



Copper(I) Halide Complexes with Triphenylphosphine and Heterocyclic Thione Ligands

Patcharanan Choto

**A Thesis Submitted in Partial Fulfillment of the Requirements for
the Degree of Master of Science in Physical Chemistry**

Prince of Songkla University

2010

Copyright of Prince of Songkla University

Thesis Title Copper(I) Halide Complexes with Triphenylphosphine and
 Heterocyclic Thione Ligands

Author Miss Patcharanan Choto

Major Program Physical Chemistry

Major Advisor :

.....Chairperson
(Asst. Prof. Dr. Chaveng Pakawatchai)

Examining Committee :

.....Chairperson
(Asst. Prof. Dr. Orawan Sirichote)

.....
(Asst. Prof. Dr. Chaveng Pakawatchai)

.....
(Dr. Weena Aemaeg Tapachai)

.....
(Dr. Nararak Leesakul)

.....
(Asst. Prof. Dr. Hirihattaya Phetmung)

The Graduate School, Prince of Songkla University, has approved this thesis as partial fulfillment of the requirements for the Master of Science Degree in Physical Chemistry

.....
(Prof. Dr. Amornrat Phongdara)

Dean of Graduate School

ชื่อวิทยานิพนธ์	สารประกอบเชิงซ้อนกوبเปอร์(I) เอไอล์ด์กับไตรฟินิลฟอสฟีนและເຫດອໂຣໄไซคลິກໄໂອນລີແກນດໍ
ผู้เขียน	นางสาวพัชรนันท์ ໂຈໂຕ
สาขาวิชา	เคมีเชิงพิสิกส์
ปีการศึกษา	2553

บทคัดย่อ

ปฏิวิຍาระหว่างกوبเปอร์(I) ເຊື້ໄລດໍກັບໄຕຣີຟິນິລີຝອສີົິນ (PPh₃) ແລະ ລີແກນດໍເຫດອໂຣໄໄສຄລິກໄໂອນ ໄດ້ແກ່ 2-ໄໂອນບົວທຸຽກ ແອຊີດ ແລະ 4,6-ໄຄມ່ທີລພິຣິມິດິນ-2(1H)-ໄໂອນ (dmpymtH) ໄທ້สารประกอบเชิงซ้อนມອນອົງເຄີລິຢີ [CuCl(PPh₃)₂(TBA)]·H₂O (1), [CuI(PPh₃)₂(CH₃CN)] (2) ແລະ [Cu(PPh₃)₂(dmpymtH)X]; X = Cl, Br, I ((3)-(5) ຕາມລຳດັບ) ທຳກຳກາວົວເຄຣະທີ່ສາຮປະກອບເຊີງຊັ້ນ (1) ແລະ (3)-(5) ໂດຍກາວົວເຄຣະທີ່ປິມາພູ ຜູາຖຸທີ່ເປັນອົງກົດປະກອບ ເອກຊະເຮຍີຟຸອອເຮສເຊັນຊີສເປັກໂທຣເມຕຣີ ນິວເຄີລິຢີແມກເນັດິກເຮໂຈແນ້ນຊີສເປັກໂທຣ ສໂກປີ ແລະ ອິນຟຣາເຣດສເປັກໂທຣສໂກປີ ນອກຈາກນີ້ຢືນສຶກຂາໂຄຮສ້າງ ໂມເລກຸລຂອງ ສາຮປະກອບທີ່ໜົດໂດຍເຫດນິກການເລີ່ມວັນນອງຮັງສີເອກຊັບນີ້ເລີກເດືອນ ໂພນວ່າໂຄຮສ້າງ ໂມເລກຸລ ຂອງສາຮປະກອບເຊີງຊັ້ນທີ່ໜົດຍົກເວັນສາຮປະກອບເຊີງຊັ້ນ (2) ມີຮູປກຮງທາງເຮາຄົມືຕອບ ອະຕອມກົບປະກົບປະກົບ ເປັນແບນທຽບສີເອກຊັບນີ້ເລີກເດືອນ (1) ແລະ ລີແກນດໍ dmpymtH ຂອງສາຮປະກອບເຊີງຊັ້ນ (3)-(5) ສຳຫຼັບສາຮປະກອບເຊີງຊັ້ນ (2) ອະຕອມກົບປະກົບປະກົບ ໃນກົບກົບສີເອກຊັບນີ້ເລີກເດືອນ (1) ແລະ (2) ຕົກພລືກອູ່ໃນຮະບນມອນອົກລິນິກ ມູ່ປະກົມ P2₁/c ສາຮປະກອບເຊີງຊັ້ນ (3) ແລະ (4) ມີໂຄຮສ້າງທີ່ເໜືອນກັນ (isomorphous) ຕົກພລືກອູ່ໃນຮະບນມອນອົກລິນິກ ມູ່ປະກົມ P2₁/c ໃນຂະໜາດທີ່ສາຮປະກອບ (5) ຕົກພລືກອູ່ໃນຮະບນໄຕຣຄລິນິກ ມູ່ປະກົມ P1 ໂຄຮສ້າງພລືກຂອງ ສາຮປະກອບເຊີງຊັ້ນ 1 ບ່ານອກວ່າທີ່ສຕານະຂອງແບ່ງ ພັນຈະໄອໂຄຣເຈນຮ່ວ່າ ໂມເລກຸລຂອງນໍ້າ ແລະ ລີແກນດໍ TBA ທຳໄໜ້ເກີດໂຄຮສ້າງແບນໂຈ່ 1 ມິຕີ ແລະ ພັນຈະໄອໂຄຣເຈນຮ່ວ່າ ລີແກນດໍ TBA ຂອງໂຈ່ 2 ສາຍທຳໄໜ້ເກີດໂຄຮສ້າງຊູປຣາ ໂມເລກຸລແບນ 1 ມິຕີ

Thesis Title	Copper(I) Halide Complexes with Triphenylphosphine and Heterocyclic Thione Ligands
Author	Miss Patcharanan Choto
Major Program	Physical Chemistry
Academic Year	2010

ABSTRACT

The reaction of copper(I) halides with triphenylphosphine (PPh_3) and 2-thiobarbituric acid (TBA) or 4,6-dimethylpyrimidine-2(1*H*)-thione (dmpymtH) gives rise to the formation of monomeric mixed-ligand complexes of the formula $[\text{CuCl}(\text{PPh}_3)_2(\text{TBA})]\cdot\text{H}_2\text{O}$ (1), $[\text{CuI}(\text{PPh}_3)_2(\text{CH}_3\text{CN})]$ (2) and $[\text{Cu}(\text{PPh}_3)_2(\text{dmpymtH})\text{X}]$; X = Cl, Br, I ((3)-(5), respectively). Complexes (1), (3)-(5) have been characterized by elemental analysis, X-ray fluorescence spectrometry, Fourier transform nuclear magnetic resonance spectroscopy and Fourier transform infrared spectroscopy. In addition, all of the complexes have also been characterized crystallographically by single crystal X-ray diffractometry, which reveals that each structure except complex (2) features a distorted tetrahedral arrangement of ligands around the central copper atom with dmpymtH or TBA acting as a neutral S donor ligand in a terminal S-bonding mode. For complex (2), the TBA ligand is not involved in the crystal structure, but the acetonitrile (solvent) molecule is bonded to the copper atom, resulting in a distorted tetrahedral geometry. Complexes (1) and (2) crystallize in monoclinic system, space group $P2_1/c$. For complexes (3)-(5), complexes (3) and (4) are isomorphous with monoclinic system, space group $P2_1/c$, while complex (5) crystallizes in triclinic system, space group $P\bar{1}$. In solid state, the water molecules of complex (1) interlink with the neutral $[\text{Cu}(\text{PPh}_3)_2(\text{TBA})\text{Cl}]$ units through hydrogen bonds forming a 1D chain. Furthermore, the hydrogen bonding interactions between TBA ligands of neighboring chains through O-H \cdots O hydrogen bonds combined two chains forming a 1D supramolecular double-chains to stabilize the structure.

ACKNOWLEDGEMENTS

I would like to express my deepest and sincere gratitude to my supervisor, Assistant Professor Dr. Chaveng Pakawatchai, for his valuable instructions, excellent suggestions, expert guidance and kindness.

My sincere thank is expressed to Assistant Professor Dr. Hirihattaya Phetmung of Thaksin University, Dr. Chomchai Suksai of Burapha University, for their kindly helpful teaching X-ray structure determination programs. Special thank is addressed to Miss Ruthairat Nimthong for her suggesting in research method. I also would like to thank Assistant Professor Dr. Orawan Sirichote, Dr. Weena Aemaeg Tapachai and Dr. Nararak Leesakul for valuable suggestions.

I greatly appreciate and wish to thank to the Center of Excellence for Innovation in Chemistry (PERCH-CIC), Commission on Higher Education, Ministry of Education and the Graduate School for partial financial supports.

I would also like to thank the staff of Department of Chemistry for their kind help and offer the convenience.

Finally, none of this would have been possible without love and encouragement of my family. I am very grateful to M.Sc., Ph.D. students and friends, for their kind help and assistance during my studies and research activities.

Patcharanan Choto

CONTENTS

	Page
CONTENTS	vii
LIST OF TABLES	ix
LIST OF ILLUSTRATIONS	xi
LIST OF ABBREVIATIONS AND SYMBOLS	xiv
1. INTRODUCTION	1
1.1 Introduction	1
1.2 Literature reviews	4
1.3 Objectives	18
2. EXPERIMENT	19
2.1 Materials and Instruments	19
2.2 Chemicals	19
2.3 Preparation of complexes	20
2.3.1 Preparation of $[\text{CuCl}(\text{PPh}_3)_2(\text{TBA})(\text{J}\cdot\text{H}_2\text{O}]$ complex	20
2.3.2 Preparation of $[\text{Cu}(\text{PPh}_3)_2(\text{CH}_3\text{CN})]$ complex	20
2.3.3 Preparation of $[\text{CuCl}(\text{PPh}_3)_2(\text{dmpytmH})]$ complex	20
2.3.4 Preparation of $[\text{CuCl}(\text{PPh}_3)_2(\text{dmpytmH})]$ complex	21
2.3.5 Preparation of $[\text{CuCl}(\text{PPh}_3)_2(\text{dmpytmH})]$ complex	21
2.4 Characterization	21
2.4.1 Melting point measurement	21
2.4.2 Elemental analysis	21
2.4.3 Fourier transform infrared spectroscopy (FT-IR)	22
2.4.4 Fourier transform NMR spectroscopy (FT-NMR)	22
2.4.5 Crystal structure determination	23
3. RESULTS	33
3.1 The studies for preparation of complexes	33
3.2 Elemental analysis	35
3.3 X-ray fluorescence spectrometry	36

CONTENTS (continued)

	Page
3.3 X-ray fluorescence spectrometry	36
3.4 Infrared spectroscopy	46
3.5 ^1H NMR and ^{13}C NMR spectroscopy	53
3.6 Single crystal X-ray diffractometry	67
4. DISCUSSION	91
4.1 Preparation of complexes	91
4.2 Elemental analysis	91
4.3 X-ray fluorescence spectrometry	92
4.4 Infrared spectroscopy	92
4.5 ^1H NMR and ^{13}C NMR spectroscopy	95
4.6 X-ray structure determination	99
4.6.1 The structure of $[\text{CuCl}(\text{PPh}_3)_2(\text{TBA})(\text{J}\cdot\text{H}_2\text{O})$	99
4.6.2 The structure of $[\text{Cu}(\text{IPPh}_3)_2(\text{CH}_3\text{CN})]$	102
4.6.3 The structure of $[\text{CuCl}(\text{PPh}_3)_2(\text{dmpymtH})]$ and $[\text{CuBr}(\text{PPh}_3)_2(\text{dmpymtH})]$	103
4.6.4 The structure of $[\text{CuCl}(\text{PPh}_3)_2(\text{dmpymtH})]$	104
5. CONCLUSION	107
REFERENCES	119
APPENDIX	116
VITAE	138

LIST OF TABLES

able	Page
1 Preparation conditions of complexes	33
2 The physical properties of ligands and complexes	40
3 The partial elemental analyses of the complexes	35
4 The crystallographic data for $[\text{CuCl}(\text{PPh}_3)_2(\text{TBA})]\cdot\text{H}_2\text{O}$ (1) and $[\text{CuI}(\text{PPh}_3)_2(\text{CH}_3\text{CN})]$ (2)	67
5 The crystallographic data for $[\text{CuX}(\text{PPh}_3)_2(\text{dmpytmH})]$ ($\text{X} = \text{Cl}, \text{Br}, \text{I}$)	68
6 Non-hydrogen interatomic distances of $[\text{CuCl}(\text{PPh}_3)_2(\text{TBA})]\cdot\text{H}_2\text{O}$	69
7 Non-hydrogen interatomic distances of $[\text{CuCl}(\text{PPh}_3)_2(\text{CH}_3\text{CN})]$	70
8 Non-hydrogen interatomic distances of $[\text{CuCl}(\text{PPh}_3)_2(\text{dmpytmH})]$	71
9 Non-hydrogen interatomic distances of $[\text{CuBr}(\text{PPh}_3)_2(\text{dmpytmH})]$	77
10 Non-hydrogen interatomic distances of $[\text{CuI}(\text{PPh}_3)_2(\text{dmpytmH})]$	78
11 Non-hydrogen interbond angles of $[\text{CuCl}(\text{PPh}_3)(\text{TBA})\cdot\text{H}_2\text{O}]$	79
12 Non-hydrogen interbond angles of $[\text{CuI}(\text{PPh}_3)_2(\text{CH}_3\text{CN})]$	81
13 Non-hydrogen interbond angles of $[\text{CuCl}(\text{PPh}_3)_2(\text{dmpytmH})]$	84
14 Non-hydrogen interbond angles of $[\text{CuBr}(\text{PPh}_3)_2(\text{dmpytmH})]$	87
15 Non-hydrogen interbond angles of $[\text{CuI}(\text{PPh}_3)_2(\text{dmpytmH})]$	90
16 IR frequencies (cm^{-1}) of TBA and its complex, $[\text{CuCl}(\text{PPh}_3)_2(\text{TBA})]\cdot\text{H}_2\text{O}$	94
17 IR frequencies (cm^{-1}) of dmpytmH and its complexes, $[\text{CuCl}(\text{PPh}_3)_2(\text{dmpytmH})]$, $[\text{CuBr}(\text{PPh}_3)_2(\text{dmpytmH})]$ and $[\text{CuI}(\text{PPh}_3)_2(\text{dmpytmH})]$	95
18 Experimental ^1H NMR spectra of the compounds in $\text{DMSO}-d_6$ solvent	97
19 Experimental ^{13}C NMR spectra of the compounds in $\text{DMSO}-d_6$ solvent	102
20 The equation of calculation of unit cell volume depend on crystal system	116
21 Atomic coordinates ($\times 10^4$) and equivalent isotropic displacement parameters ($\text{\AA}^2 \times 10^3$) for $[\text{CuCl}(\text{PPh}_3)_2(\text{TBA})]\cdot\text{H}_2\text{O}$	118
22 Anisotropic displacement parameters ($\text{\AA}^2 \times 10^3$) for $[\text{CuCl}(\text{PPh}_3)_2(\text{TBA})]\cdot\text{H}_2\text{O}$	120
23 Atomic coordinates ($\times 10^4$) and equivalent isotropic displacement parameters ($\text{\AA}^2 \times 10^3$) for $[\text{CuI}(\text{PPh}_3)_2(\text{CH}_3\text{CN})]$	122

LIST OF TABLES (continued)

Table	Page
24 Anisotropic displacement parameters ($\text{\AA}^2 \times 10^3$) for $[\text{CuI}(\text{PPh}_3)_2(\text{CH}_3\text{CN})]$	124
25 Atomic coordinates ($\times 10^4$) and equivalent isotropic displacement parameters ($\text{\AA}^2 \times 10^3$) for $[\text{CuCl}(\text{PPh}_3)_2(\text{dmpymtH})]$	125
26 Anisotropic displacement parameters ($\text{\AA}^2 \times 10^3$) for $[\text{CuCl}(\text{PPh}_3)_2(\text{dmpymtH})]$	128
27 Atomic coordinates ($\times 10^4$) and equivalent isotropic displacement parameters ($\text{\AA}^2 \times 10^3$) for $[\text{CuBr}(\text{PPh}_3)_2(\text{dmpymtH})]$	130
28 Anisotropic displacement parameters ($\text{\AA}^2 \times 10^3$) for $[\text{CuBr}(\text{PPh}_3)_2(\text{dmpymtH})]$	132
29 Atomic coordinates ($\times 10^4$) and equivalent isotropic displacement parameters ($\text{\AA}^2 \times 10^3$) for $[\text{CuI}(\text{PPh}_3)_2(\text{dmpymtH})]$	134
30 Anisotropic displacement parameters ($\text{\AA}^2 \times 10^3$) for $[\text{CuI}(\text{PPh}_3)_2(\text{dmpymtH})]$	136

LIST OF ILLUSTRATIONS

Figure	Page
1 Various coordination modes of heterocyclic thiones	2
2 The structure of the tautomeric species of 4,6-dimethylpyrimidine-2(1 <i>H</i>)-thione (dmpymtH)	3
3 The structure of tautomeric species of 2-thiobarbituric acid (TBA)	3
4 The structure of triphenylphosphine (PPh_3)	4
5 The structure of $[(\text{PPh}_3)_3\text{Cu}_2\text{Br}_2]$ in the monoclinic crystal	4
6 The structure of $[\text{Cu}(\text{PPh}_3)_2(\text{bztdtH})\text{C1}]\text{CH}_3\text{COCH}$	5
7 The structure of $[\text{Cu}(\text{bztdtH})(\text{PPh}_3)\text{Br}]_2$	6
8 The structure of $[\text{Cu}(\text{PPh}_3)_2(\text{tzdtH})\text{Cl}]$	7
9 A single molecule of $[\text{CuI}(\text{PPh}_3)(\text{C}_9\text{H}_7\text{N})]_2$	7
10 A single molecule of $[\text{Cu}_2(\text{CN})_2(\text{PPh}_3)_4(\text{hppH})]$	8
11 A single molecule of trigonal $[\text{Cu}(\text{PPh}_3)_3\text{Br}]$ viewed down Cu-Br bond	9
10 A single molecule of $[\text{Cu}(\text{PPh}_3)_3\text{Br}] \bullet 2\text{Me}_2\text{CO}$, projected down the Cu-Br bond	8
11 The structure of $[(\text{CuBr}(\text{PPh}_3))_2(\text{pym})]$	9
12 The structure of $[(\text{CuBr}(\text{PPh}_3))_2(\text{Trz})]$	9
13 The structure of $[\text{Cu}(\text{oxine})(\text{PPh}_3)_2](\text{BF})_4$	10
14 The structure of $[\text{Cu}(\text{quin})(\text{PPh}_3)_2](\text{BF})_4$	10
15 1D infinite chain structure (b) of $\{[\text{Cu}_2(\text{L}_1)(\text{PPh}_3)_2\text{I}_2]\text{2CH}_2\text{Cl}_2\}_n$ with $(\text{PPh}_3)_2\text{Cu}_2(\mu\text{-I})_2$ unit (a)	11
16 1D infinite chain structure of $\{[\text{Cu}_2(\text{L}_2)(\text{PPh}_3)_2]\text{BF}_4\}_n$	12
17 The structure of $[\text{Cu}_2(\text{L}_4)(\text{PPh}_3)_4\text{I}_2]$	12
18 The structure of $[\text{Cu}_2(\text{L}_4)(\text{PPh}_3)_4\text{I}_2]$	13
19 The structure of $[\text{Cu}(\text{A})(\text{PPh}_3)_2]\text{ClO}_4$	14
20 Two crystallographically independent molecules of $[\text{CuCl}(1\kappa\text{SimzSH})(\text{PPh}_3)_2] \cdot [\text{CuCl}(\text{PPh}_3)_2]$	14
21 The structure of $[\text{Cu}(\text{H}_2\text{L})(\text{PPh}_3)_2]\text{NO}_3 \cdot 0.5\text{H}_2\text{O}$	15

LIST OF ILLUSTRATIONS (continued)

Figure	Page
22 The structure of $[\text{Cu}(\text{dmpymtH})_3]_2[\text{BF}_4]_2 \cdot 2\text{H}_2\text{O}$	16
23 The structure of $[\text{CuCl}(\text{dmpymtH})_2]_2$	16
24 The structure of $[\text{Cu}(\text{N}_3)(\text{dmpymtH})(\text{PPh}_3)_2]$	17
25 The structure of $[\text{Cu}(\text{NCS})(\text{dmpymtH})(\text{PPh}_3)_2]$	17
26 SMART APEX system components	23
27 A flowchart for the step involved in a crystal structure determination	25
28 (a) Crystal mounting, (b) the Goniometer base and head and (c) crystal center on cross-hairs	27
29 The $\text{Cu}(K_\alpha)$ spectrum of $[\text{CuCl}(\text{PPh}_3)_2(\text{TBA})] \cdot \text{H}_2\text{O}$	36
30 The $\text{S}(K_\alpha)$, $\text{S}(K_\beta)$, $\text{P}(K_\alpha)$, $\text{P}(K_\beta)$ and $\text{Cl}(K_\alpha)$ spectrum of $[\text{CuCl}(\text{PPh}_3)_2(\text{TBA})] \cdot \text{H}_2\text{O}$	37
31 The $\text{Cu}(K_\alpha)$ spectrum of $[\text{CuCl}(\text{PPh}_3)_2(\text{dmpymtH})]$	38
32 The $\text{S}(K_\alpha)$, $\text{S}(K_\beta)$, $\text{P}(K_\alpha)$, $\text{P}(K_\beta)$ and $\text{Cl}(K_\alpha)$ spectrum of $[\text{CuCl}(\text{PPh}_3)_2(\text{dmpymtH})]$	39
33 The $\text{Cu}(K_\alpha)$ spectrum of $[\text{CuBr}(\text{PPh}_3)_2(\text{dmpymtH})]$	40
34 The $\text{S}(K_\alpha)$, $\text{S}(K_\beta)$, $\text{P}(K_\alpha)$ and $\text{P}(K_\beta)$ spectrum of $[\text{CuBr}(\text{PPh}_3)_2(\text{dmpymtH})]$	41
35 The $\text{Br}(K_\alpha)$ and $\text{Br}(K_\beta)$ spectrum of $[\text{CuBr}(\text{PPh}_3)_2(\text{dmpymtH})]$	42
36 The $\text{Cu}(K_\alpha)$ spectrum of $[\text{CuI}(\text{PPh}_3)_2(\text{dmpymtH})]$	43
37 The $\text{S}(K_\alpha)$, $\text{S}(K_\beta)$ and $\text{P}(K_\beta)$ spectrum of $[\text{CuI}(\text{PPh}_3)_2(\text{dmpymtH})]$	44
38 The $\text{I}(K_\alpha)$ spectrum of $[\text{CuI}(\text{PPh}_3)_2(\text{dmpymtH})]$	45
39 The infrared spectrum of 2-thiobarbituric acid (TBA)	46
40 The infrared spectrum of dimethylpyrimidine-2(1H)-thione (dmpymtH)	47
41 The infrared spectrum of Triphenylphosphine (PPh_3)	48
42 The infrared spectrum of $[\text{CuCl}(\text{PPh}_3)_2(\text{TBA})] \cdot \text{H}_2\text{O}$	49
43 The infrared spectrum of $[\text{CuCl}(\text{PPh}_3)_2(\text{dmpymtH})]$	50
44 The infrared spectrum of $[\text{CuBr}(\text{PPh}_3)_2(\text{dmpymtH})]$	51
45 The infrared spectrum of $[\text{CuI}(\text{PPh}_3)_2(\text{dmpymtH})]$	52
46 ^1H NMR spectrum of 2-thiobarbituric acid (TBA)	53

LIST OF ILLUSTRATIONS (continued)

Figure	Page
47 ^1H NMR spectrum of dimethylpyrimidine-2(1H)-thione (dmpytmH)	54
48 ^1H NMR spectrum of Triphenylphosphine (PPh_3)	55
49 ^1H NMR spectrum of $[\text{CuCl}(\text{PPh}_3)_2(\text{TBA})]\cdot\text{H}_2\text{O}$	56
50 ^1H NMR spectrum of $[\text{CuCl}(\text{PPh}_3)_2(\text{dmpytmH})]$	57
51 ^1H NMR spectrum of $[\text{CuBr}(\text{PPh}_3)_2(\text{dmpytmH})]$	58
52 ^1H NMR spectrum of $[\text{CuBr}(\text{PPh}_3)_2(\text{dmpytmH})]$	59
53 ^{13}C NMR spectrum of 2-thiobarbituric acid (TBA)	60
54 ^{13}C NMR spectrum of dimethylpyrimidine-2(1H)-thione (dmpytmH)	61
53 ^{13}C NMR spectrum of Triphenylphosphine (PPh_3)	62
56 ^{13}C NMR spectrum of $[\text{CuCl}(\text{PPh}_3)_2(\text{TBA})]\cdot\text{H}_2\text{O}$	63
57 ^{13}C NMR spectrum of $[\text{CuCl}(\text{PPh}_3)_2(\text{dmpytmH})]$	64
58 ^{13}C NMR spectrum of $[\text{CuBr}(\text{PPh}_3)_2(\text{dmpytmH})]$	65
59 ^{13}C NMR spectrum of $[\text{CuI}(\text{PPh}_3)_2(\text{dmpytmH})]$	66
60 Unit cell contents of $[\text{CuCl}(\text{PPh}_3)_2(\text{TBA})]\cdot\text{H}_2\text{O}$	89
61 Unit cell contents of $[\text{CuI}(\text{PPh}_3)_2(\text{CH}_3\text{CN})]$	89
62 Unit cell contents of $[\text{CuCl}(\text{PPh}_3)_2(\text{dmpytmH})]$ and $[\text{CuBr}(\text{PPh}_3)_2(\text{dmpytmH})]$	90
63 Unit cell contents of $[\text{CuI}(\text{PPh}_3)_2(\text{dmpytmH})]$	90
64 Atom nomenclature employed for NMR assignments, (a) complex $[\text{CuCl}(\text{PPh}_3)_2(\text{TBA})]\cdot\text{H}_2\text{O}$, (b) complexes 3-5	96
65 Two keto-enol tautomeric forms of 2-thiobarbituric acid	96
66 The structure of $[\text{CuCl}(\text{PPh}_3)_2(\text{TBA})]\cdot\text{H}_2\text{O}$ (1)	100
67 The intra-interaction hydrogen bonding in complex $[\text{CuCl}(\text{PPh}_3)_2(\text{TBA})]\cdot\text{H}_2\text{O}$	101
68 1D supramolecular double-chains of complex $[\text{CuCl}(\text{PPh}_3)_2(\text{TBA})]\cdot\text{H}_2\text{O}$	101
69 The structure of $[\text{CuI}(\text{PPh}_3)_2(\text{CH}_3\text{CN})]$	102
70 The structure of $[\text{CuX}(\text{PPh}_3)_2(\text{dmpytmH})]$ ($\text{X} = \text{Cl}, \text{Br}$ and I)	103
71 The parallel arrangement of structure of $[\text{CuX}(\text{PPh}_3)_2(\text{dmpytmH})]$ ($\text{X} = \text{Cl}, \text{Br}$)	104

LIST OF ILLUSTRATIONS (continued)

Figure	Page
72 The intra-interaction hydrogen bonding in $[\text{CuX}(\text{PPh}_3)(\text{dmpymtH})]$ (X= Cl, Br, I) Complexes	105
73 The resonance structure of complexes (3), (4) and (5) (X; Cl, Br ,I)	106
74 The Bravais lattices	117

LIST OF ABBREVIATIONS AND SYMBOLS

°	=	degree
Å	=	Angstrom unit ($1 \text{ \AA} = 10^{-10}$ metre)
°C	=	degree celsius
A.R.	=	Analytical Reagent
cm ⁻¹	=	wave number
D _c	=	calculated density
D _m	=	measured density
EDXRF	=	Energy Dispersive X-ray Fluorescence
g	=	gram
g/cm ³	=	gram per cubic centimetre
hr.	=	hour
K	=	Kelvin
KeV	=	kilo electron volt
mg	=	milligram
kg	=	kilogram
L.R.	=	Lab Reagent
mL	=	millilitre
mm.	=	millimetre
mmol	=	millimole
M	=	molar
V	=	volume
ptu	=	N-phenylthiourea
PPh ₃	=	triphenylphosphine
CuI	=	Copper(I) iodide
CuBr	=	Copper(I) bromide
CuCl	=	Copper(I) chloride
s	=	singlet
m	=	multiplet

LIST OF ABBREVIATIONS AND SYMBOLS (continued)

br	=	broad
nm	=	nanometre
mp.	=	melting point
cm^{-1}	=	reciprocal centimetre (wave number)
δ	=	chemical shift relative to TMS
λ_{\max}	=	maximum absorption wavelength
λ	=	wavelength
ν	=	absorption frequency
ε	=	molar extinction coefficient
MHz	=	MegaHertz
Hz	=	hertz
ppm	=	part per million
Fig.	=	Figure
IR	=	Infrared
UV-Vis	=	Ultraviolet-Visible
NMR	=	Nuclear magnetic resonance
DMSO- d_6	=	hexadeutero-dimethyl sulphoxide

CHAPTER 1

Introduction

1.1 Introduction

Copper (Cu) is a metallic chemical element in Group 11 of the periodic table, together with silver (Ag) and gold (Au). The electronic configuration of elemental copper is $[1s^2 2s^2 2p^6 3s^2 3p^6]3d^{10}4s^1$ or $[Ar] 3d^{10}4s^1$. Copper has two common different positive oxidation numbers, it can either be copper(I), which has an oxidation number of +1. The other possibility is copper(II), which has an oxidation number of +2. Copper(I) is a soft Lewis acid metal ion, it is well-coordinated with soft ligands. This is the main reason that the complexes of copper(I) have been studied extensively during the last several years. However, this thesis will focus on the complexes of copper(I).

There are many previous research publications on the synthesis and coordination chemistry of copper(I) complexes. The interaction of copper(I) with nitrogen, sulfur, phosphorous and oxygen-donors has yielded complexes which gave wide variation in structural format and rich photo-physical and chemical properties. The structure and stereochemistry of copper(I) complexes exhibit coordination number dependent structures, three coordination prefers trigonal planar and four coordination prefers distorted tetrahedral. Many of these complexes have been reported to be luminescent (Su *et al.*, 1997) and their emission behavior varies with structures, identities of halides, and steric and electronic effects of used ligands (Li *et al.*, 2005). Some of these complexes have been found to be unusual structural features, catalytic activity in photoredox reactions (Miller *et al.*, 2001), exhibit corrosion inhibiting properties (Tian *et al.*, 2004), phosphorescence due to close Cu…Cu interactions (Fu *et al.*, 2004), precursors to blue copper–protein model (Fujisawa *et al.*, 2004), superconductors (Karppinen *et al.*, 2004) and catalysts in enantiomer selective Diels–Alder reactions (Mancheno *et al.*, 2004). Moreover, the

role of copper(I) is evident in several biologically important reactions, such as a dioxygen carrier and models for several enzymes (Lantie *et al.*, 1984).

There are many complexes of copper(I) generated with a variety of heterocyclic thiones because of the presence of various donor atoms. The chemistry of heterocyclic thiones that incorporate both sulfur and nitrogen atoms in their structure is rich because these compounds can coordinate as monodentate ligands (Lobana *et al.*, 2008) and more frequently as polydentate ligands either to a single metal center, acting as a chelating ligand (Sheldrick, *et al.*, 1998), or to several metal centers as a bridging ligand (Raper, 1996). In addition, these copper(I) complexes have wide ranging application as metal corrosion inhibitors and biologically active molecules (Sakhawat *et al.*, 1990). There is indeed a considerable versatility in the coordination modes of these molecules which may include monodentate binding through S(I) or through N(II), bridging through a single S(III), bridging through both S and N(IV) or chelating via the S-to-N backbone (VI) (Akrivos, 2001) (Figure 1). In addition, copper(I) compounds, usually are air and moisture sensitive, therefore as the secondary ligands the tertiary phosphines were chosen for stabilizing the coordination sphere of copper(I) (Grodzicki, *et al.*, 2005). Especially, the presence of tertiary phosphines play an important role in enhancing the solubility of copper(I) compounds of heterocyclic thione ligands (Lobana, *et al.*, 2002), therefore the copper(I) complexes with heterocyclic thiones in the presence of tertiary phosphines have attracted considerable attention.

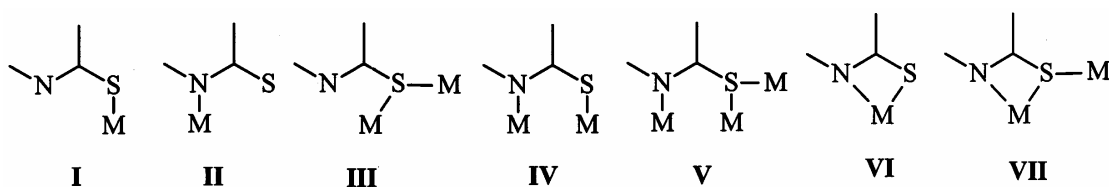


Figure 1 Various coordination modes of heterocyclic thiones.

Two compounds, 4,6-dimethylpyrimidine-2(1*H*)-thione (dmpymtH) and 2-thiobarbituric acid (TBA) are heterocyclic thione compounds. The first compound, 4,6-dimethylpyrimidine-2(1*H*)-thione, exhibit tautomeric equilibrium between thiol

and thione as a consequence of the highly mobile protons that it possess (Figure 2). The predominant form largely depends on the state and conditions of the molecule (Martos-Calvente, *et al.*, 2003). Its complexes with some divalent metal ions (Battistuz and Peyronel, 1980) as well as monovalent silver ion (Goodgame, *et al.*, 1980) have been previously studied. The seconded compound, 2-thiobarbituric acid (TBA), is a substituted mercaptopyrimidine with three mobile H atoms and two tautomeric forms (Figure 3). 2-Thiobarbituric acid is a class of drugs that utilized as anesthetics and sleeping agent and is used for treatment of anxiety, epilepsy and other psychiatric disorders, and possess effects on the motor and sensory functions (Earnshaw *et al.*, 1968). However, in spite of that, the preparation of the transition metal complexes of 2-thiobarbituric acid has been reported (Masoud, *et al.*, 1983) and by screening the literature survey, no studies of the crystal structure of copper(I) and 2-thiobarbituric acid have been reported.

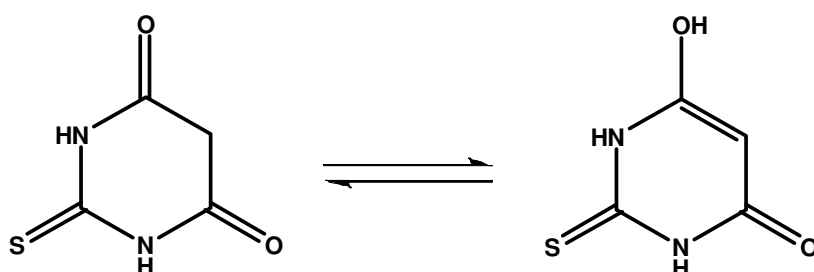
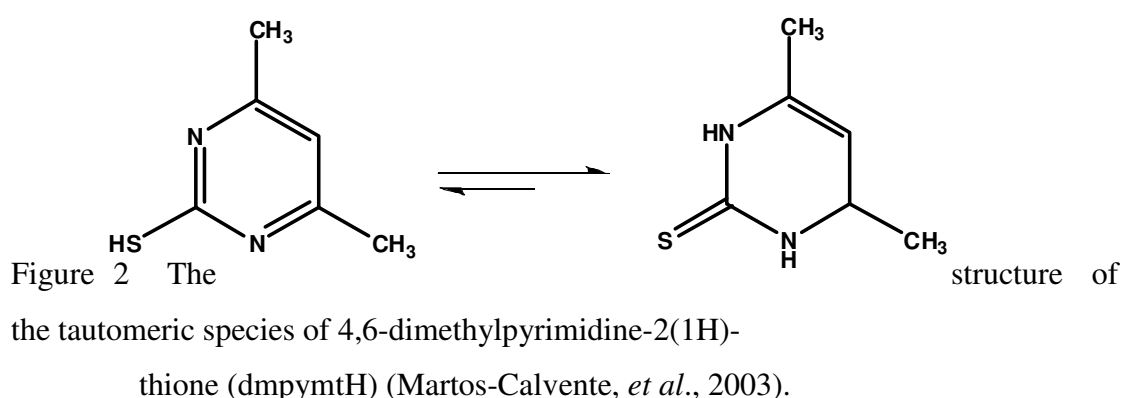


Figure 3 The structure of tautomeric species of 2-thiobarbituric acid (TBA) (Mendez, *et al.*, 2007).

Tertiary phosphine such as triphenylphosphine (PPh_3) is an important agent for organic synthesis. The replacement of triphenylphosphine from various metal triphenylphosphine complexes with heterocyclic thione ligands have been studied. The structure of triphenylphosphine is shown in Figure 4.

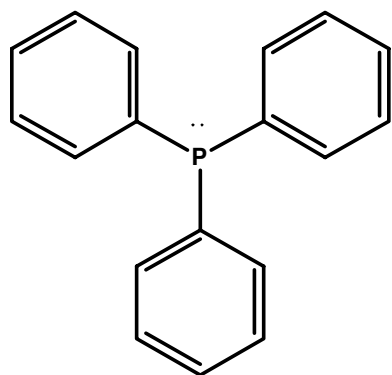


Figure 4 The structure of triphenylphosphine (PPh_3).

From the above viewpoints, the copper(I) halide complexes of ligands containing the $-\text{NH}-\text{C}(=\text{S})-$ moiety, 4,6-dimethylpyrimidine-2(1*H*)-thione (dmpymtH) and 2-thiobarbituric acid (TBA) with triphenylphosphine (PPh_3) as a co-ligand have been prepared and characterized in this work, named the replacement of triphenylphosphine groups in $[\text{Cu}(\text{PPh}_3)_3\text{X}]$, $\text{X} = \text{Cl}, \text{Br}, \text{I}$ by heterocyclic thione molecules, 4,6-dimethylpyrimidine-2(1*H*)-thione (dmpymtH) and 2-thiobarbituric acid (TBA).

1.2 Literature reviews

Complexes of copper(I) with triphenylphosphine, PPh_3 as well as complexes of copper(I) with mixed PPh_3 and ligand containing sulfur or nitrogen donor atom have been studied in previous publications as follow:

Dyason (Dyason *et al.*, 1985) synthesized dinuclear complex of the formula $[(\text{PPh}_3)_3\text{Cu}_2\text{Br}_2]$. The complex crystallizes in the monoclinic space group $P2_1/c$ with cell parameters $a = 19.390(8)$, $b = 9.912(5)$, $c = 26.979(9)$ Å, $\beta = 112.33(3)^\circ$; $R = 0.043$. Crystallographic analysis indicated that the complex consists of both three- and four-coordinated copper atoms as shown in Figure 5.

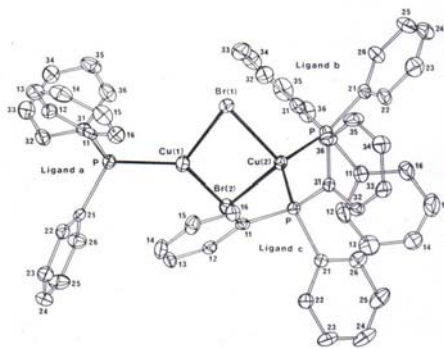


Figure 5 The structure of $[(\text{PPh}_3)_3\text{Cu}_2\text{Br}_2]$ in the monoclinic crystal.

Voutsas (Voutsas *et al.*, 1995) prepared copper(I) complex of the general formula $[\text{Cu}(\text{PPh}_3)_2(\text{bztdtH})\text{C1}]\text{CH}_3\text{COCH}_3$ from the reaction of copper(I) chloride and benz-1,3-thiazolidine-2-thione (bztdtH). The copper(I) complex crystallizes in the monoclinic space group $P2_1/c$ with unit-cell parameters of $a = 13.172$, $b = 18.713$, $c = 17.357$ Å, $\beta = 95.65^\circ$ and $Z = 4$. The structure of $[\text{Cu}(\text{PPh}_3)_2(\text{bztdtH})\text{C1}]\text{CH}_3\text{COCH}_3$ exhibits a distorted tetrahedral as shown in Figure 6.

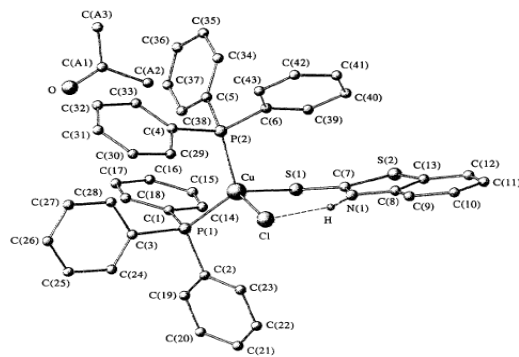


Figure 6 The structure of $[\text{Cu}(\text{PPh}_3)_2(\text{bztdtH})\text{C1}]\text{CH}_3\text{COCH}_3$.

Lang and Tatsumi (Lang and tatsumi, 1995) studied the solid state reaction of copper(I) bromide with PPh_3 and benz-1,3-thiazolidine-2-thione (bztzdtH). The crystal structure was determined by single-crystal X-ray diffraction method. The complex $[\text{Cu}(\text{bztzdtH})(\text{PPh}_3)\text{Br}]_2$ is monoclinic, space group $C2/c$ with $a = 25.991(14)$, $b = 9.206(1)$, $c = 19.943(3)$ Å, $\beta = 100.02$ (1) $^\circ$ and $Z = 4$. The two crystallographically equivalent copper atoms have a pseudo-tetrahedral geometry. The sulfur atoms of two bztzdtH ligands link the two copper atoms, forming a planar Cu_2S_2 moiety as shown in Figure 7.

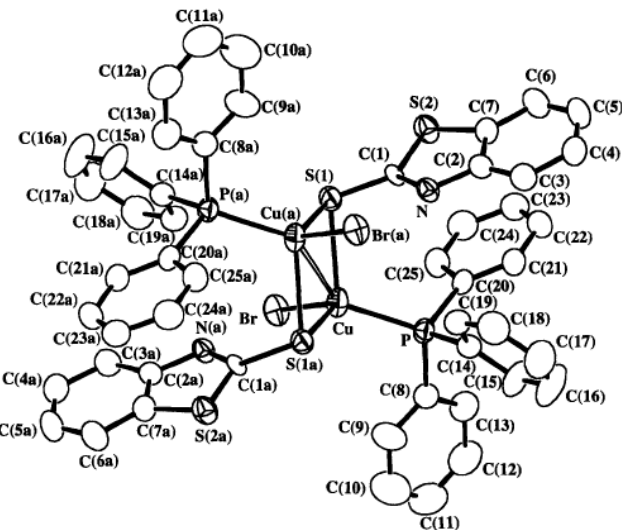


Figure 7 The structure of $[\text{Cu}(\text{bztzdtH})(\text{PPh}_3)\text{Br}]_2$

Aslanidis (Aslanidis *et al.*, 1998) studied the reaction of $[\text{Cu}(\text{PPh}_3)_3\text{Cl}]$ with heterocyclic thiones, 1,3-thiazolidine-2-thione (tzdtH). The complex $[\text{Cu}(\text{PPh}_3)_2(\text{tzdtH})\text{Cl}]$ was characterized by various physicochemical methods. The crystal structure was determined by single-crystal X-ray diffraction method. The crystals are monoclinic, space group $P2_1/c$ with $a = 14.31(2)$, $b = 10.099(10)$, $c = 24.52(2)$ Å, $\beta = 93.53(7)$ $^\circ$ and $Z = 4$. The copper atom has a pseudo-tetrahedral geometry as shown in Figure 8.

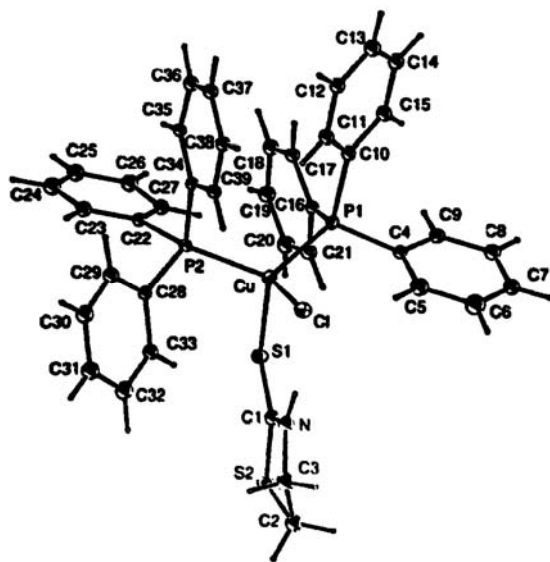


Figure 8 The structure of $[\text{Cu}(\text{PPh}_3)_2(\text{tzdtH})\text{Cl}]$.

Jin (jin *et al.*, 1999) synthesized dinuclear complex by the reaction of quinoline ($\text{C}_9\text{H}_7\text{N}$) and PPh_3 . The complex $[\text{CuI}(\text{PPh}_3)(\text{C}_9\text{H}_7\text{N})]_2$ crystallizes in the triclinic space group $P\bar{1}$ with cell parameters $a = 9.304(2)$, $b = 10.9792(13)$, $c = 13.685(3)$ Å, $\alpha = 107.896(10)$, $\beta = 107.812(4)$, $\gamma = 96.383(11)^\circ$ and $Z = 1$. The structure of complex exhibits a distorted tetrahedral as shown in Figure 9.

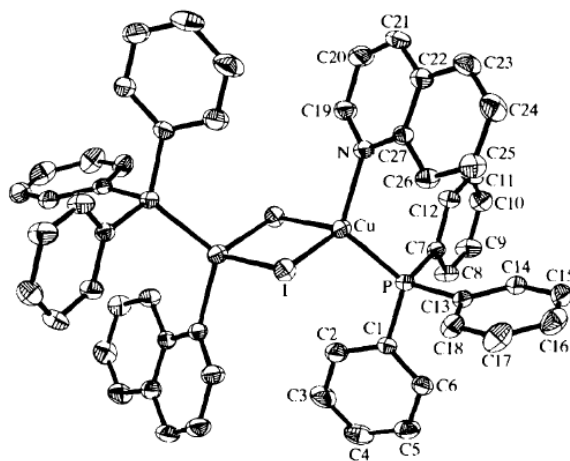


Figure 9 A single molecule of $[\text{CuI}(\text{PPh}_3)(\text{C}_9\text{H}_7\text{N})]_2$.

Coles (Coles *et al.*, 2001) synthesized the complex with the formula $[\text{Cu}_2(\text{CN})_2(\text{PPh}_3)_4(\text{hppH})]$. The complex was characterized by elemental analysis, IR,

and NMR spectroscopy. X-rays diffraction study revealed that the solid-state structure of $[\text{Cu}_2(\text{CN})_2(\text{PPh}_3)_4(\text{hppH})]$ is consistent with a zwitterionic complex, comprising of $[\text{Cu}^{(+)}(\text{PPh}_3)_2(\text{hppH})]$ and $[\text{Cu}^{(-)}(\text{CN})_2(\text{PPh}_3)_2]$ metal centres, linked by a cyanide bridge as shown in Figure 10. The complex crystallizes in the triclinic space group $P\bar{1}$ with cell parameters $a = 13.501(6)$, $b = 14.3767(4)$, $c = 19.6377(8)$ Å, $\alpha = 81.818(3)$, $\beta = 78.002(2)$, $\gamma = 83.788(3)^\circ$ and $Z = 2$.

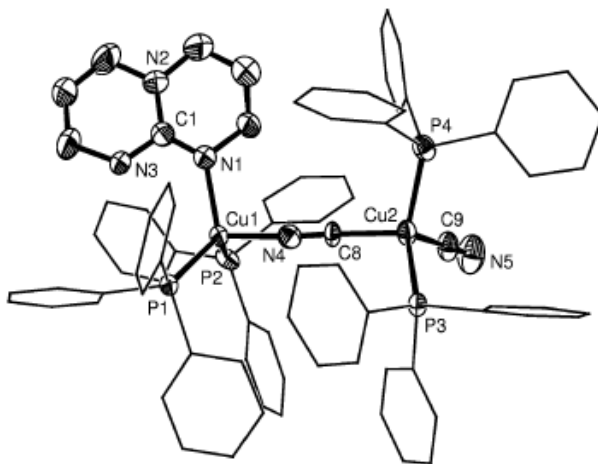


Figure 10 A single molecule of $[\text{Cu}_2(\text{CN})_2(\text{PPh}_3)_4(\text{hppH})]$.

Maeyer (Maeyer, *et al.*, 2003) studied the coordination of pyrimidine (pym) and triazine (trz) bridging ligands with CuBr. The X-ray structures of $[(\text{CuBr}(\text{PPh}_3))_2\text{B}]$ ($\text{B} = \text{pym, trz}$) show 1D chains formed from rhomboidal $(\text{CuL})_2\text{Br}_2$ units linked by the B ligand as shown in Figures 11 and 12. The complex $[(\text{CuBr}(\text{PPh}_3))_2(\text{pym})]$ crystallizes in the triclinic space group $P\bar{1}$ with cell parameters $a = 10.2411(17)$, $b = 12.647(2)$, $c = 14.897(3)$ Å, $\alpha = 98.630(3)$, $\beta = 99.884(3)$, $\gamma = 104.433(3)^\circ$ and $Z = 2$. For complex $[(\text{CuBr}(\text{PPh}_3))_2(\text{trz})]$, crystallizes in the triclinic space group $P\bar{1}$ with cell parameters $a = 10.1583(13)$, $b = 12.1583(15)$, $c = 14.7891(18)$ Å, $\alpha = 95.289(2)$, $\beta = 103.401(2)$, $\gamma = 101.887(2)^\circ$ and $Z = 2$.

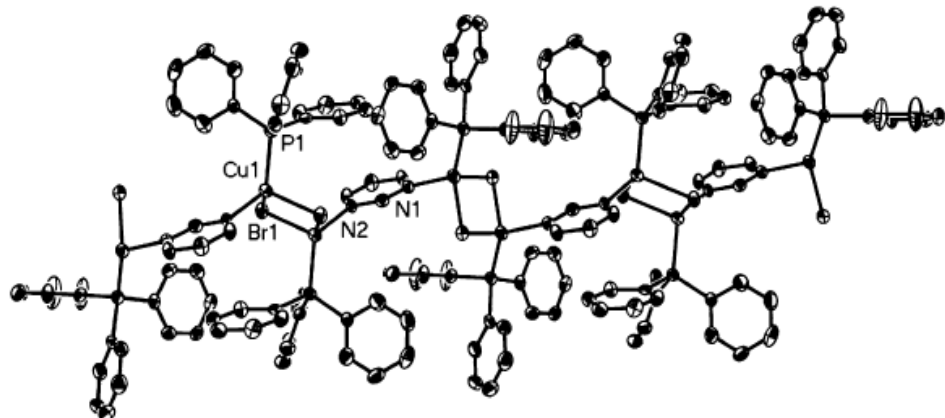


Figure 11 The structure of $[(\text{CuBr}(\text{PPh}_3)_2(\text{pym})]$.

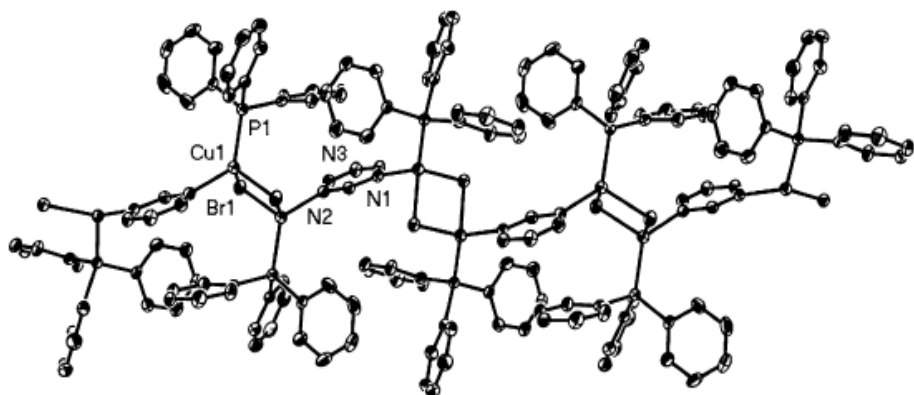


Figure 12 The structure of $[(\text{CuBr}(\text{PPh}_3)_2(\text{Trz})]$.

Li (Li *et al.*, 2003) synthesized the two mononuclear copper(I) complexes, $[\text{Cu}(\text{oxine})(\text{PPh}_3)_2](\text{BF}_4)$ and $[\text{Cu}(\text{PPh}_3)_2(\text{quin})]\text{BF}_4$ by the reaction of 8-hydroxyquinoline (oxine) with $[\text{Cu}(\text{MeCN})_2(\text{PPh}_3)_2](\text{BF}_4)$ and quinoline (quin) with $[\text{Cu}(\text{MeCN})_2(\text{PPh}_3)_2](\text{BF}_4)$ respectively. Their structures were determined by X-ray crystallography as shown in Figures 13 and 14. The complex $[\text{Cu}(\text{oxine})(\text{PPh}_3)_2](\text{BF}_4)$ crystallizes in the monoclinic space group $P2_1/n$, $a = 11.372(3)$, $b = 22.171(5)$, $c = 16.038(4)$ Å, $\beta = 97.942(5)^\circ$ and $Z = 4$. For complex $[\text{Cu}(\text{PPh}_3)_2(\text{Quin})]\text{BF}_4$ crystallizes in the monoclinic space group $P2_1/c$, $a = 19.445(5)$, $b = 11.878(3)$, $c = 17.637(4)$ Å, $\beta = 94.009(4)^\circ$ and $Z = 4$.

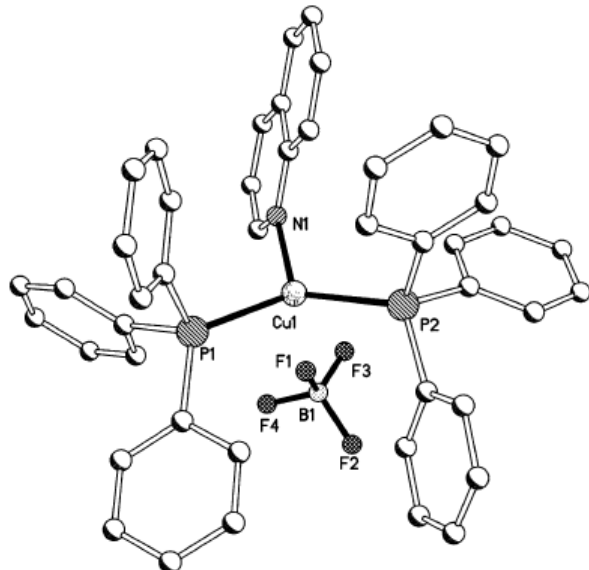


Figure 13 The structure of $[\text{Cu}(\text{oxine})(\text{PPh}_3)_2](\text{BF}_4)_2$.

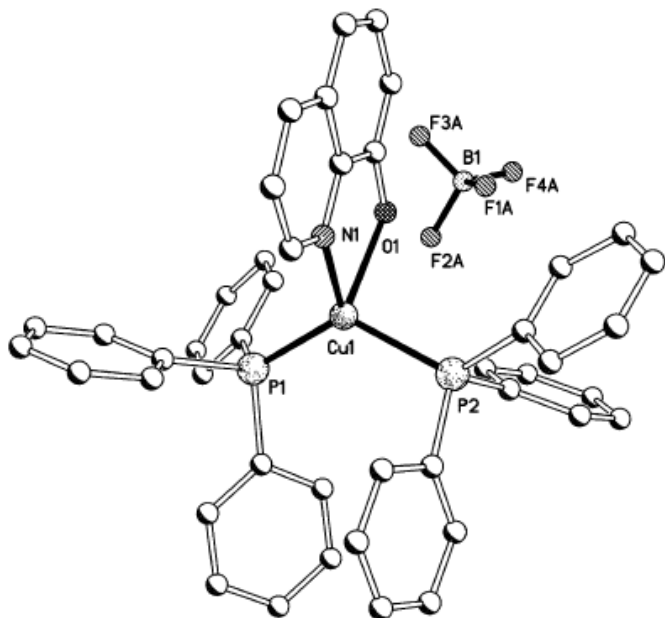


Figure 14 The structure of $[\text{Cu}(\text{quin})(\text{PPh}_3)_2](\text{BF}_4)_2$.

Zhou (Zhou *et al.*, 2006) synthesized and studied photoluminescence property of copper(I) complexes with bis(schiff base) ligands. The crystal structures of all the complexes were determined by X-ray crystallography as follows:

The complex $\{[\text{Cu}_2(\text{L}1)(\text{PPh}_3)_2\text{I}_2]\text{2CH}_2\text{Cl}_2\}_n$ was prepared by the reaction of pyridine-4-carbaldehyde azine (L1) with PPh_3 and copper(I) iodide. The structure contains $(\text{PPh}_3)_2\text{Cu}_2(\mu\text{-I})_2$ units bridging by L1 to construct an infinite chain structure as in 4,4'-bipyridine analogue as shown in Figures 15a and 15b. The complex crystallizes in the triclinic space group $P\bar{1}$ with unit-cell parameters of $a = 9.915(3)$, $b = 11.214(3)$, $c = 13.049(4)$ Å, $\alpha = 77.275(5)$, $\beta = 70.730(5)$, $\gamma = 76.875(5)$ ° and $Z = 2$.

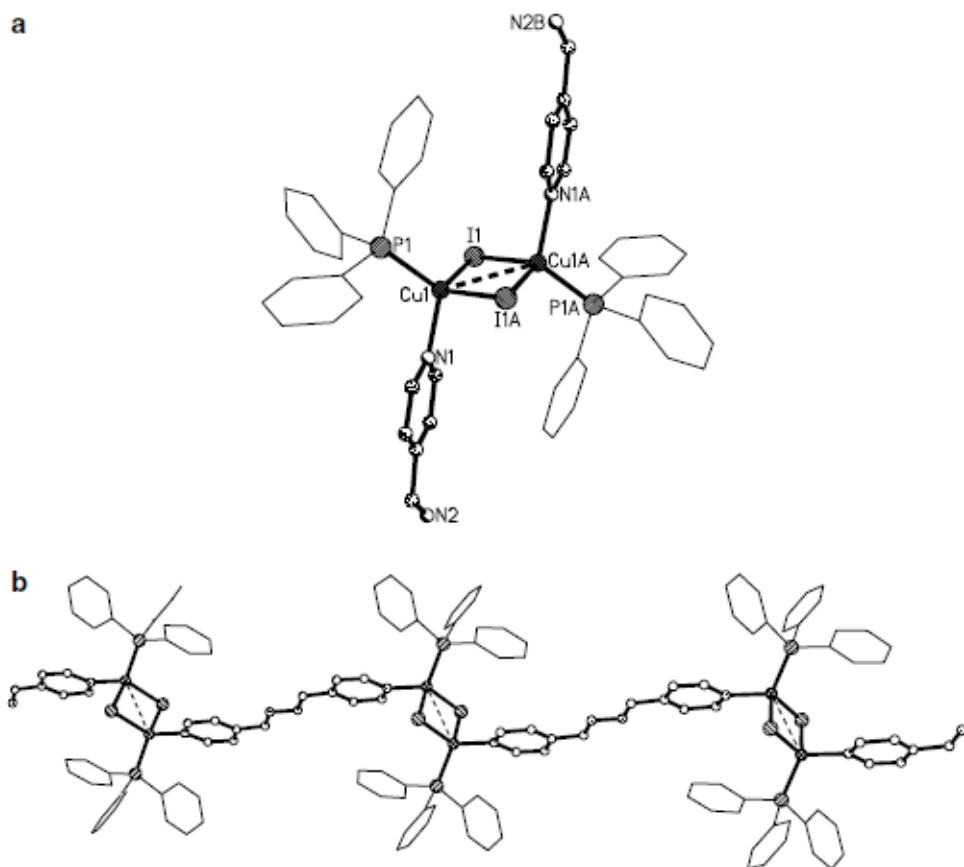


Figure 15 1D infinite chain structure (b) of $\{[\text{Cu}_2(\text{L}1)(\text{PPh}_3)_2\text{I}_2]\text{2CH}_2\text{Cl}_2\}_n$ with $(\text{PPh}_3)_2\text{Cu}_2(\mu\text{-I})_2$ unit (a).

The complex $\{[\text{Cu}_2(\text{L}_2)(\text{PPh}_3)_2]\text{BF}_4\}_n$ was prepared by the reaction of 2-bis(4'-pyridylmethyleneamino)ethane (L_2) with $[\text{Cu}(\text{CH}_3\text{CN})_4]\text{BF}_4$ and PPh_3 . The coordination atoms around copper(I) atom are two pyridyl nitrogen atoms from two different L_2 ligands and two phosphorus atoms from two different PPh_3 molecules as shown in Figure 16. The complex crystallizes in the monoclinic space group $P2_1/c$ with $a = 13.4414(10)$, $b = 24.6684(10)$, $c = 13.8239(10)$ Å, $\beta = 96.796(5)^\circ$ and $Z = 4$.

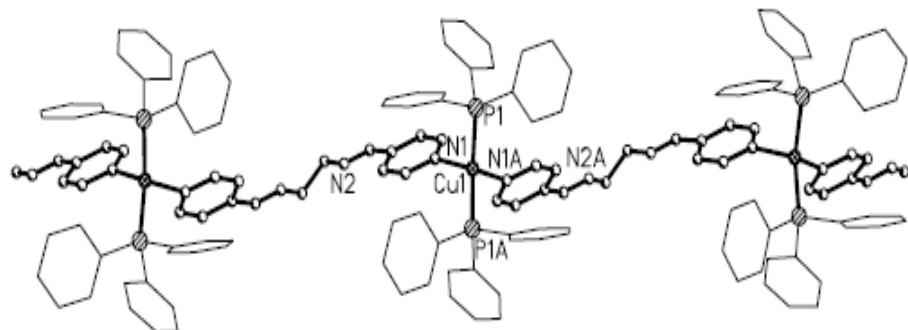


Figure 16 1D infinite chain structure of $\{[\text{Cu}_2(\text{L}_2)(\text{PPh}_3)_2]\text{BF}_4\}_n$.

The complex $[\text{Cu}_2(\text{L}_3)(\text{PPh}_3)_4\text{I}_2]2\text{CH}_2\text{Cl}_2$ was synthesized by the reaction of pyridine-3-carbaldehyde azine (L_3) with copper(I) iodide and PPh_3 . Ligand L_3 acts as a monodentate ligand to coordinate two copper(I) atoms yielding a dimer as shown in Figure 17. The complex crystallizes in the triclinic space group $P\bar{1}$ with unit-cell parameters of $a = 11.0924(9)$, $b = 13.1742(11)$, $c = 14.6867(12)$ Å, $\alpha = 99.2890(10)$, $\beta = 93.5390(10)$, $\gamma = 102.4750(10)^\circ$ and $Z = 1$.

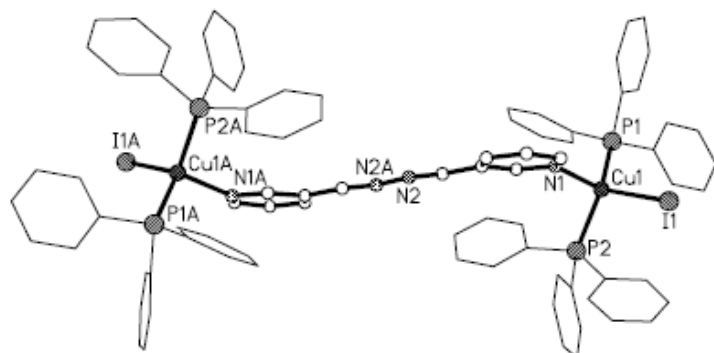


Figure 17 The structure of $[\text{Cu}_2(\text{L}_3)(\text{PPh}_3)_4\text{I}_2]2\text{CH}_2\text{Cl}_2$.

The complex $[\text{Cu}_2(\text{L}_4)(\text{PPh}_3)_4\text{I}_2]$ was synthesized by the reaction of 1,2-bis(3'-pyridylmethyleneamino) ethane (L_4) with copper(I) iodide and PPh_3 . Ligand L_4 acts as a monodentate ligand to coordinate two copper(I) atoms and no solvent molecule exists in this complex as shown in Figure 18. The complex crystallizes in the monolinic space group $P2_1/n$ with unit-cell parameters of $a = 13.9744(7)$, $b = 17.8186(10)$, $c = 15.3126(8)$ Å, $\beta = 90.8490(10)^\circ$ and $Z = 2$.

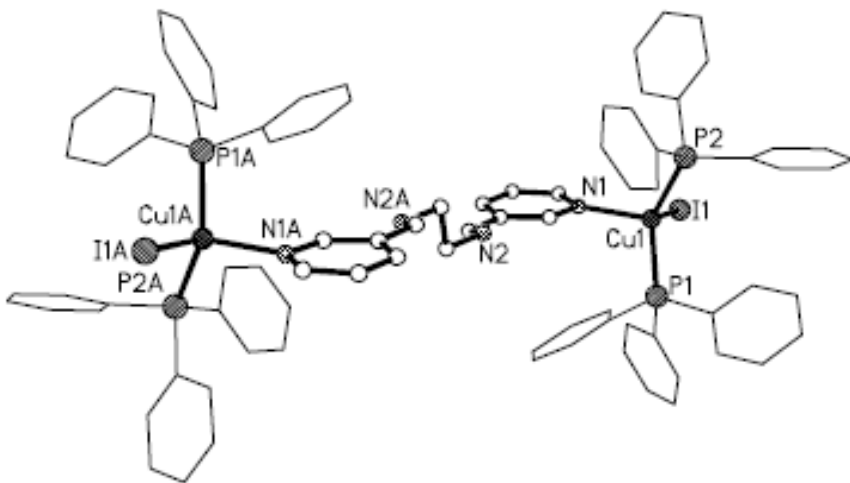


Figure 18 The structure of $[\text{Cu}_2(\text{L}_4)(\text{PPh}_3)_4\text{I}_2]$.

Dehghanpou (Dehghanpou *et al.*, 2007) synthesized (4-methyl-phenyl)-pyridin-2-ylmethylen-amine (A) ligand and its corresponding copper(I) complex, $[\text{Cu}(\text{A})(\text{PPh}_3)_2]\text{ClO}_4$. The complex has been characterized by CHN analyses, ^1H and ^{13}C NMR, IR and UV–Vis spectroscopy. The crystal structure of $[\text{Cu}(\text{A})(\text{PPh}_3)_2]\text{ClO}_4$ was determined from single crystal X-ray diffraction. The coordination about the copper(I) center in the the complex is best described as a distorted tetrahedral as shown in Figure 19, and crystallizes in the triclinic space group $P\bar{1}$ with unit-cell parameters of $a = 11.0500(10)$, $b = 12.676(2)$, $c = 32.847(5)$ Å, $\alpha = 79.13(5)$, $\beta = 81.31(4)$, $\gamma = 85.21(7)^\circ$ and $Z = 2$.

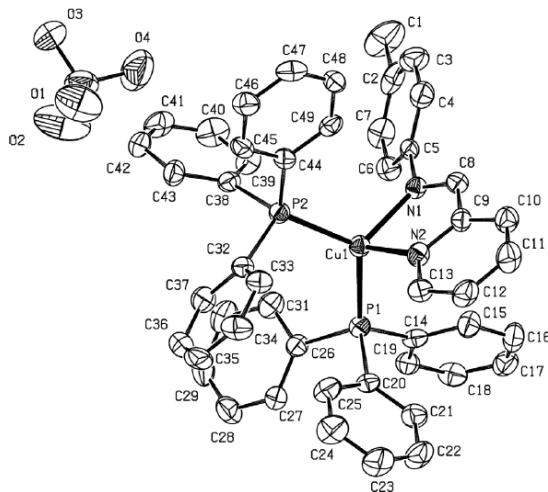


Figure 19 The structure of $[\text{Cu}(\text{A})(\text{PPh}_3)_2]\text{ClO}_4$.

Lobana (Lobana *et al.*, 2008) studied the reaction of copper(I) chloride with 1,3-imidazoline-2-thione (imzSH) in the presence of PPh_3 in 1:2:2 or 1:1:2 (M:L:PPh_3) molar ratios yielded a compound of unusual composition, $[\text{CuCl}(\text{1}\kappa\text{SimzSH})(\text{PPh}_3)_2] \cdot [\text{CuCl}(\text{PPh}_3)_2]$, whose X-ray crystallography has shown that its crystals consist of four coordinated $[\text{CuCl}(\text{1}\kappa\text{S-imzSH})(\text{PPh}_3)_2]$ and three coordinated $[\text{Cu}(\text{PPh}_3)_2\text{Cl}]$ independent molecules in the same unit cell as shown in Figure 20. The complex crystallizes in the triclinic space group $P\bar{1}$ with unit-cell parameters of $a = 9.992(1)$, $b = 17.6240(10)$, $c = 19.902(2)$ Å, $\alpha = 84.18(1)$, $\beta = 87.50(1)$, $\gamma = 78.26(1)$ ° and $Z = 2$.

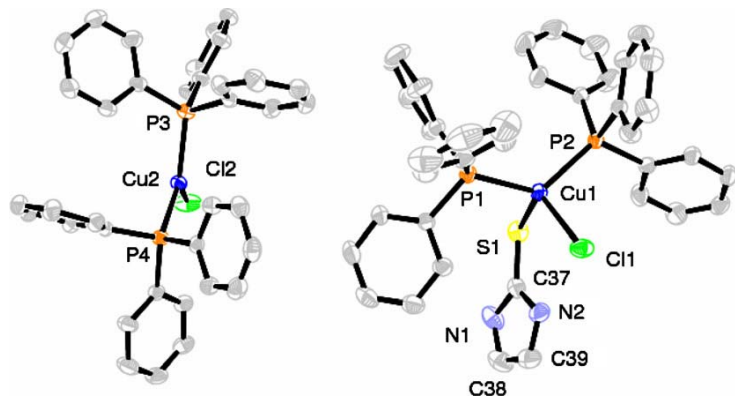


Figure 20 Two crystallographically independent molecules of $[\text{CuCl}(\text{1}\kappa\text{SimzSH})(\text{PPh}_3)_2] \cdot [\text{CuCl}(\text{PPh}_3)_2]$.

Singh (Singh *et al.*, 2008) synthesized a new *N,N'*-ethane-1,2-bis(4-methoxyphenyl)carbothioamide ligand and its Cu(I) complex of the formula $[\text{Cu}(\text{H}_2\text{L})(\text{PPh}_3)_2]\text{NO}_3 \cdot 0.5\text{H}_2\text{O}$. The synthesized compound have been characterized with the help of elemental analyses, IR, ^1H , ^{13}C and ^{31}P NMR spectroscopy. The crystal structure has been determined by single crystal X-ray diffraction technique. The ligand acts as a neutral S-donor and forms a nine-membered chelate ring in $[\text{Cu}(\text{H}_2\text{L})(\text{PPh}_3)_2]\text{NO}_3 \cdot 0.5\text{H}_2\text{O}$ as shown in Figure 21. The complex crystallizes in the triclinic space group $P\bar{1}$ with unit-cell parameters of $a = 10.399(3)$, $b = 12.933(3)$, $c = 20.330(4)$ Å, $\alpha = 88.887(6)$, $\beta = 85.594(7)$, $\gamma = 69.275(6)$ ° and $Z = 2$.

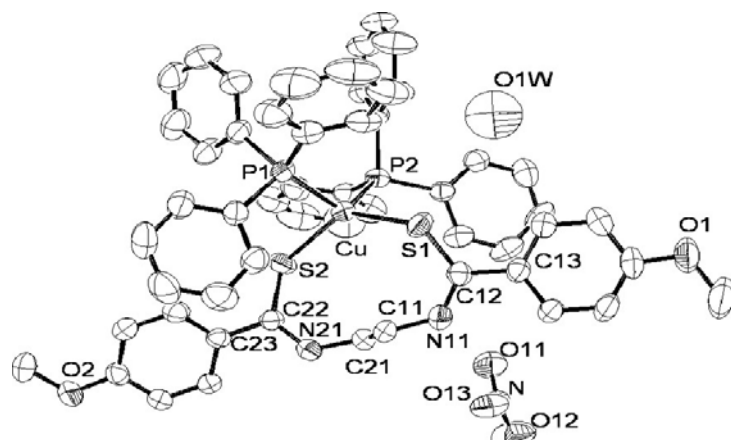


Figure 21 The structure of $[\text{Cu}(\text{H}_2\text{L})(\text{PPh}_3)_2]\text{NO}_3 \cdot 0.5\text{H}_2\text{O}$.

The X-ray crystal structures of copper(I) complexes with 4,6-dimethylpyrimidine-2(1H)-thione (dmpytmH) as well as copper(I) complexes with mixed 4,6-dimethylpyrimidine-2(1H)-thione and triphenylphosphine have been previously studied are as follows.

Falcomer (Falcomer *et al.*, 2006) synthesized the copper(I) complexes by the reaction of dmpytmH with the parent complex $[\text{Cu}(\text{MeCN})_4][\text{BF}_4]$ affords the dinuclear copper(I) complex $[\text{Cu}(\text{dmpytmH})_3]_2[\text{BF}_4]_2 \cdot 2\text{H}_2\text{O}$ and the reaction of Cu_2O and the hydrochloride salt of dmpytmH gives the dinuclear complex $[\text{CuCl}(\text{dmpytmH})_2]_2$ as shown in Figures 22 and 23 respectively. In both complex,

the neutral dmpymtH is acting as a bridging ligand. The complex $[\text{Cu}(\text{dmpymtH})_3]_2[\text{BF}_4]_2 \cdot 2\text{H}_2\text{O}$ crystallizes in the triclinic space group $P\bar{1}$ with unit-cell parameters of $a = 7.365(1)$, $b = 12.786(2)$, $c = 14.852(2)$ Å, $\alpha = 70.622(4)$, $\beta = 81.781(5)$, $\gamma = 74.195(8)$ ° and $Z = 1$. For complex $[\text{CuCl}(\text{dmpymtH})_2]_2$, crystallizes in the monolinic space group $P2_1/c$ with unit-cell parameters of $a = 12.7208(8)$, $b = 8.8949(5)$, $c = 14.7208(6)$ Å, $\beta = 101.284(3)$ ° and $Z = 2$.

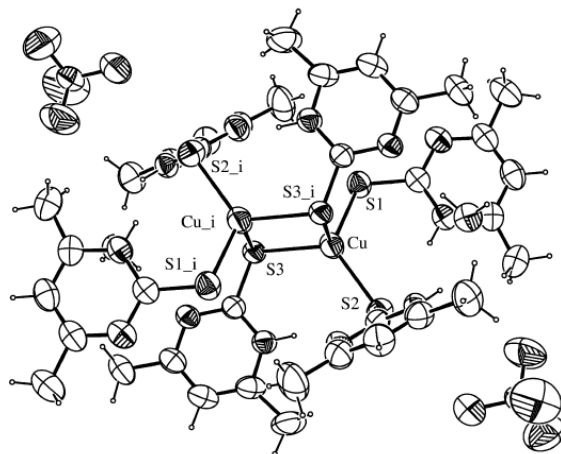


Figure 22 The structure of $[\text{Cu}(\text{dmpymtH})_3]_2[\text{BF}_4]_2 \cdot 2\text{H}_2\text{O}$.

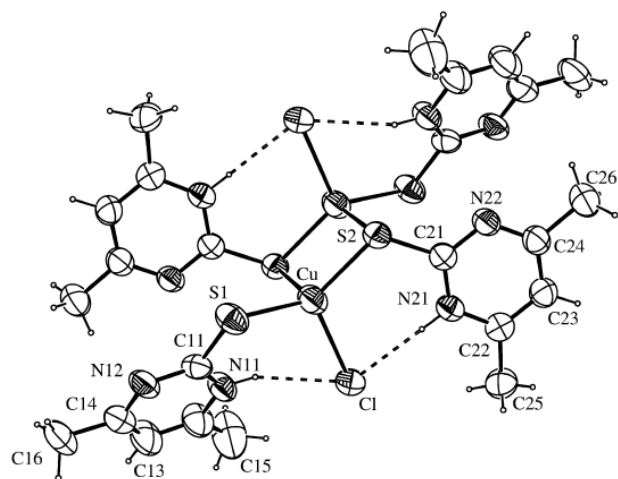


Figure 23 The structure of $[\text{CuCl}(\text{dmpymtH})_2]_2$.

Lemos (Lemos *et al.*, 2001) prepared mixed-ligand copper(I) coordination compounds containing pseudohalides (azide and thiocyanate), 4,6-dimethylpyrimidine-2(1H)-thione (dmpymtH) and triphenylphosphine. The crystal structures of $[\text{Cu}(\text{N}_3)(\text{dmpymtH})(\text{PPh}_3)_2]$ and $[\text{Cu}(\text{NCS})(\text{dmpymtH})(\text{PPh}_3)_2]$ have been determined by X-ray diffraction method. The copper atom has a tetra-coordinate CuNP_2S chromophore with distorted tetrahedral coordination in both complexes as shown in Figures 24 and 25. The complex $[\text{Cu}(\text{N}_3)(\text{dmpymtH})(\text{PPh}_3)_2]$ crystallizes in the monolinic space group, $P2_1/c$ with $a = 9.829(16)$, $b = 17.7041(11)$, $c = 22.3169(18)$ Å, $\beta = 101.416(8)^\circ$ and $Z = 4$. For complex $[\text{CuCl}(\text{dmpymtH})_2]_2$, crystallizes in the monolinic space group $P2_1/c$ with unit-cell parameters of $a = 15.1388(17)$, $b = 12.9769(5)$, $c = 20.0351(7)$ Å, $\beta = 94.467(5)^\circ$ and $Z = 4$.

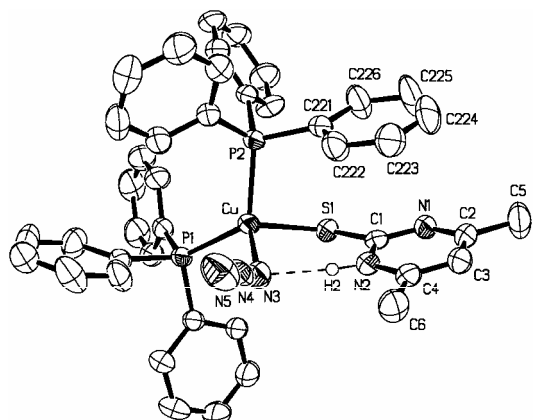


Figure 24 The structure of $[\text{Cu}(\text{N}_3)(\text{dmpymtH})(\text{PPh}_3)_2]$.

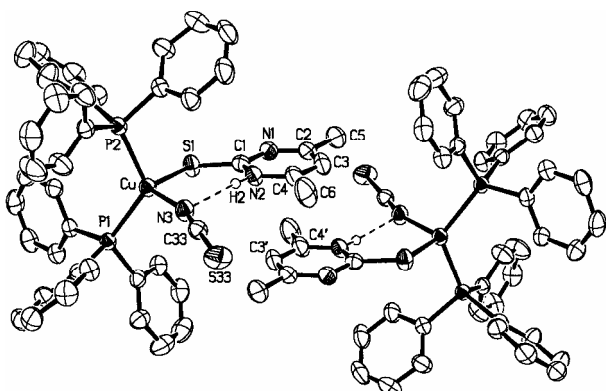


Figure 25 The structure of $[\text{Cu}(\text{NCS})(\text{dmpymtH})(\text{PPh}_3)_2]$.

1.3 Objectives

1. To study the method and find out the optimum condition for synthesized Cu(I) complexes with mixed ligands of triphenylphosphine and heterocyclic thione ligands, 4,6-dimethylpyrimidine-2(1H)-thione and 2-thiobarbituric acid by varying mole ratio of reactants, solvents, temperature of reaction and so on.
2. To characterize the structures of these complexes by single crystal diffraction technique, IR ,NMR and XRF spectroscopies.
3. To study molecular structure and arrangement of the molecules in unit cell, including crystal system, cell parameters and space group of the complexes.
4. To be the fundamental informations for other researchers who take them to find more applications.
5. To present the research in academic conferences or publish in chemistry journals.

CHAPTER 2

Experiment

2. Method of study

2.1 Materials and Instruments

1. Thermometer, Gallenkamp, England 0-360 °C
2. Capillary tube
3. Capillary melting point apparatus, Thomas Hoover, Unimelt 0-360 °C
4. Hot plate stirrer with magnetic bar
5. Ultrasonic cleaner, model AS7240 AT, Tianjin
6. X-ray fluorescence spectrometer model PW 2400, Philips
7. Fourier transform infrared spectrometer, model 783, Perkin - Elmer
8. Fourier transform NMR spectrometer 500 MHz, Model UNITY INOVA, Varian
9. Bruker SMART APEX CCD diffractometer
10. UHU epoxy adhesive
11. Fiber glass, 0.1-0.4 mm. (in diameter)
12. Bee wax

2.2 Chemicals

Products of Fluka Chemical, Buchs, Switzerland

2-Thiobarbituric acid C₄H₄O₂N₂S, purum
4,6-Dimethyl-2-mercaptopurimidin C₆H₈N₂S,
Triphenylphosphine, C₁₈H₁₈P, purum
Copper(I) chloride, CuCl, L.R. grade
Copper(I) bromide, CuBr, L.R. grade

Products of Lab-Scan Analytical Science

Methanol, CH₃OH, A.R. grade

Acetonitrile, CH₃CN, A.R. grade

Products of Aldrich Chemical Company, Inc

Copper(I) iodide, CuI, L.R. grade

2.3 Preparation of complexes

2.3.1 Preparation of [CuCl(TBA)(PPh₃)₂]·H₂O complex

A solution of triphenylphosphine (0.53g, 2.02 mmol) in 30 mL of acetonitrile was stirred at 70 °C then CuCl (0.10g, 1.01 mmol) solid was added and stirred for 2 hours. Solid of 2-thiobarbituric acid (0.15g, 1.01 mmol) was added and heated with continuous stirring for a period of 5 hours. The clear yellow solution was formed then filtered off and cooled slowly to room temperature. Slow evaporation of the solvent gave the pink colored crystalline solids, which were filtered off and dried in vacuo.

2.3.2 Preparation of [CuI(PPh₃)₂(CH₃CN)] complex

A solution of triphenylphosphine (0.27g, 1.05 mmol) and CuI (0.1g, 0.52 mmol) in 30 cm³ of acetonitrile was irradiated in a water bath of the ultrasonic cleaner at frequency of 40 kHz and power of 200 watts at 40 °C for 15 minutes. The reaction mixture was followed by adding TBA (0.08g, 0.52 mmol) then irradiated for 30 minutes. The resulting solution was filtered off and the clear solution was kept at room temperature. Slow evaporation of the solvent at room temperature gave the microcrystalline solids, which were filtered off and dried in vacuo.

2.3.3 Preparation of [CuCl(dmpymtH)(PPh₃)₂] complex

A solution of 4,6-dimethyl-2-mercaptopyrimidin (0.14g, 1.01 mmol) in 30 mL of methanol was stirred at 60 °C then CuCl (0.10g, 1.01 mmol) solid was added and stirred for 3 hours. Solid of triphenylphosphine (0.53g, 2.02 mmol) was added and heated with continuous stirring for a period of 2 hours. The clear yellow solution was formed then filtered off and kept at room temperature. Slow evaporation of the

solvent gave the yellow colored crystalline solids, which were filtered off and dried in vacuo.

2.3.4 Preparation of $[\text{CuBr}(\text{dmpymtH})(\text{PPh}_3)_2]$ complex

A solution of 4,6-dimethyl-2-mercaptopurimidin (0.10g, 0.70 mmol) in 30 mL of methanol was stirred at 60 °C then CuBr (0.10g, 0.70 mmol) solid was added and stirred for 3 hours. Solid of triphenylphosphine (0.37g, 1.40 mmol) was added and heated with continuous stirring for a period of 2 hours. The clear yellow solution was formed then filtered off and kept at room temperature. Slow evaporation of the solvent gave the yellow colored crystalline solids, which were filtered off and dried in vacuo.

2.3.5 Preparation of $[\text{CuI}(\text{dmpymtH})(\text{PPh}_3)_2]$ complex

A solution of 4,6-dimethyl-2-mercaptopurimidin (0.08g, 0.52 mmol) in 30 mL of methanol was stirred at 60 °C then CuI (0.10g, 0.52 mmol) solid was added and stirred for 3 hours. Solid of triphenylphosphine (0.27g, 1.04 mmol) was added and heated with continuous stirring for a period of 2 hours. The clear yellow solution was formed then filtered off and kept at room temperature. Slow evaporation of the solvent gave the yellow colored crystalline solids, which were filtered off and dried in vacuo.

2.4 Characterization

2.4.1 Melting point measurement

Melting points of the complexes were measured on Capillary Melting Point Apparatus, Thomas Hoover, Unimelt 0-360 °C.

2.4.2 Elemental analysis

Carbon, hydrogen, nitrogen, sulfur, phosphorus and oxygen contents in the synthetic crystals were determined by CE Instruments Flash 1112 Series EA CHNS-O Analyser.

2.4.3 Fourier transform infrared spectroscopy (FT-IR)

Infrared spectra were measured in the region 4000-400 cm^{-1} on a Perkin-Elmer 783 Infrared Spectrophotometer and Perkin-Elmer Spectrum GX FTIR-spectrophotometer using potassium bromide disc.

2.4.4 Fourier transform NMR spectroscopy (FT-NMR)

^1H and ^{13}C -NMR spectra were recorded in $\text{DMSO}-d_6$ and chloroform- d on a Varian Inova spectrometer at 500 MHz. The chemical shift values are on δ scale and the coupling constants (J) are in Hz.

2.4.5 X-ray fluorescence spectrometry

Cu, S, P and halides (Cl, Br and I) qualitative analyses of $[\text{Cu}(\text{TBA})(\text{PPh}_3)_2\text{Cl}]$, $[\text{Cu}(\text{dmpymtH})(\text{PPh}_3)_2\text{Cl}]$, $[\text{Cu}(\text{dmpymtH})(\text{PPh}_3)_2\text{Br}]$ and $[\text{Cu}(\text{dmpymtH})(\text{PPh}_3)_2\text{I}]$ were performed by X-ray Fluorescence spectrometer (Perkin Elmer, PW2400).

2.4.6 Crystal structure determination by single crystal X-ray diffraction

The X-ray diffraction data of $[\text{Cu}(\text{TBA})(\text{PPh}_3)_2\text{Cl}]\text{H}_2\text{O}$, $[\text{Cu}(\text{PPh}_3)_2(\text{CH}_3\text{CN})\text{I}]$, $[\text{Cu}(\text{dmpymtH})(\text{PPh}_3)_2\text{Cl}]$, $[\text{Cu}(\text{dmpymtH})(\text{PPh}_3)_2\text{Br}]$ and $[\text{Cu}(\text{dmpymtH})(\text{PPh}_3)_2\text{I}]$ were performed at 293 K with graphite-monochromated Mo $K\alpha$ radiation on a Bruker SMART APEX CCD diffractometer ($\lambda=0.71073\text{\AA}$) at Department of Chemistry, Faculty of Science, Prince of Songkla University, the SMART/APEX CCD system is shown in Figure 26. Integration and absorption corrections were used with SAINT (Bruker, 2003) and, SADABS (Bruker, 2003), respectively. The structures of the complexes were solved by direct methods using the SHELXTL program. All of the non-hydrogen atoms were refined anisotropically by full-matrix least-squares based on F^2 . All hydrogen atoms were fixed geometrically and allowed to ride on those atoms, to which they are attached.

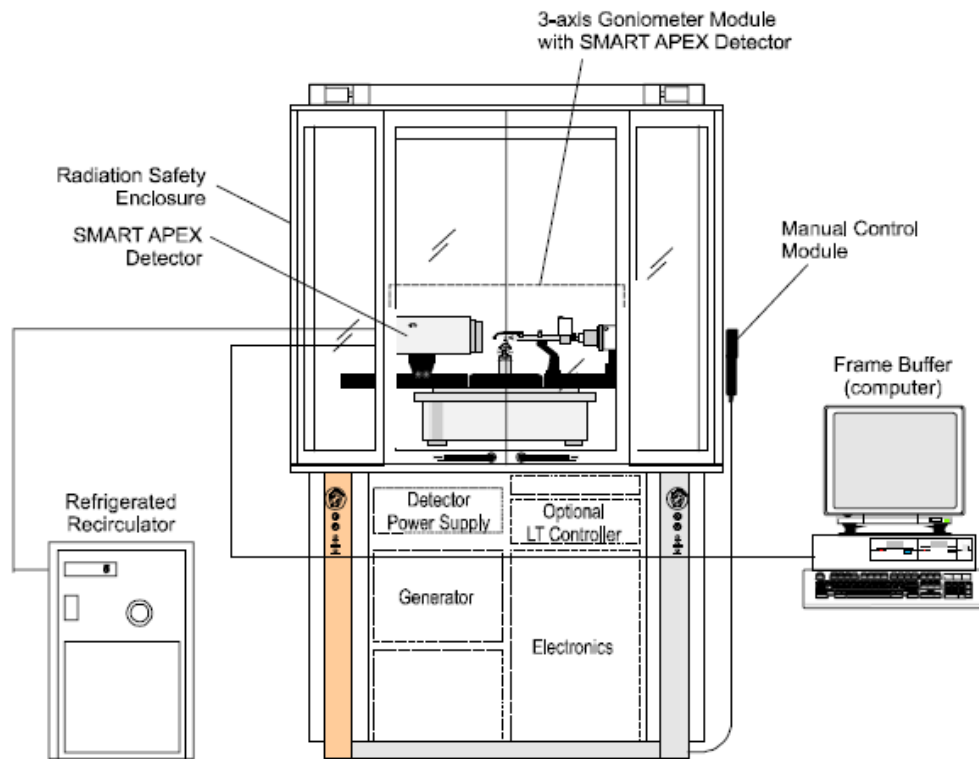


Figure 26 SMART APEX system components.

The SMART APEX system incorporates a software suite for instrument control and structure determination:

- SMART program controls the diffractometer to collect the experimental data used by the other programs in the system program suite
- D8TOOLS software package helps users and service staff with maintenance, error diagnosis and correction of the diffractometer
- VIDEO program controls the real-time video images from the video camera
- RLATT program displays reflections in reciprocal space
- ASTRO and COSMO set up the data collection strategy
- SAINTPLUS integrates the raw data to provide the best intensities for each indexed reflection
- SADABS does absorption and other corrections

- XPREP displays the indexed reflections in layers similar to Precession photographs, calculates the space group, performs face-indexed absorption corrections, and displays calculated Patterson sections
- XS and XL perform structure solution and refinement, respectively
- XP and XSHELL visualize molecular and crystal structure and plot diagrams;
- XCIF produces reports from standard CIF files

The structure of the synthesized crystals were determined by following steps in Figure 27, illustrating common step employed in the determination of crystal structure. The involved steps are in the boxes. To the right of each is listed the information obtained and to the left an indication of the time-scale involved in carrying out the operation.

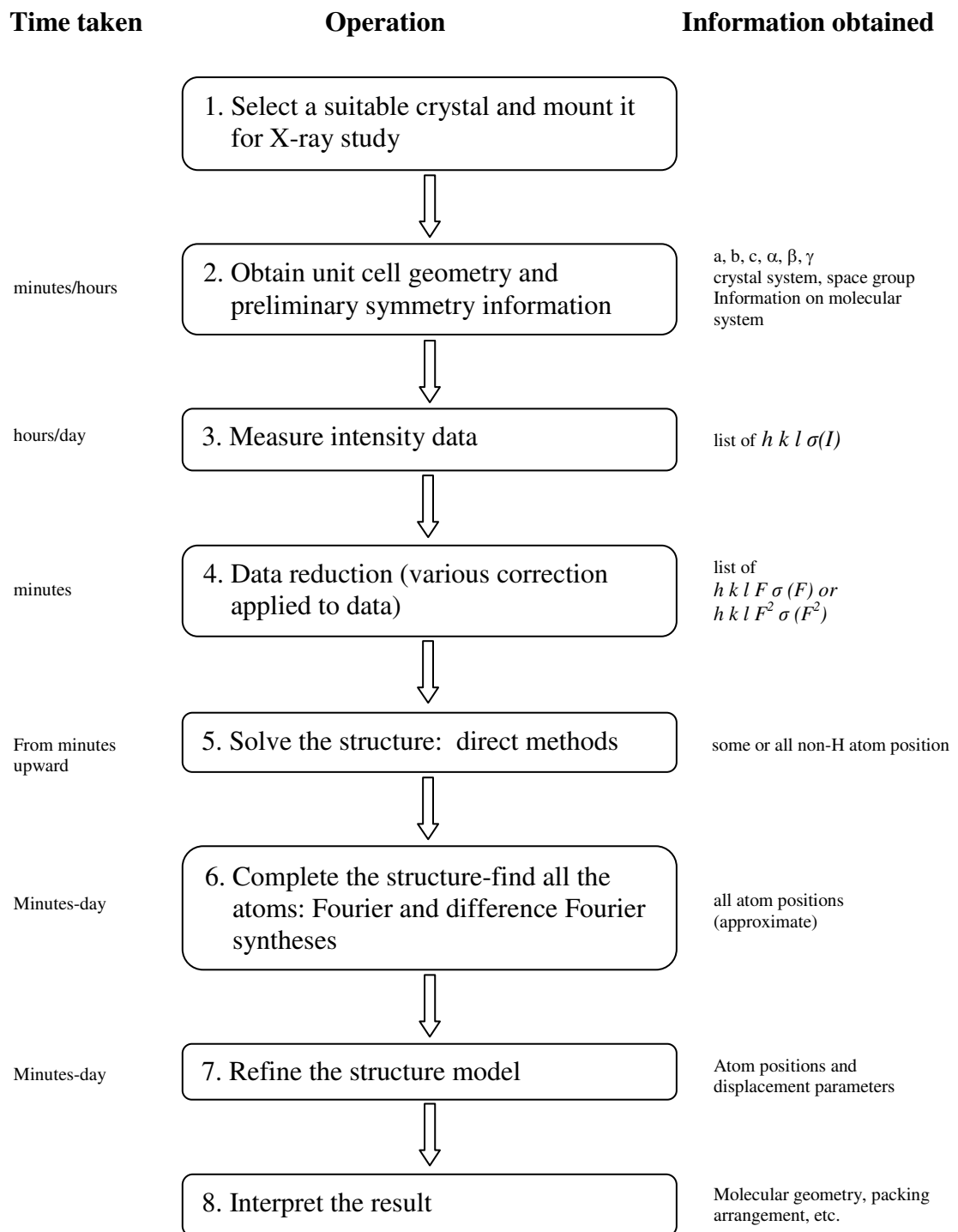


Figure 27 A flowchart for the step involved in a crystal structure determination (Clegg, 1998).

(1) Selection a suitable crystal and mount it.

(1.1) Crystal selection.

If a crystal is to be satisfactory for collecting X-ray diffraction data, two main requirements must be met (Stout and Jensen, 1989);

(1.1.1) Crystal must posses uniform internal structure.

Crystals suitable for x-ray diffraction were selected by examining them under a polarizing microscope. A crystal must be pure at the molecular, ionic, or atomic level. It must be a single crystal in the usual sense, that is, it should not be twinned, grossly fractured, bent, or otherwise physically distorted.

(1.1.2) Crystal must be of proper size.

Scattering intensity is proportional to crystal volume, but X-ray absorption increases exponentially with size and useful sample size is limited by X-ray beam diameter (0.1–0.7 mm for standard laboratory setup). The crystal size for X-ray diffraction is generally preferred in 0.1-0.3 mm.

(1.2) Crystal mounting

Crystal mountings must be rigid enough to hold the sample in a fixed orientation and must minimize the amount of extraneous material that is in the incident and diffracted beam paths. The sample support is usually made from an amorphous material such as glass or plastic that is held in a metal pin and clamped onto a goniometer head. Solid glass fibers may be used. Air stable crystals are usually glued to the end of a glass fiber. In this research, all studied crystal were mounted on the tip of a thin glass fiber using an epoxy glue. (Figure 28a). The crystal should be mounted with its smallest surface attached to the end of the glass fiber to minimize absorption effects and to minimize background scattering from the sample mount. This fiber is attached to a brass mounting pin using modeling clay, and the pin is then inserted into the goniometer head (Figure 28b). The goniometer head and crystal are then affixed to the diffractometer. Samples can be centered by viewing the sample under an attached microscope or video camera and adjusting the X,Y and Z directions

until the sample is centered under the cross-hairs for all crystal orientations (Figure 28c).

It is more difficult to mount air sensitive crystal. There are two main choices of method;

The first method for mildly air unstable compounds, a crystal can be coated with epoxy or an inert viscous material such as Paratone-N oil. These mountings are usually carried out in an inert atmosphere such as a dish filled with argon gas. The crystal is further kept from reacting during data collection by cooling the sample in a chilled, inert (nitrogen) gas stream.

The second method for the very reactive compounds, a crystal must be mounted in a glove bag or glove box. Crystals of these compounds may be mounted using an inert coating on the crystal as described above or may be mounted in glass capillaries. If capillaries are chosen as the sample support, the crystals may be wedged in place or may be held in place by a small amount of (stopcock) grease. Capillary tubes containing unstable compounds must be sealed by melting the ends of the glass tube.

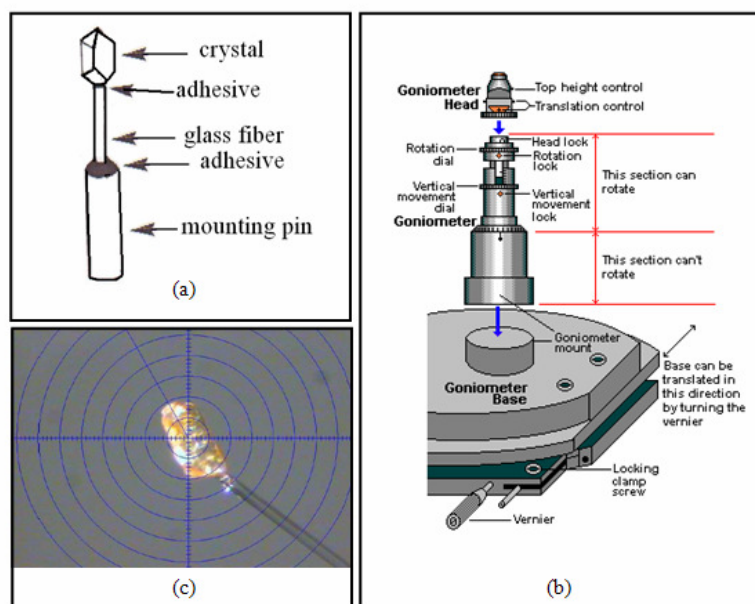


Figure 28 (a) Crystal mounting, (b) the Goniometer base and head and (c) crystal center on cross-hairs.

(2) Obtain unit cell geometry and preliminary symmetry information.

Crystal needs to be rotated in the X-ray beam to observe all the reflections. A photograph or single exposure on an area detector involves a small rotation (a fraction of a degree to several degrees); more gives too much overlap. Bruker SMART APEX CCD diffractometer use a SMART APEX detector, which measures directions and intensities of many reflections simultaneously. Unit cell and crystal orientation are derived by application of Bragg equation (Eq. (1.1)) and related calculations to the directions observed for a set of initially located random reflections. Space group is determined from symmetry of diffraction pattern, ‘systematic absences’ (patterns of reflections with zero intensity caused by certain types of symmetry element), statistical analysis, and other information. Unit cell contents are estimated from cell volume and chemical information, and possibly from measured density.

$$2d \sin \theta = n\lambda \quad (1.1)$$

where n is an integer determined by the order given, λ is the wavelength of the X-ray, d is the spacing between the planes in the atomic lattice, and θ is the angle between the incident ray and the scattering planes.

(3) Measure intensity data

Once the crystal orientation and unit cell are known, all reflections can be assigned indices and their intensities measured from sets of exposures, and the process takes from minutes to hours. For each reflection, the information provided are indices $(h k l)$, intensity (I) and estimate of precision of intensity (standard uncertainty, su, $\sigma(I)$).

(4) Data reduction

Conversion of raw experimental intensities (I) to structure amplitudes ($|F|$). Basically, $I \propto |F|^2$, but some corrections are necessary;

- Geometrical corrections inherent in the diffraction process, including polarization
- Variations in incident X-ray intensity (e.g. synchrotron beam decay) or scattering power of the crystal (decomposition)

- Effects of non-diffraction processes on intensities, especially absorption, which depends on crystal shape, chemical composition and X-ray wavelength
- Merge and average symmetry-equivalent data and deal with discrepancies
- Statistical analysis to indicate certain symmetry elements (especially inversion centre)

(5) Solving the structure

The structure is the Fourier transform of the diffraction pattern, but this can not be directly carried out, because not all the information is available. There are wave amplitudes, but not their relative phases. Two methods of solving this Phase Problem are common.

(a) Patterson method

The Patterson method was used to solve many early crystal structures and is still important in the location of heavy atoms by use of the Patterson function (Patterson 1934). The Patterson function at any point is given by

$$P(r) = \frac{1}{V} \sum_H |F_H|^2 \exp(-2\pi i H \cdot r) \quad (1.2)$$

where r is the position vector and H is the scattering vector.

Peaks in the Patterson synthesis correspond to vectors between pairs of atoms, and vectors between pairs of heavy atoms (many electrons) give the largest peaks. The object is to find a self-consistent set of heavy atom positions that account for the largest Patterson peaks. This locates a significant proportion of the total electron density of the structure.

(b) Direct methods

Direct methods are the preferred method for phasing structure factors produced by small or medium size molecules having up to 1,000 atoms in the

asymmetric unit. However, they are generally not feasible by themselves for larger molecules such as proteins. The direct methods exploit constraints or statistical correlations between the phases of different Fourier components. The atomicity of molecules, and the fact that the electron density should be zero or positive, at any point of the unit cell, creates certain limitations in the distribution of phases associated with the structure factors. Electron density is formed by adding up waves (equal positive and negative parts except for $F(000)$, which is positive everywhere). This imposes considerable restrictions on relationships between phases of strong reflections with related indices, and these relationships are probable sums and differences of phases. Trial phases (usually randomly generated) are assigned to strong phases and the relationships tested to find the most likely set of phases, and phases can also be improved through these relationships. The phases with the best relationships are used to calculate an electron difference map, which is examined for recognizable molecular features.

(6) Complete the structure: find all the atoms

This step is needed if not all the atoms were found in step 5. The atoms known so far are our first model structure. Calculate the diffraction pattern of this model structure (F_c with amplitudes and phases) by Fourier transform. Compare the set of $|F_c|$ with the observed $|F_o|$, define as

$$R = \frac{\sum |F_o| - |F_c|}{\sum |F_o|} \quad (1.3)$$

$$wR2 = \sqrt{\frac{\sum w(F_o^2 - F_c^2)}{\sum w(F_o^2)^2}} \quad (1.4)$$

Where w is a weight for each reflection based on its uncertainty $\sigma(F)$ or $\sigma(F^2)$. R and $wR2$ are known as *R-values*, and are the measures of how well the model agrees with the experimental data. As the model improves, these numbers should decrease.

If we calculate a reverse Fourier transform using $|F_c|$ and ϕ_c , we just regenerate the model structure, but if we use $|F_o|$ (the true amplitudes) and ϕ_c (not the true phases), we obtain a new electron density, which usually contains the atoms of the model structure together with some others. The new atoms are added to the model structure and the process of forward and reverse Fourier transform calculation is repeated until all non-H atoms are located.

If $|F_o|-|F_c|$ is used instead of $|F_o|$ in the reverse Fourier transform, a difference electron density map is obtained, showing only new atoms and not those of the model structure. H atoms are not usually found until all other atoms are located and refined.

(7) Refine the structure model

Vary the numerical parameters describing the structure, to produce the best agreement between its calculated diffraction pattern (F_c) and the observed pattern (F_o). Only amplitudes can be compared, as there are no observed phases.

The refinement process uses a well-established mathematical procedure called least-squares analysis, which minimizing the sum of squares of differences between observed and calculated values; $\sum w(|F_o|-|F_c|)^2$.

Numerical parameters of the model structure:

- 3 coordinates (x, y, z) for each atom.
- 1 (isotropic) or 6 (anisotropic) displacement (vibration) parameters for each atom.
- An overall scale factor and a few other possible parameters in some cases.

Each parameter is obtained as a value with a ‘standard uncertainty’ (su), describing its precision and reliability. A large excess of data over parameters is essential (often >10:1).

H atoms contribute little to X-ray diffraction and often need to be constrained, for example, by fixing bond lengths and angles, even when they are located in difference electron density maps.

After refinement, a final difference map (with phases from the refined model structure) should contain no significant peaks or holes. Typically, $R < 0.05$ and may be as low as 0.01–0.02.

(8) Interpret the results

Primary result: 3D electron density distribution, but usually described by an atomic model; chemical bonds are deduced from distances and angles, not directly observed.

From refinement:

- Unit cell geometry and space group
- Positions of atoms
- Displacement parameters for atoms
- All with standard uncertainties

Derived results:

- Bond lengths and other distances
- Bond angles
- Torsion angles
- Shapes and conformations (rings, chains)
- Planarity of groups of atoms
- Degree of association of molecules
- Intermolecular geometry and interactions

Graphical representations:

- Ball and stick (arbitrary atomic radii)
- Space-filling (van der Waals radii)
- Ellipsoids representing atomic displacements
- Packing diagrams (intermolecular arrangement)
- Polyhedral representations for ionic and network structures
- Ribbons and other non-atom representations for protein structures

CHAPTER 3

Results

3.1 The studies for preparation of complexes

Reaction of copper(I) halides with the phosphine ligand, triphenylphosphine and some heterocyclic thiones in methanol or acetonitrile solvent afforded crystalline solids. The complexes have been characterized using elemental analysis, IR, ¹H and ¹³C NMR spectroscopies and single crystal x-ray crystallography. Moreover, some of their physical properties together with reacting ligands are summarized in Table 2.

Table 1 Preparation conditions of complexes.

Reactants	Mole ratio	Solvent	Temp * (°C)	Complexes
CuCl:PPh ₃ : TBA	1 : 2 : 1	acetonitrile	70	[CuCl(PPh ₃) ₂ (TBA)]
CuI:PPh ₃ : TBA	1: 2 : 1	acetonitrile	40	[CuI(PPh ₃) ₂ (CH ₃ CN)]
CuCl:PPh ₃ : dmpymtH	1 : 2 : 1	mehanol	60	[CuCl(PPh ₃) ₂ (dmpymtH)]
CuBr:PPh ₃ : dmpymtH	1 : 2 : 1	mehanol	60	[CuBr(PPh ₃) ₂ (dmpymtH)]
CuI:PPh ₃ : dmpymtH	1 : 2 : 1	mehanol	60	[CuI(PPh ₃) ₂ (dmpymtH)]

*Temp = temperature

Table 2 The physical properties of ligands and complexes.

Compound	Physical properties			
	Appearance	Colour	Melting point (°C)	Solubility
Ligand TBA	Powder	White	245	x
Ligand dmpymtH	Powder	Yellow	213-216	x
Ligand PPh ₃	Powder	White	79-81	xx
[CuCl(PPh ₃) ₂ (TBA)]	cubic	Pink	179-180	xxx
[CuI(PPh ₃) ₂ (CH ₃ CN)]	Needle	Colourless	181-182	xxx
[CuCl(PPh ₃) ₂ (dmpymtH)]	Needle	Yellow	200-202	xxx
[CuBr(PPh ₃) ₂ (dmpymtH)]	Needle	Yellow	202-204	xxx
[CuI(PPh ₃) ₂ (dmpymtH)]	Needle	Yellow	196-198	xxx

soluble^x = soluble in ethanol and acetone

soluble^{xx} = soluble in ethanol, acetone and water

soluble^{xxx} = soluble in chloroform , DMSO and acetone

3.2 Elemental analysis

Table 3 The partial elemental analyses of the complexes.

Compound	%C Found (Calcd.)	%H Found (Calcd.)	%N Found (Calcd.)	%S Found (Calcd.)	%O Found (Calcd.)
[CuCl(PPh ₃) ₂ (TBA)]·H ₂ O	60.44(0.16) 61.14	4.53(0.10) 4.59	3.71(0.58) 3.57	4.28(0.48) 4.07	5.28(1.02) 6.11
[CuCl(PPh ₃) ₂ (dmpymtH)]	65.20(0.13) 66.11	4.93(0.21) 4.89	3.67(0.58) 3.67	4.31(0.85) 4.21	-
[CuBr(PPh ₃) ₂ (dmpymtH)]	62.38(0.12) 62.47	4.70(0.22) 4.62	2.66(1.25) 3.47	3.01(0.85) 3.98	-
[CuI(PPh ₃) ₂ (dmpymtH)]	60.11(0.77) 59.03	4.46(0.91) 4.37	2.88(0.99) 3.28	3.22(0.54) 3.76	-

3.3 X-ray fluorescence spectrometry

The X-ray fluorescence spectra of the complexes are shown in Figures 29-38.

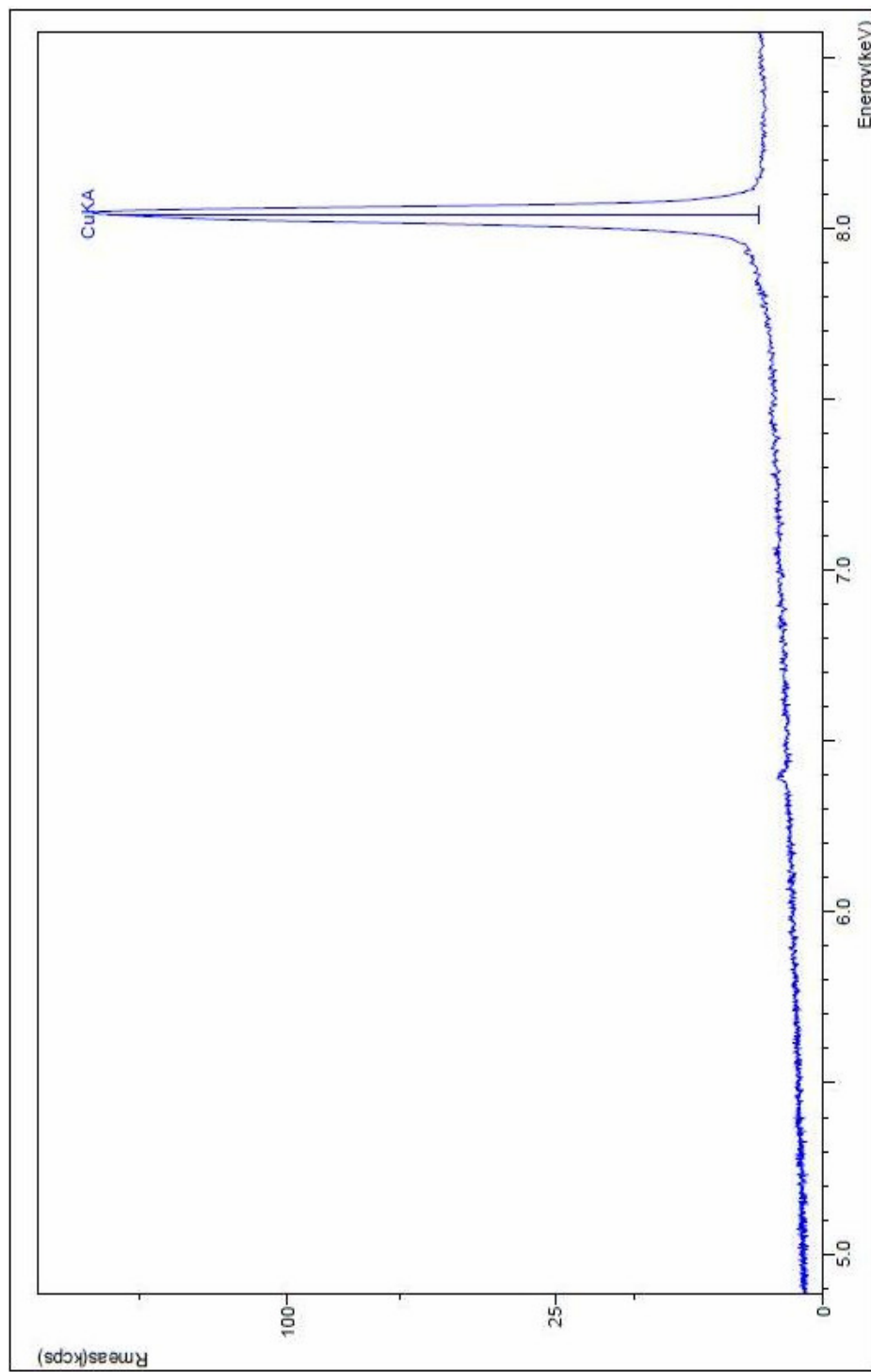


Figure 29 The Cu (K_{α}) spectrum of $[\text{CuCl}(\text{PPh}_3)_2(\text{TBA})]\cdot\text{H}_2\text{O}$ (1).

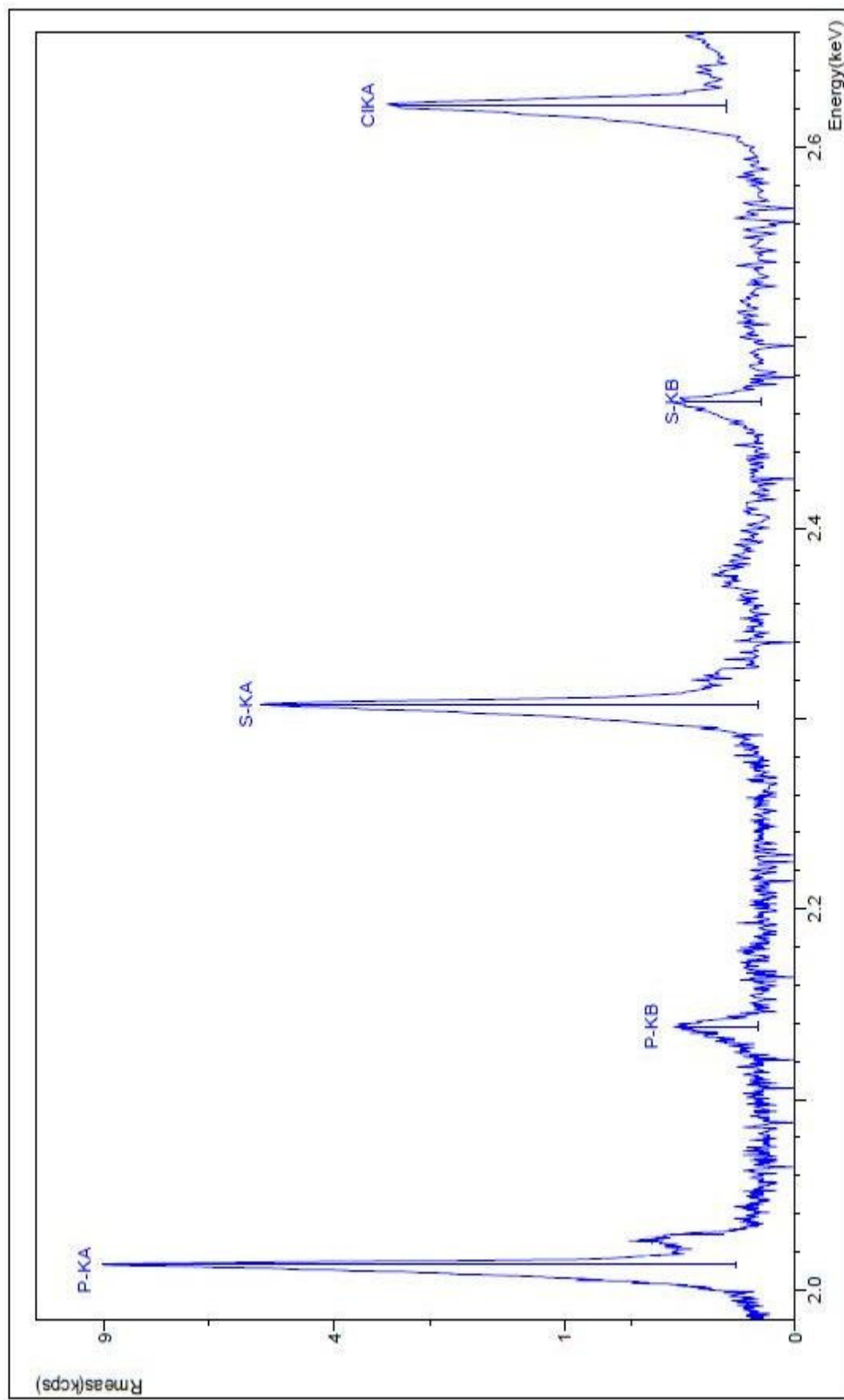


Figure 30 The $S(K_\alpha)$, $S(K_\beta)$, $P(K_\alpha)$, $P(K_\beta)$ and $Cl(K_\alpha)$ spectrum of $[CuCl(PPh_3)_2(TBA)] \cdot H_2O$ (1).

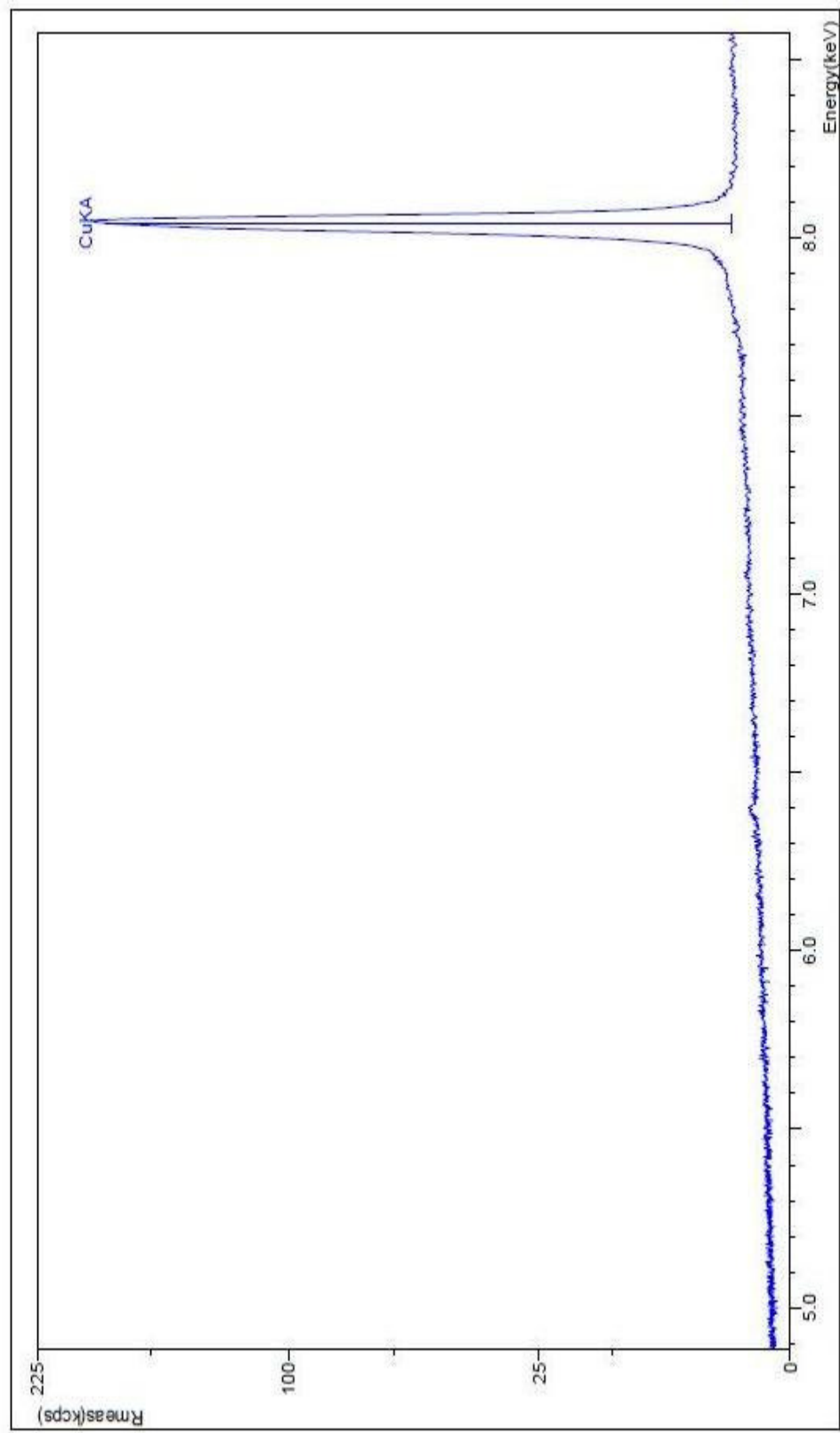


Figure 31 The Cu(K α) spectrum of [CuCl(PPh₃)₂(dmpymtH)] (3).

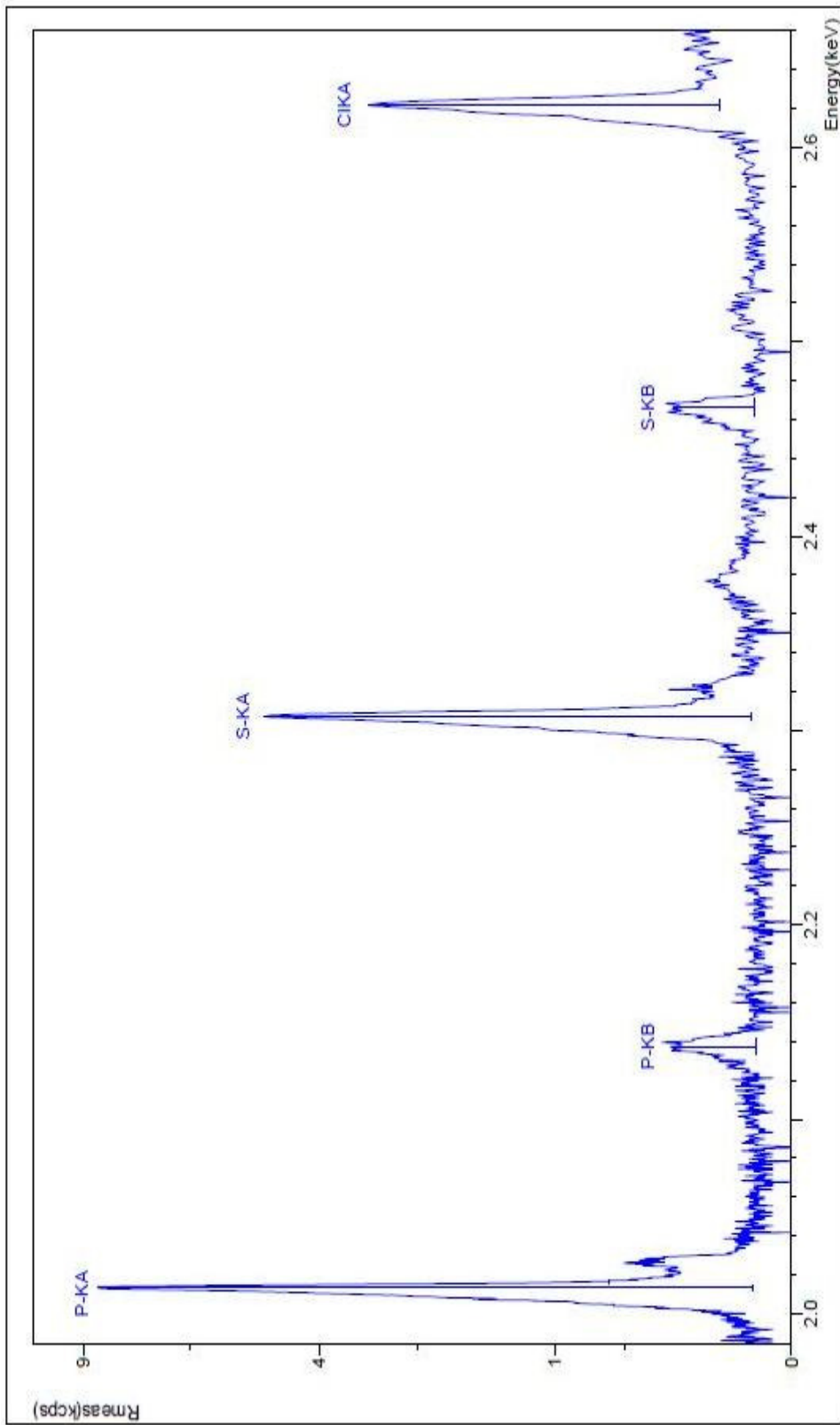


Figure 32 The $S(K_\alpha)$, $S(K_\beta)$, $P(K_\alpha)$, $P(K_\beta)$ and $Cl(K_\alpha)$ spectrum of $[CuCl(PPh_3)_2(dmpydtH)]$ (3).

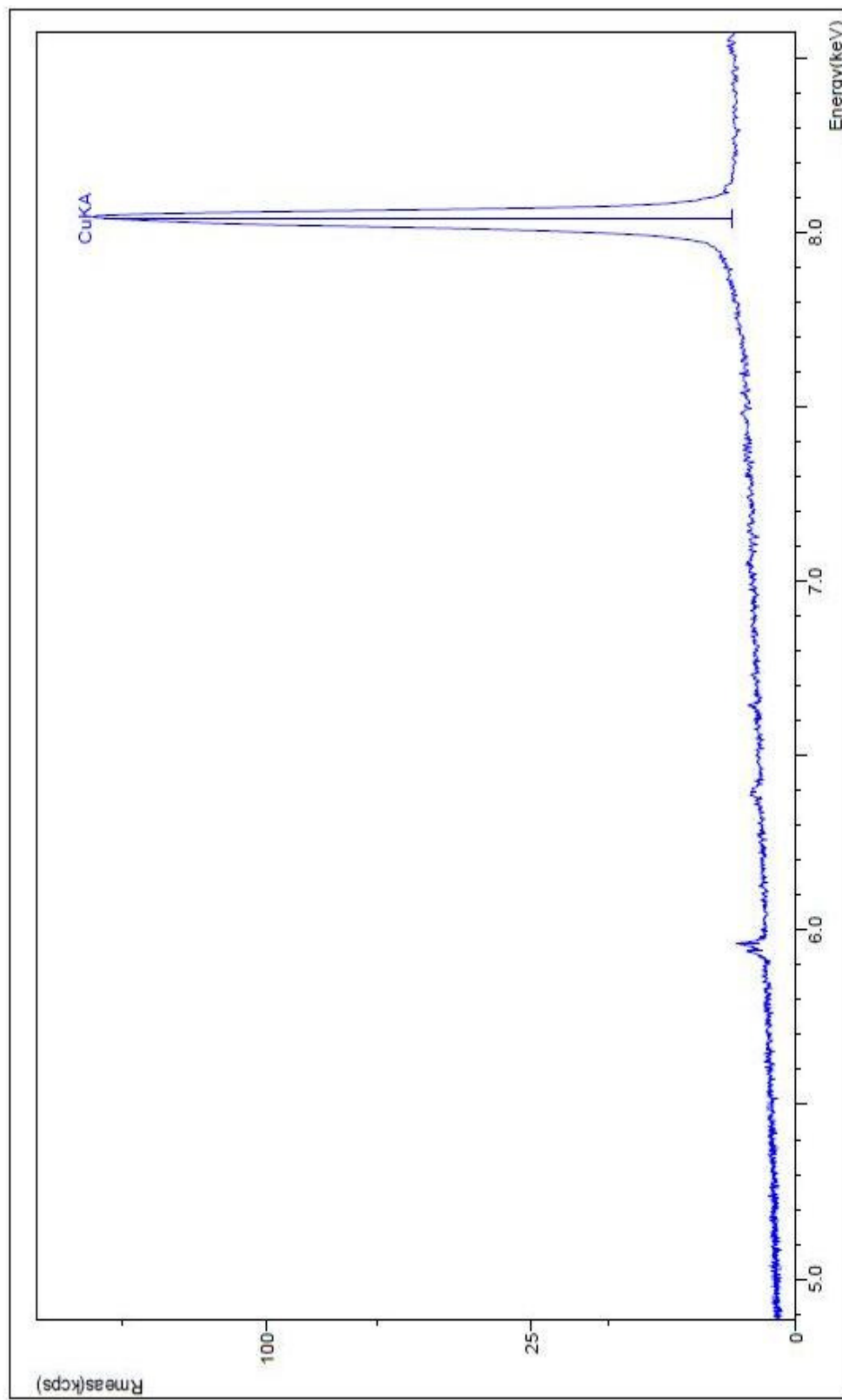


Figure 33 The Cu(K α) spectrum of [CuBr(PPh₃)₂(dmpydtH)] (4).

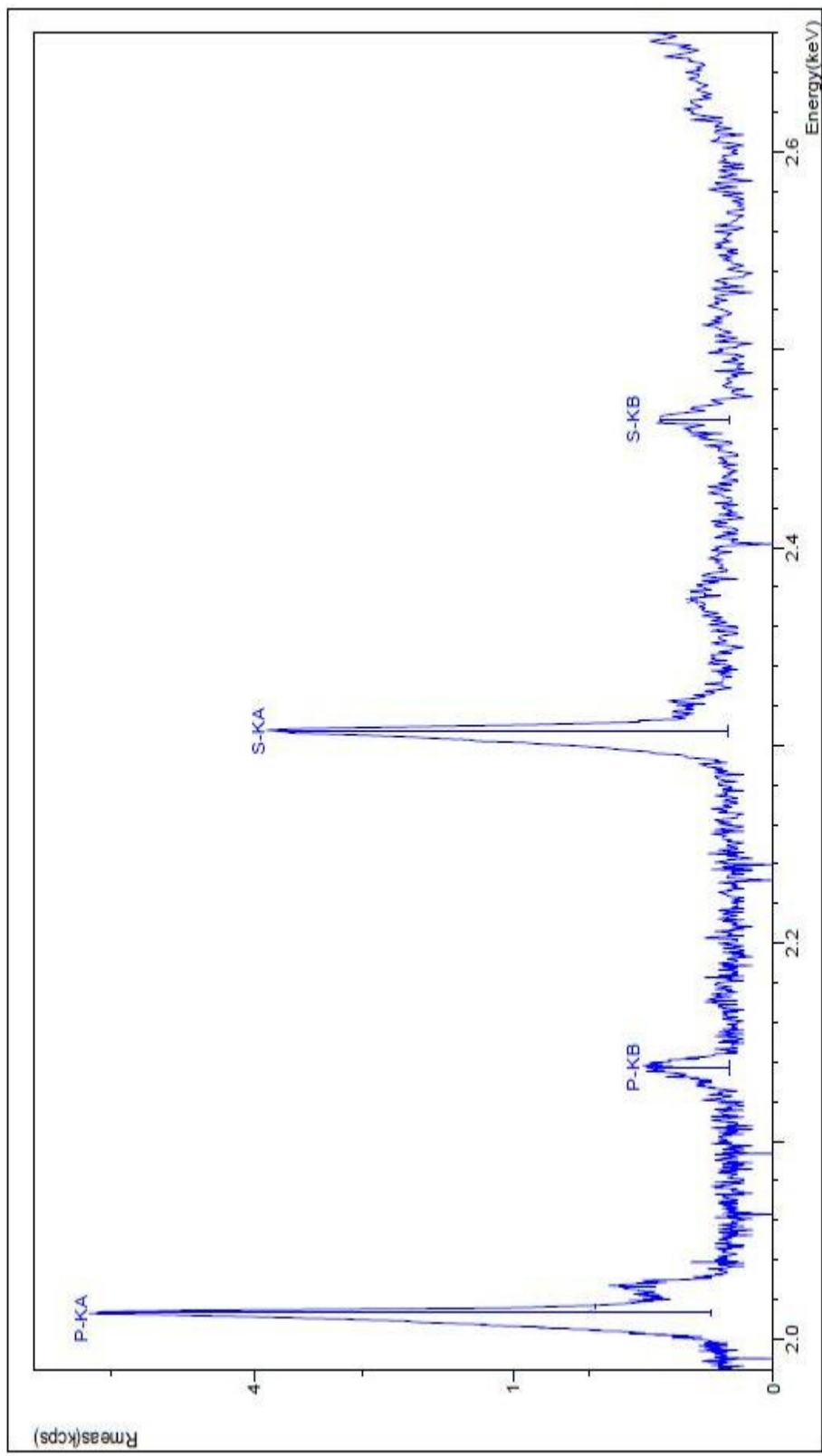


Figure 34 The $S(K_\alpha)$, $S(K_\beta)$, $P(K_\alpha)_\alpha$ and $P(K_\beta)_\beta$ spectrum of $[\text{CuBr}(\text{PPh}_3)_2(\text{dmpymth})](4)$.

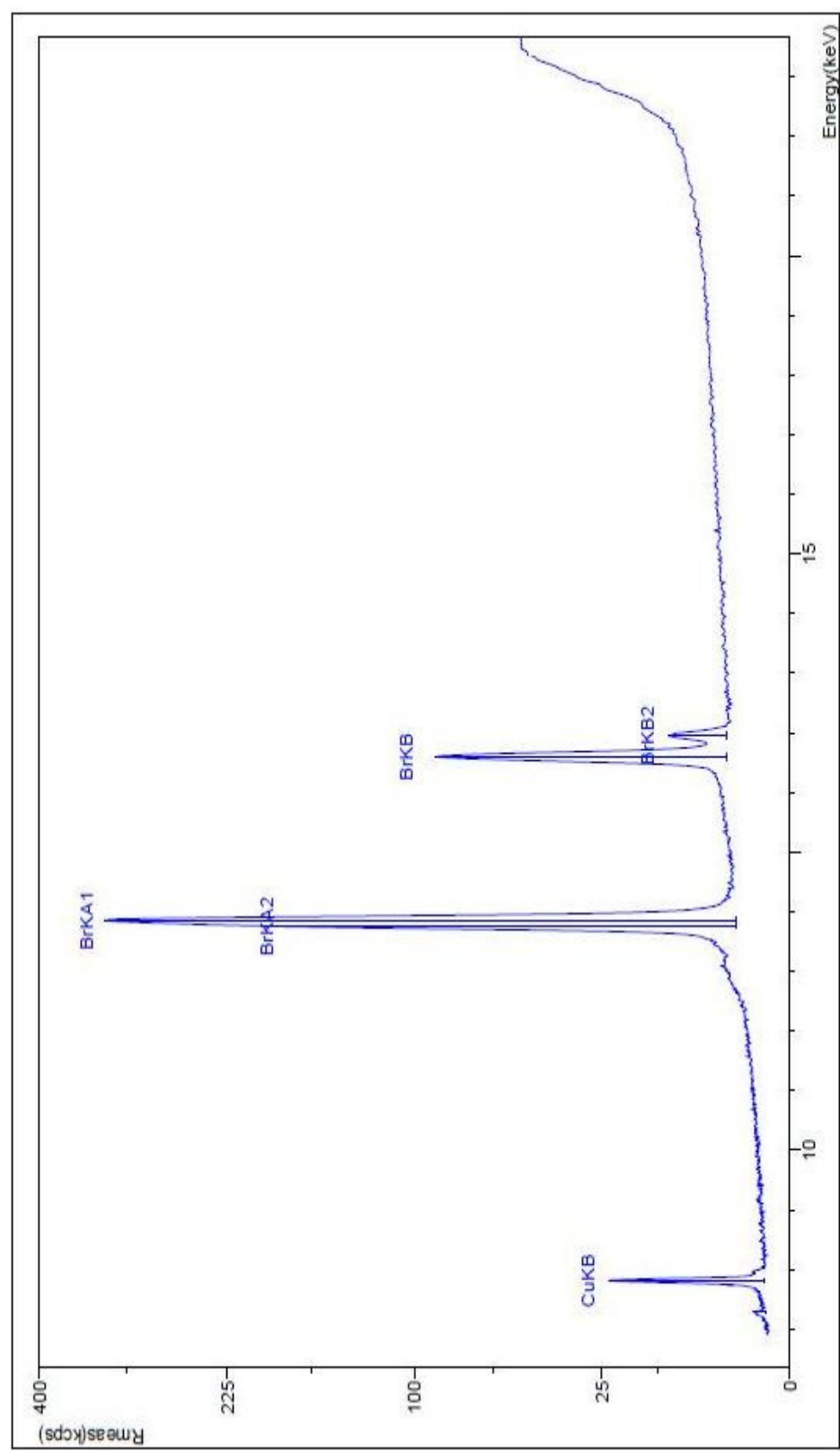


Figure 35 The $\text{Br}(K_\alpha)$ and $\text{Br}(K_\beta)$ spectrum of $[\text{CuBr}(\text{PPh}_3)_2(\text{dmpy})\text{H}]$ (4).

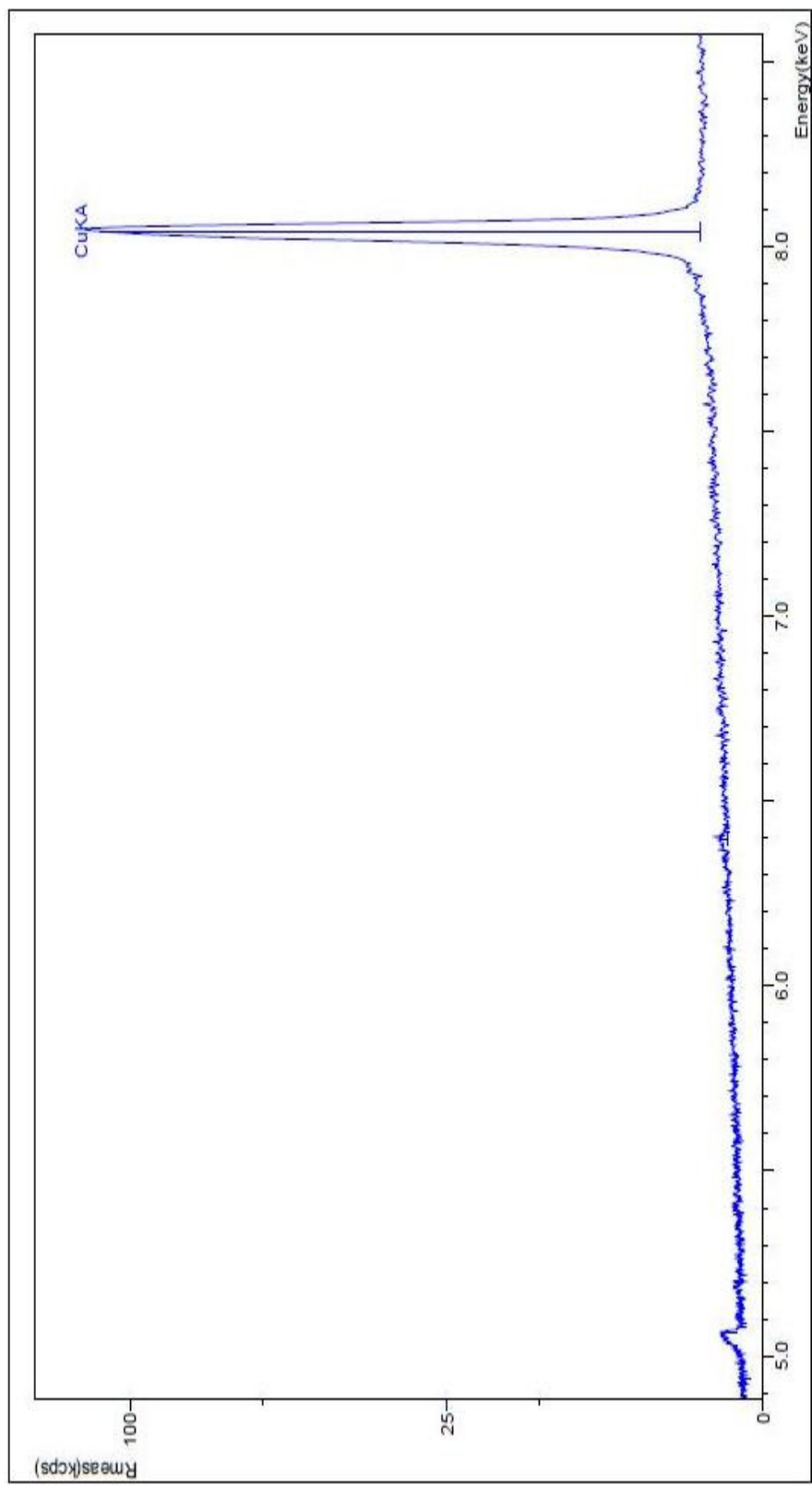


Figure 36 The Cu(K_{α}) spectrum of $[\text{CuI}(\text{PPh}_3)_2(\text{dmppymH})]$ (5).

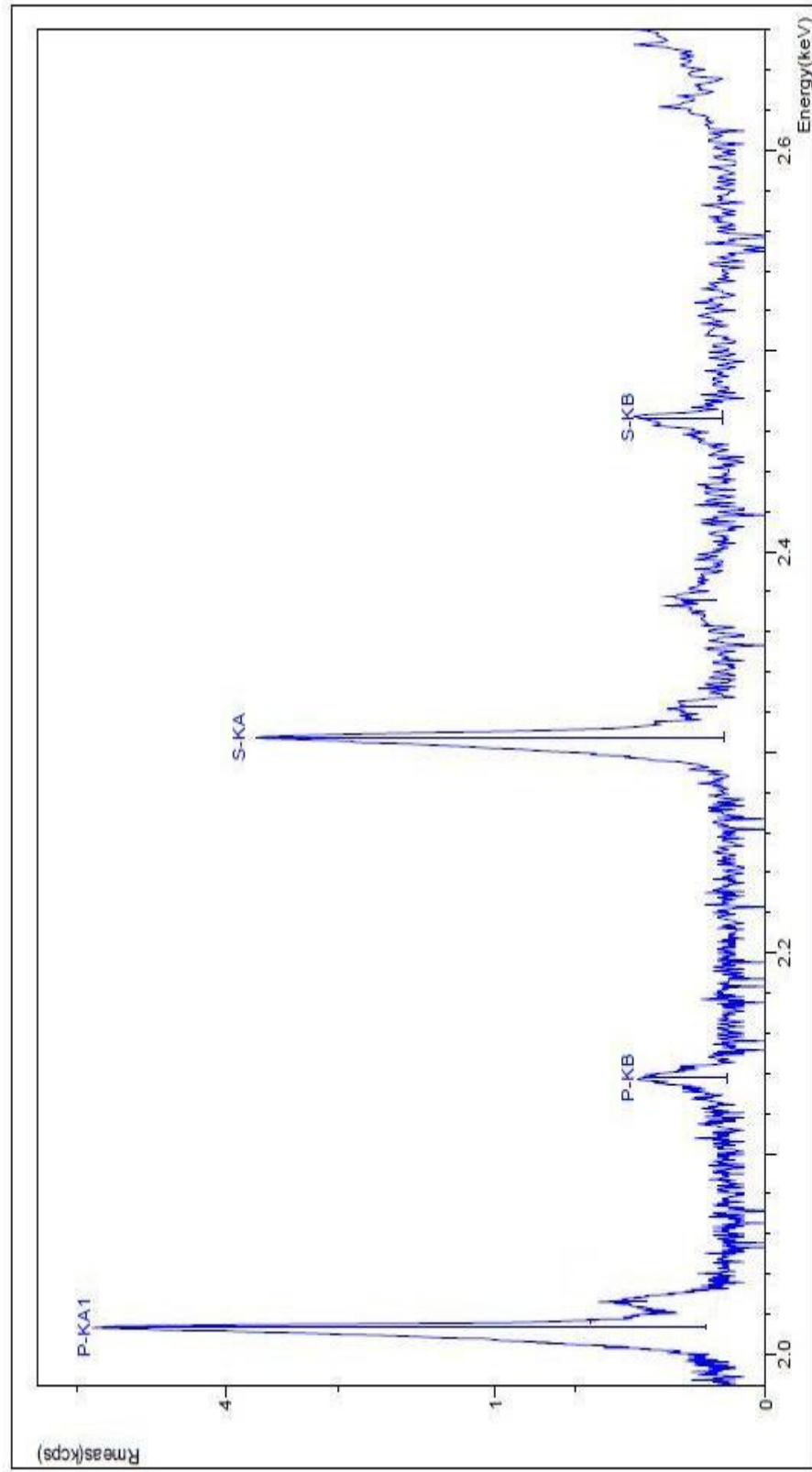


Figure 37 The $S(K_\alpha)$, $S(K_\beta)$, $P(K_\alpha)_\alpha$ and $P(K_\beta)$ spectrum of $[\text{CuI}(\text{PPh}_3)_2(\text{dmpymtH})]$ (5).

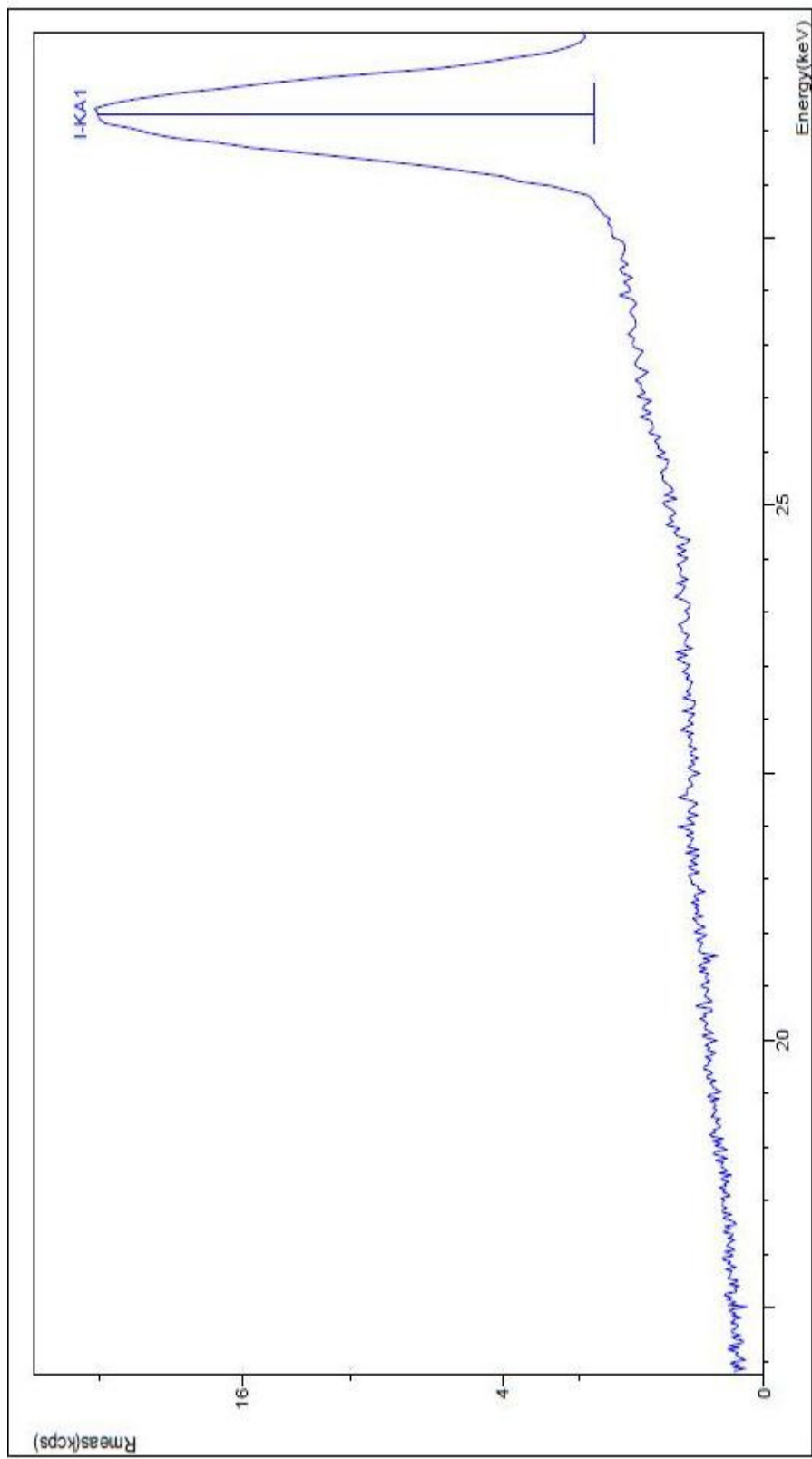


Figure 38 The I(K_{α}) spectrum of $[\text{CuI}(\text{PPh}_3)_2(\text{dmpymtH})]$ (5).

3.4 Infrared spectroscopy

The infrared spectrum of the ligands and compounds are shown in Figure 39-45.

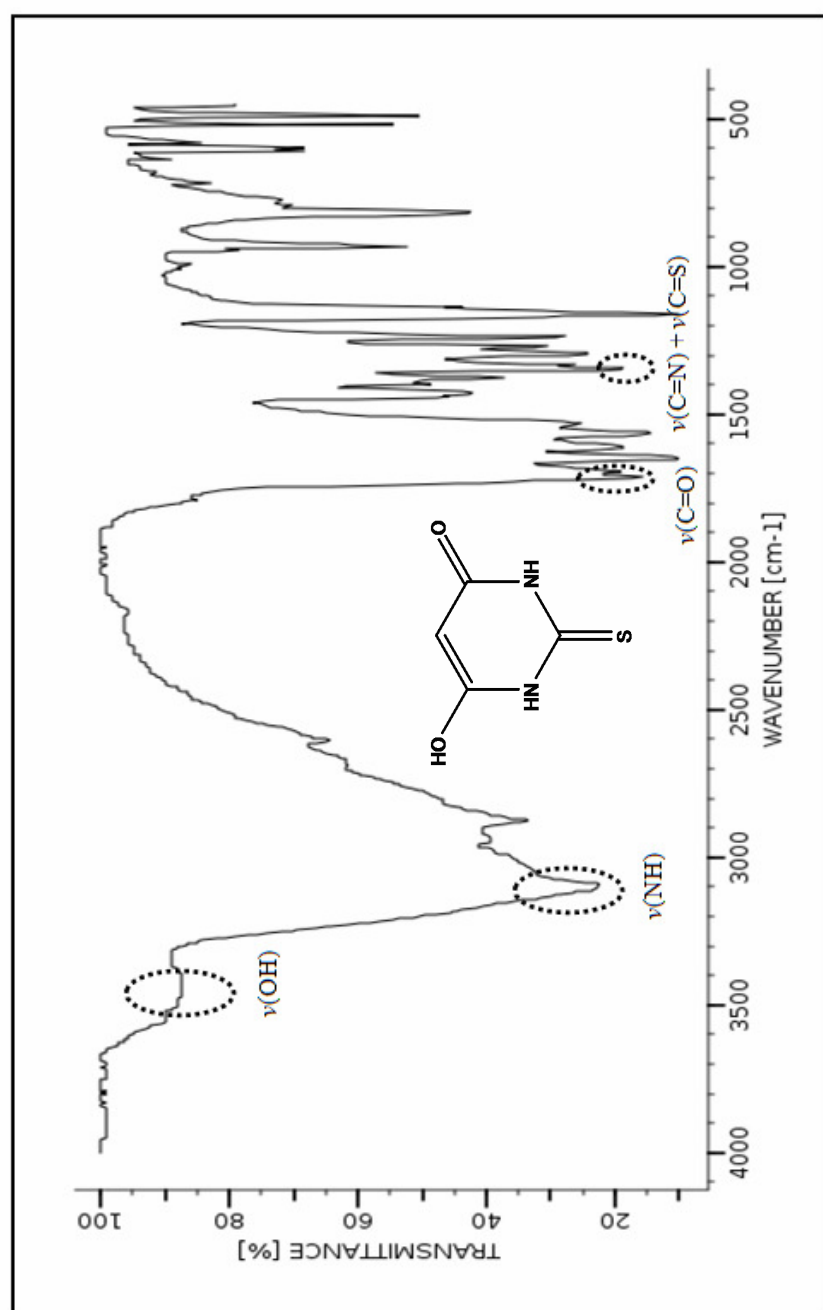


Figure 39 The infrared spectrum of 2-thiobarbituric acid (TBA).

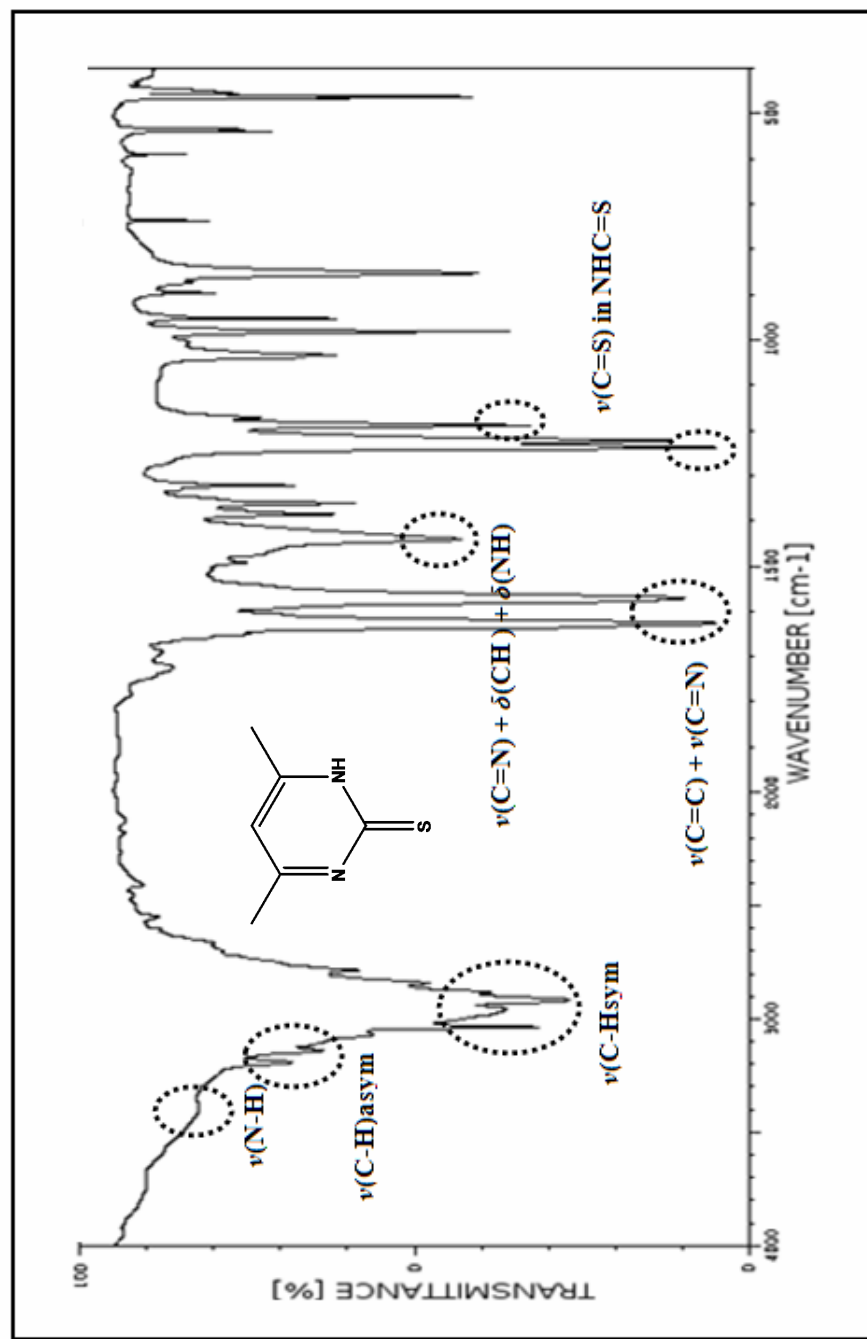


Figure 40 The infrared spectrum of dimethylpyrimidine-2(1H)-thione (dmpytmH).

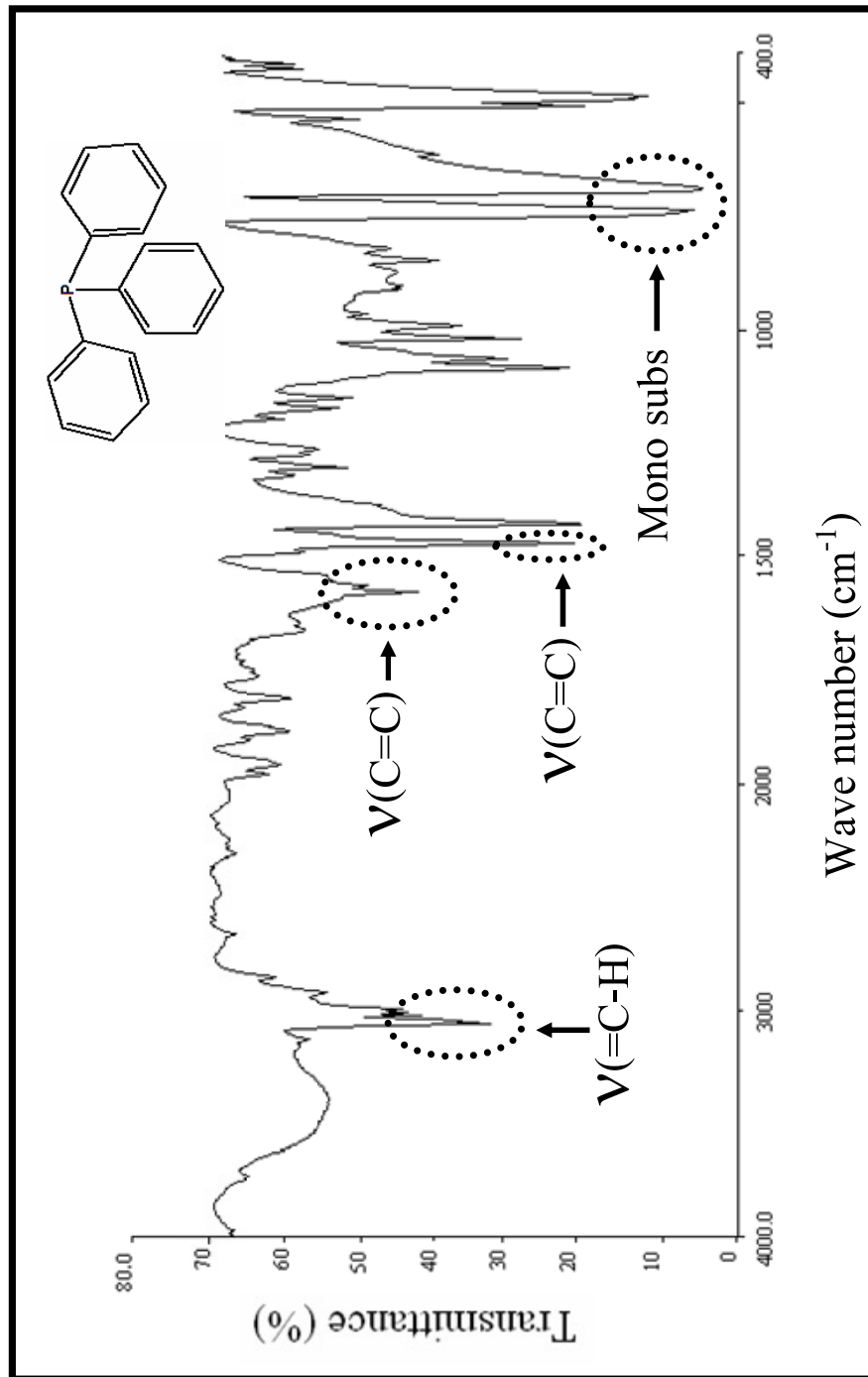


Figure 41 The infrared spectrum of Triphenylphosphine (PPh_3).

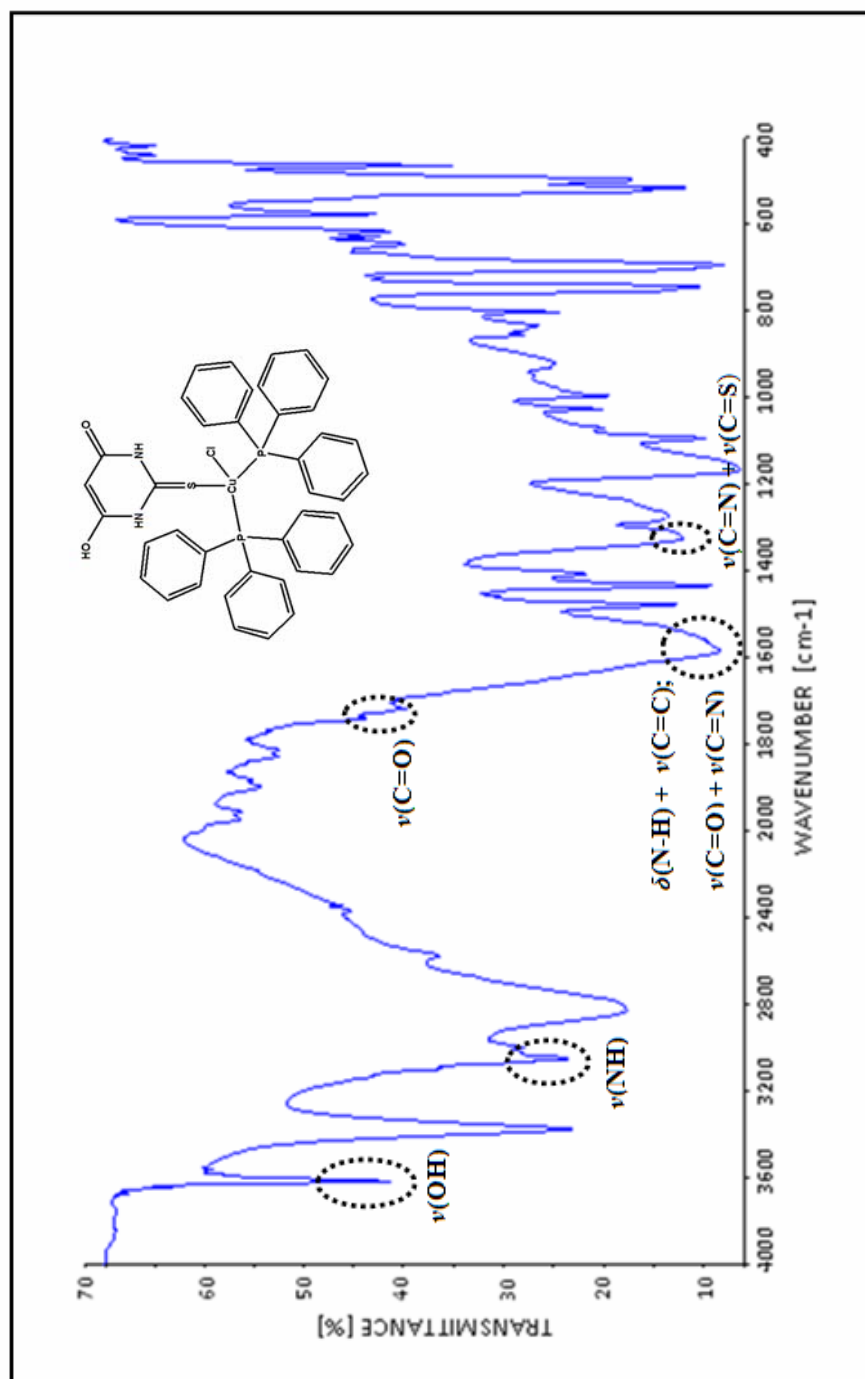


Figure 42 The infrared spectrum of $[\text{CuCl}(\text{PPh}_3)_3(\text{TBA})]\cdot\text{H}_2\text{O}$ (1).

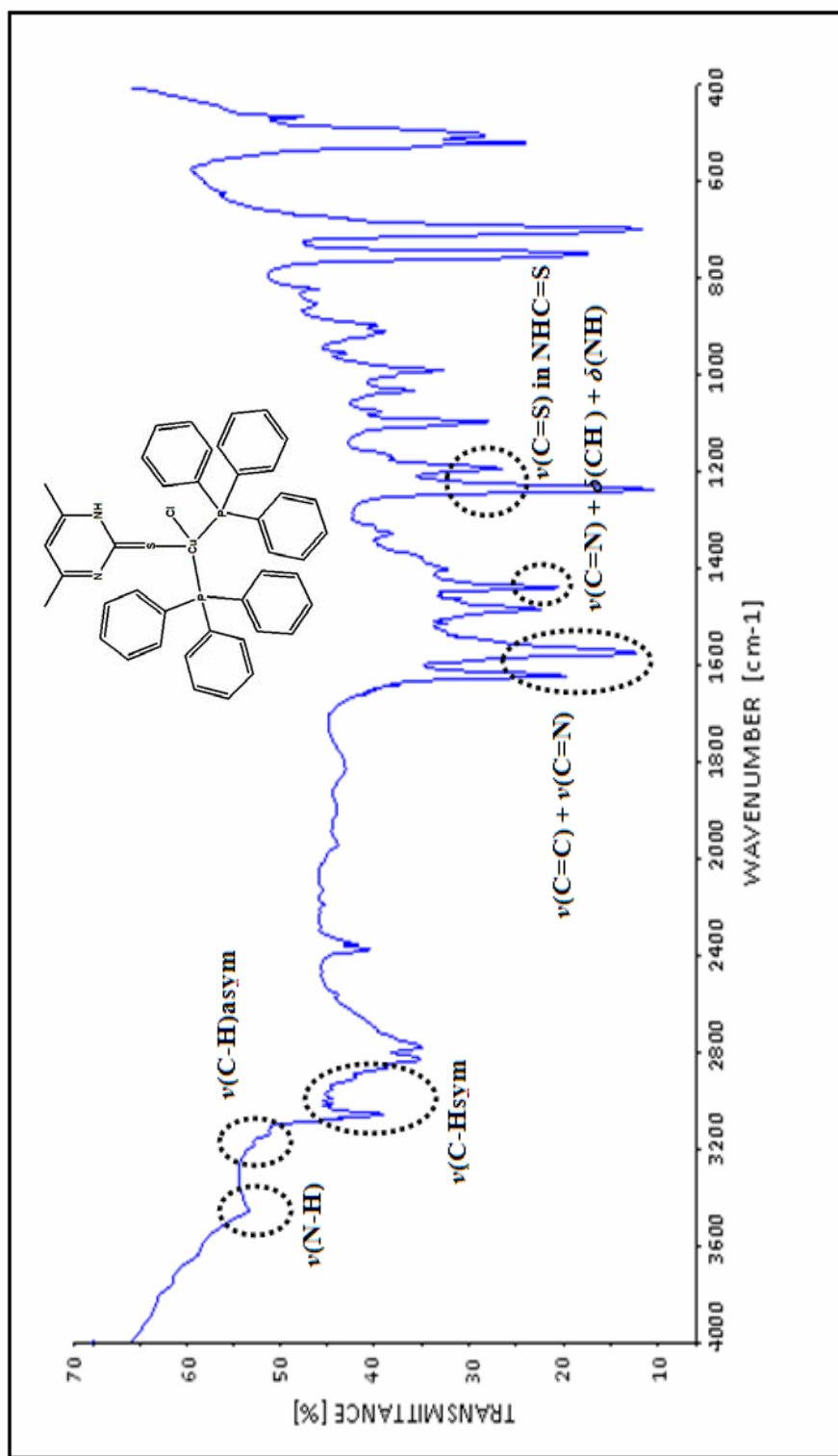


Figure 43 The infrared spectrum of $[\text{CuCl}(\text{PPh}_3)_3(\text{dmpytmH})]$ (3).

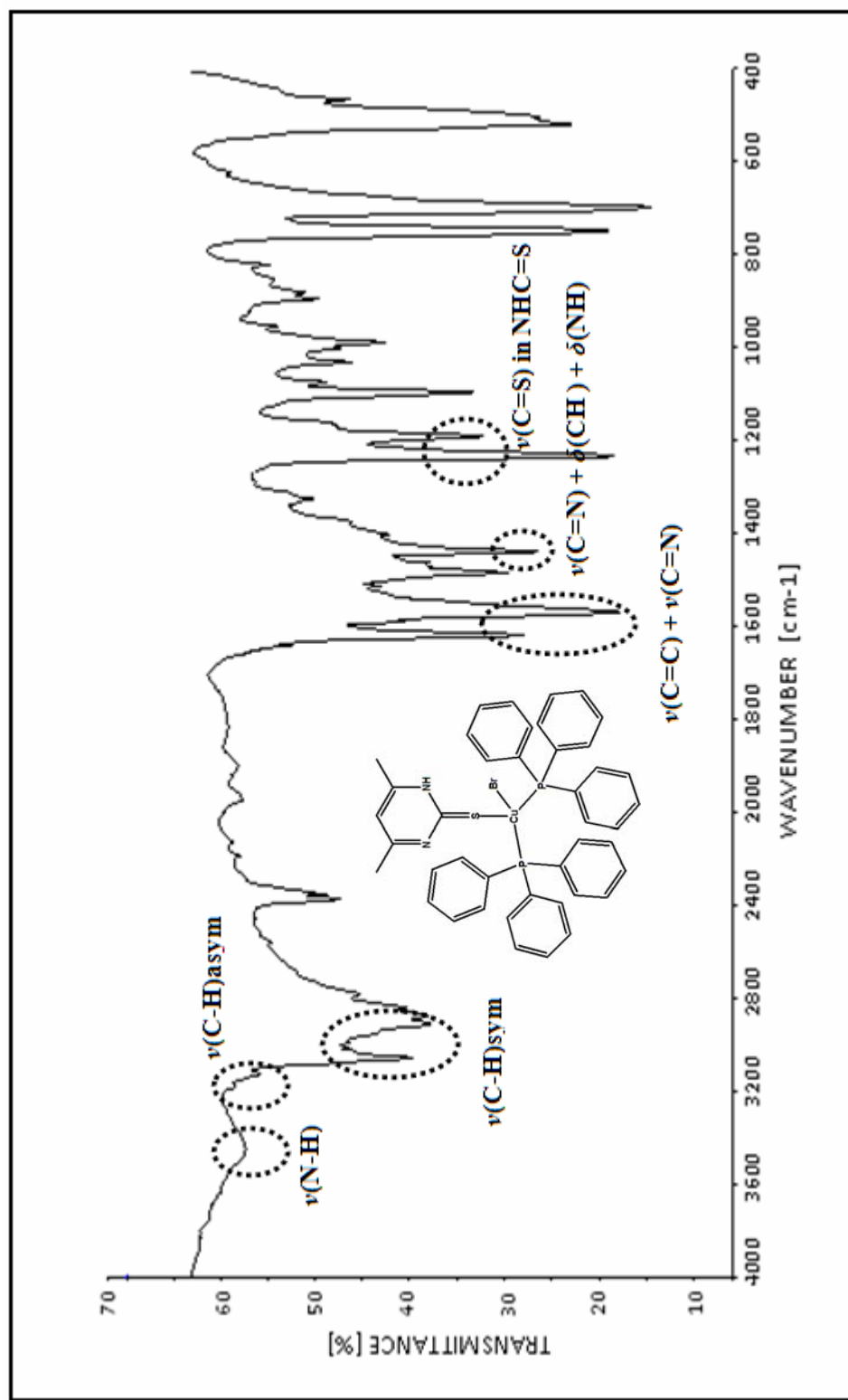


Figure 44 The infrared spectrum of $[\text{CuBr}(\text{PPh}_3)_3(\text{dmpymtH})]$ (4).

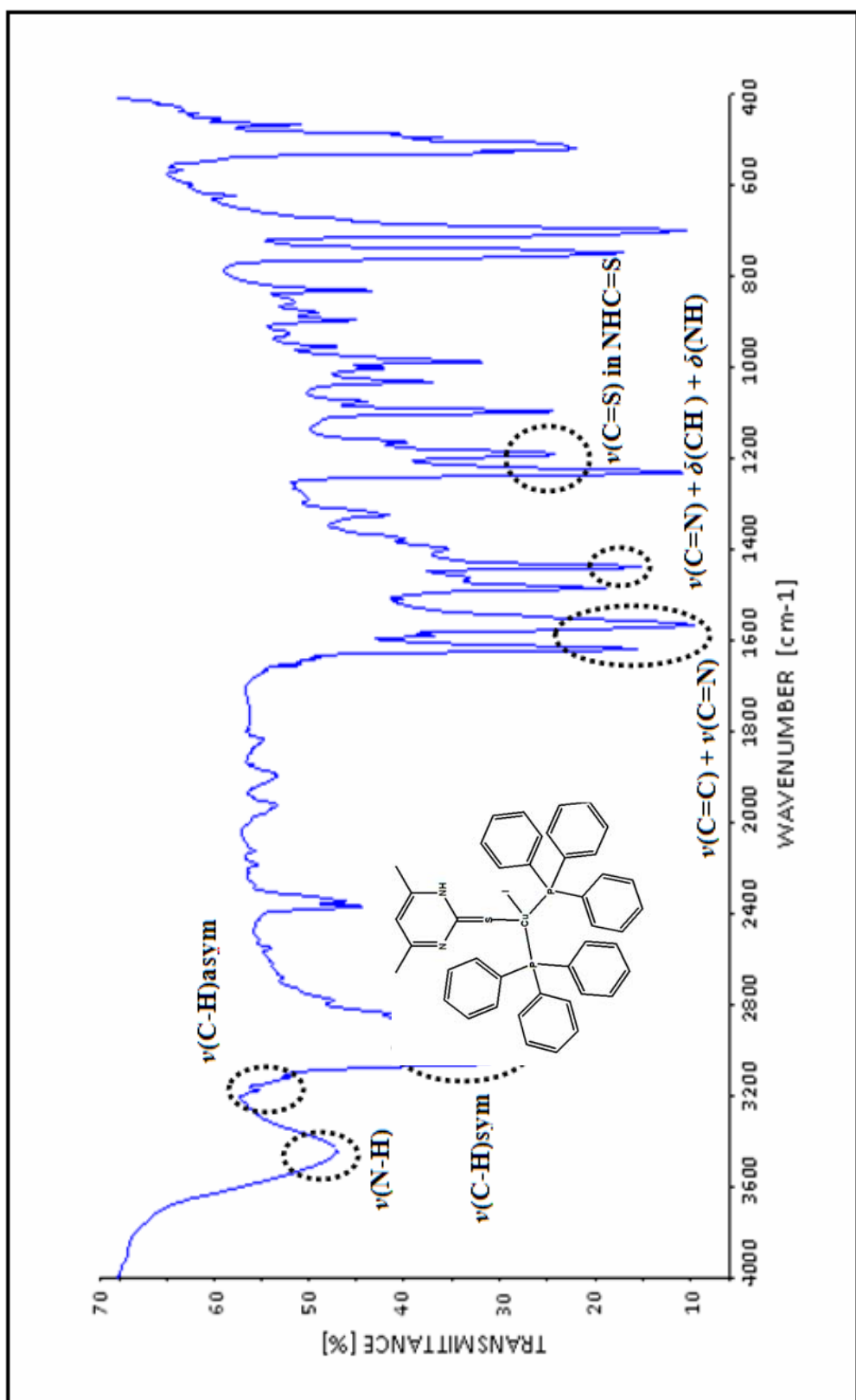


Figure 45 The infrared spectrum of $[\text{Cu}(\text{PPh}_3)_3(\text{dmpymtH})]$ (5).

3.5 ^1H NMR and ^{13}C NMR spectroscopy

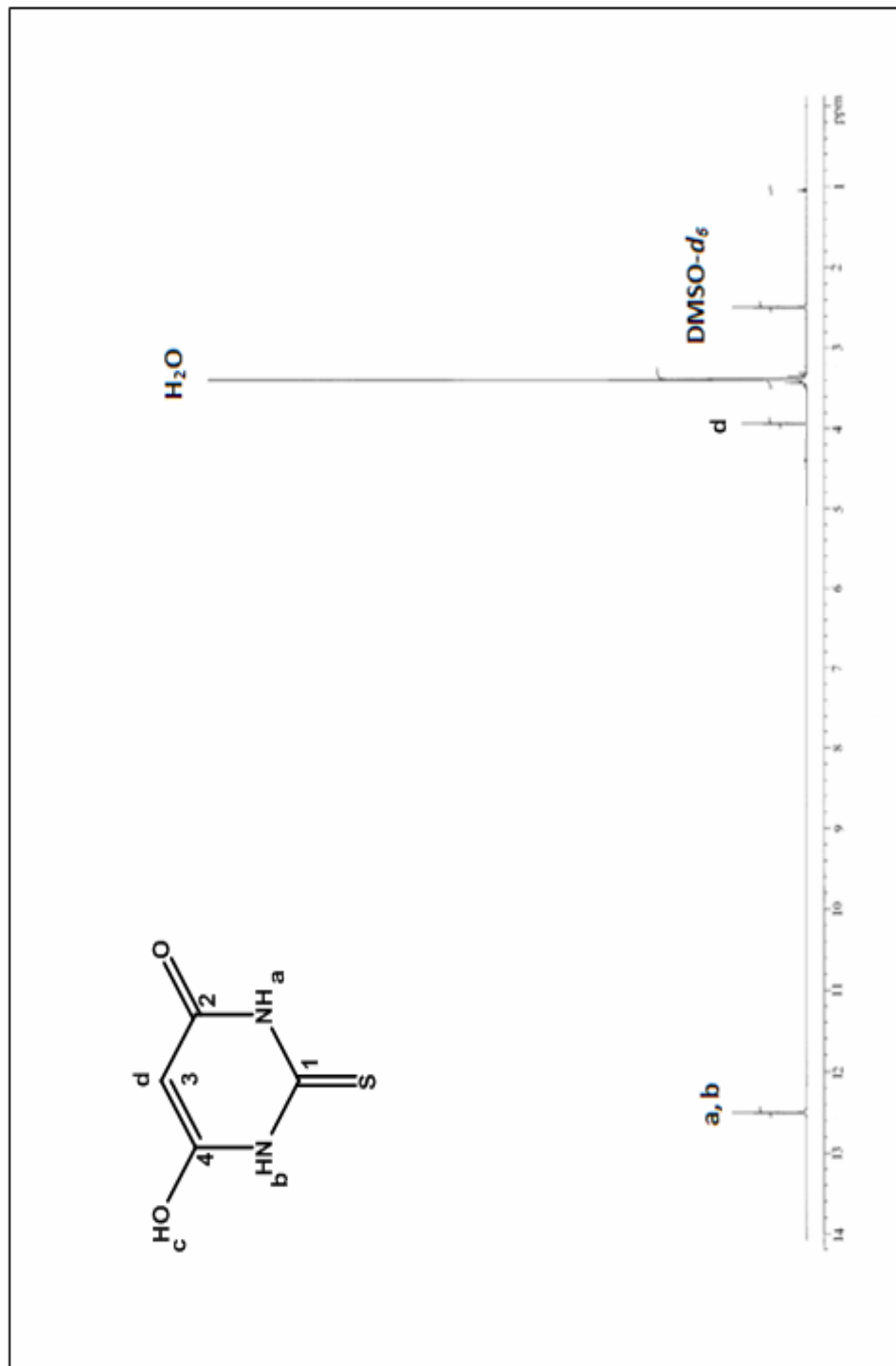


Figure 46 ^1H NMR spectrum of TBA.

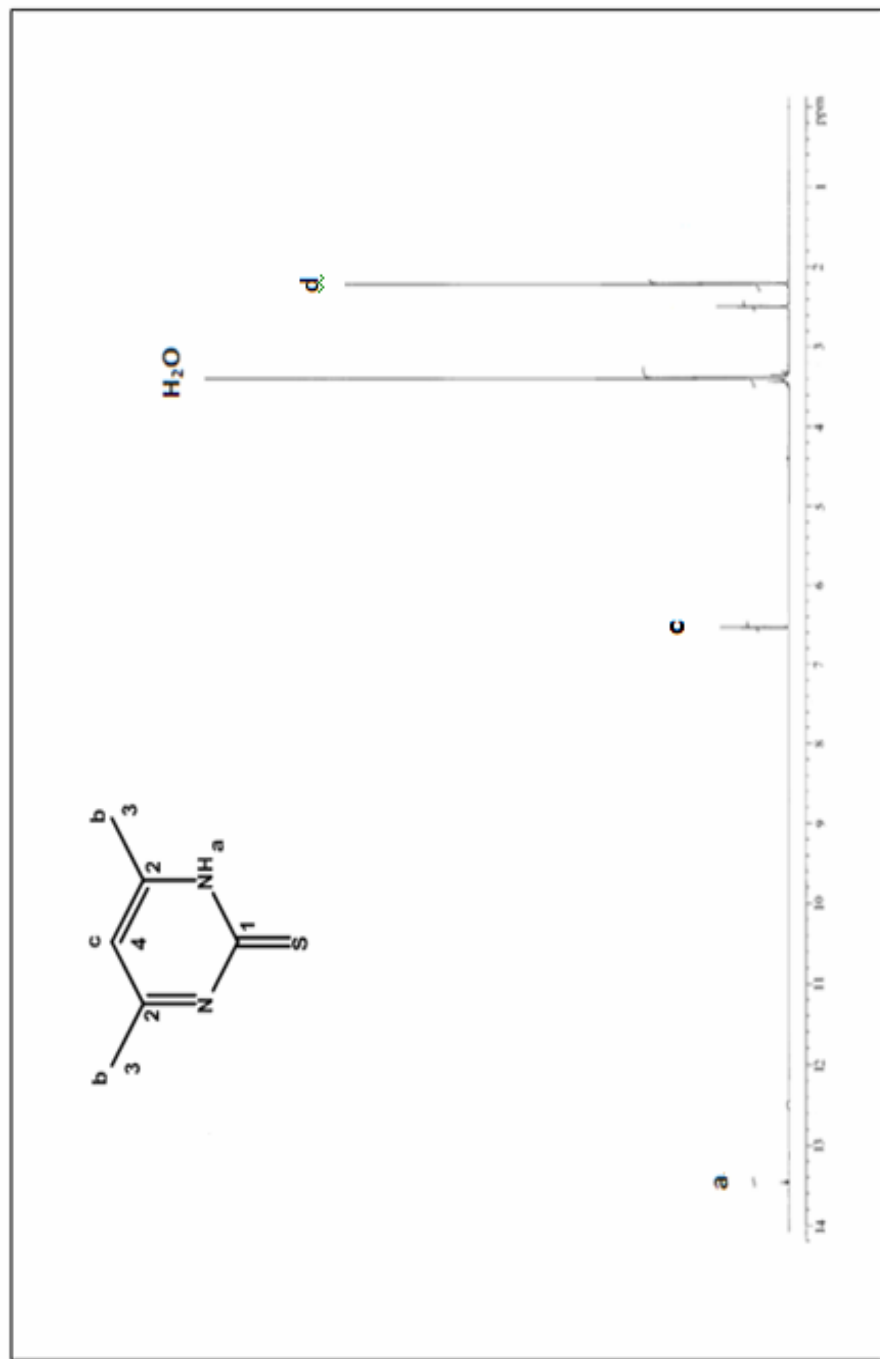


Figure 47 ^1H NMR spectrum of dmpytmH.

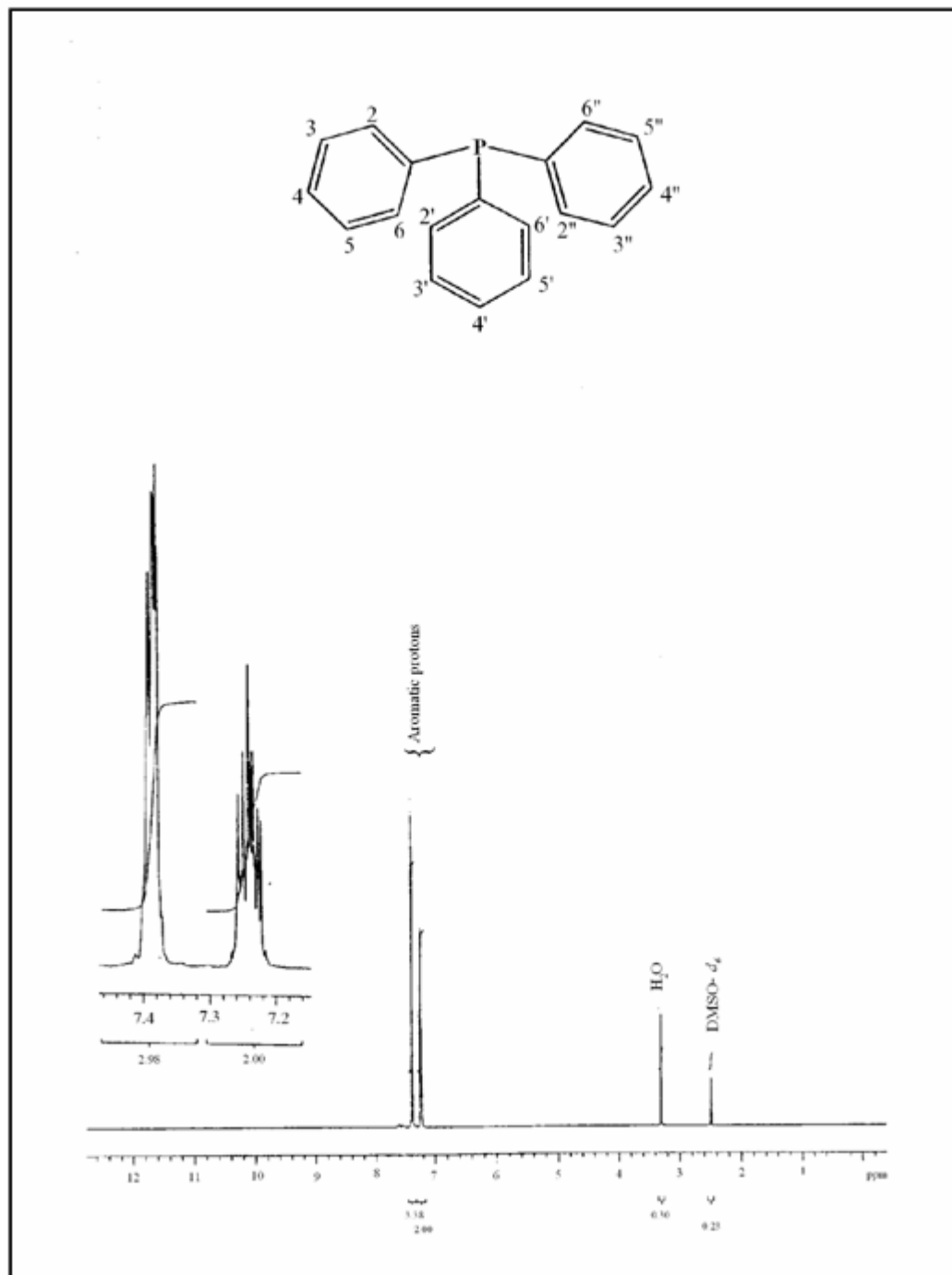


Figure 48 ^1H NMR spectrum of triphenylphosphine (PPh_3).

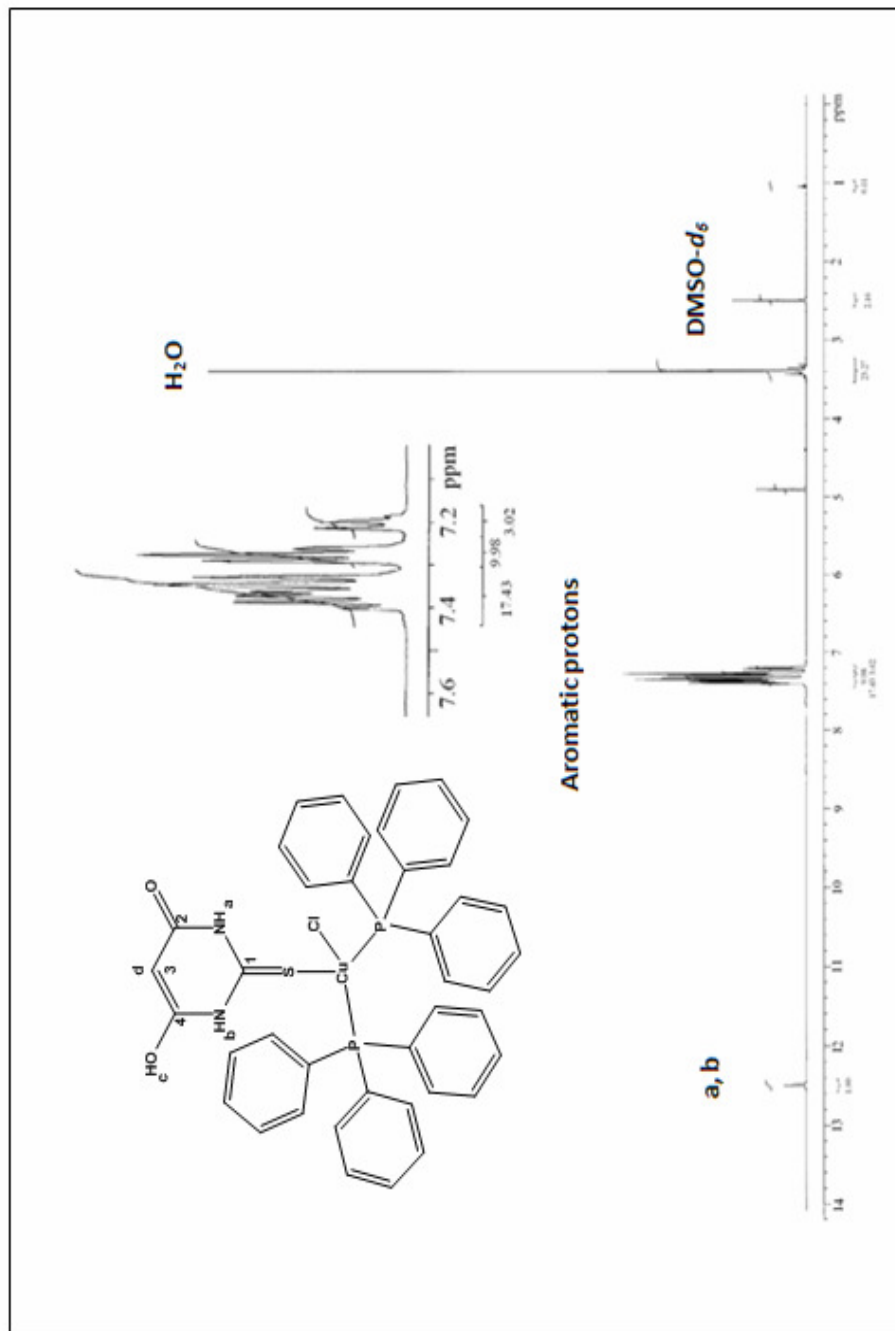


Figure 49 ¹H NMR spectrum of $[\text{CuCl}(\text{PPh}_3)_2(\text{TBA})]\cdot\text{H}_2\text{O}$ (1).

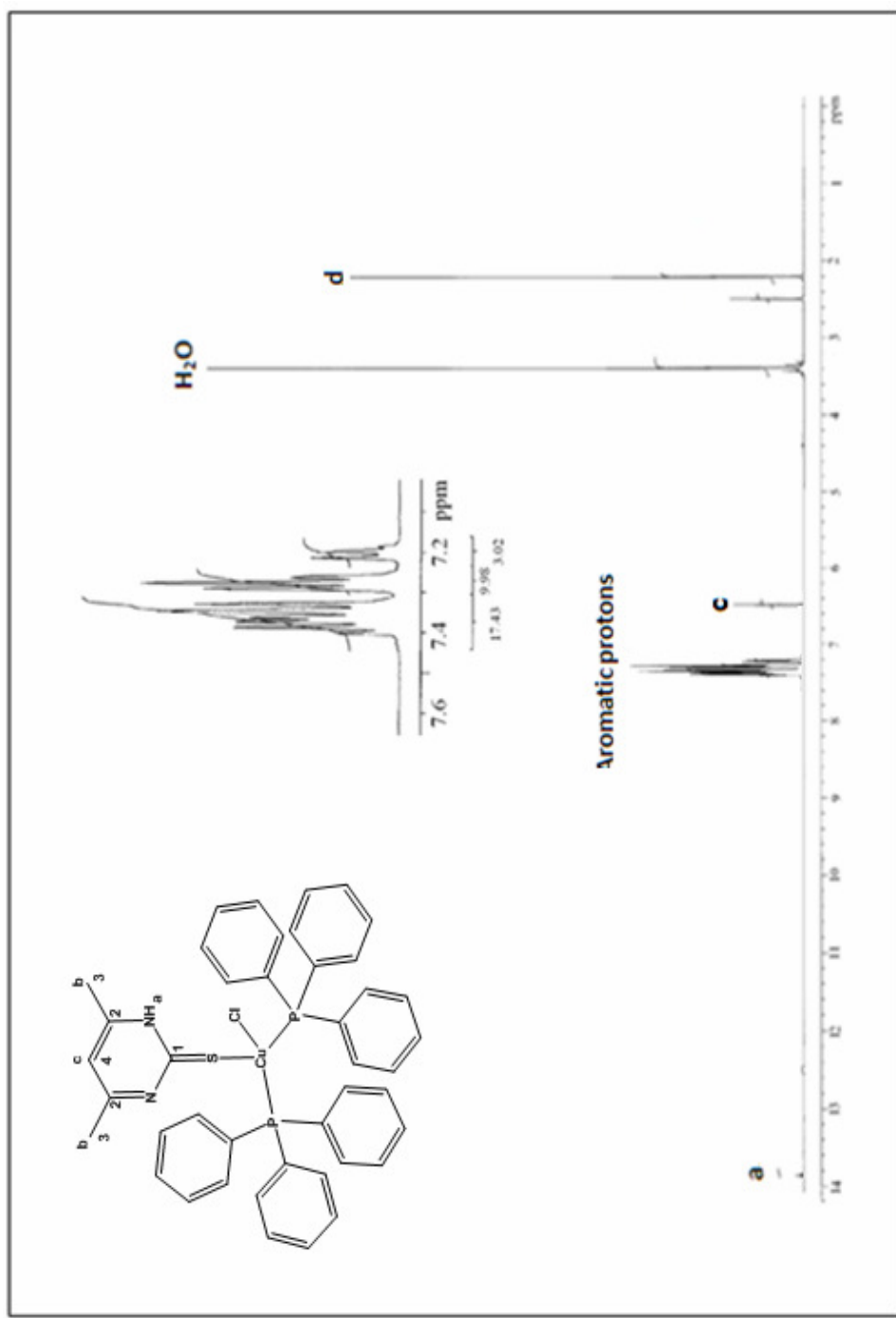


Figure 50 ^1H NMR spectrum of $[\text{CuCl}(\text{PPh}_3)_2(\text{dmpymtH})]$ (3).

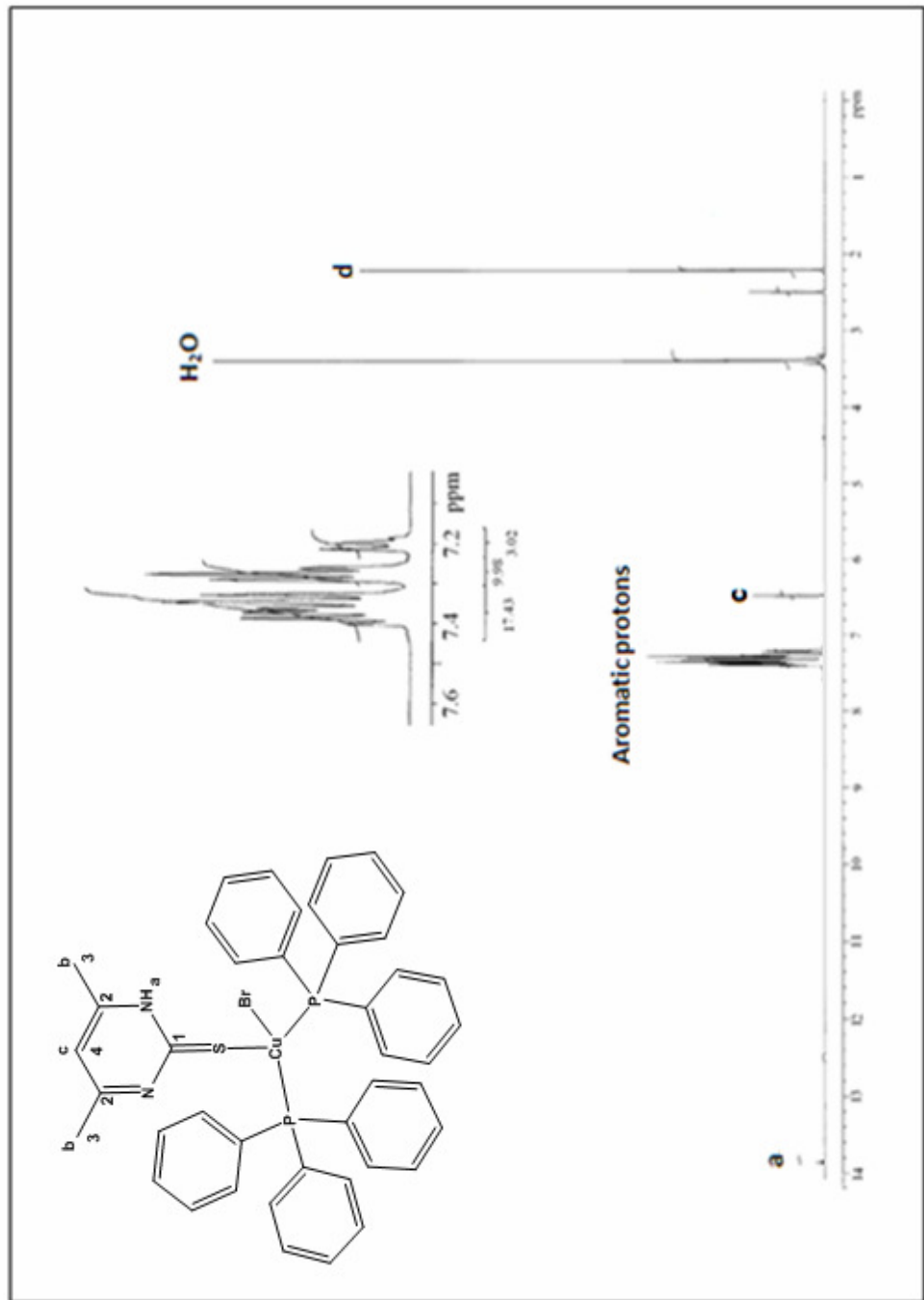


Figure 51 ^1H NMR spectrum of $[\text{CuBr}(\text{PPh}_3)_2(\text{dmpytmH})]$ (4).

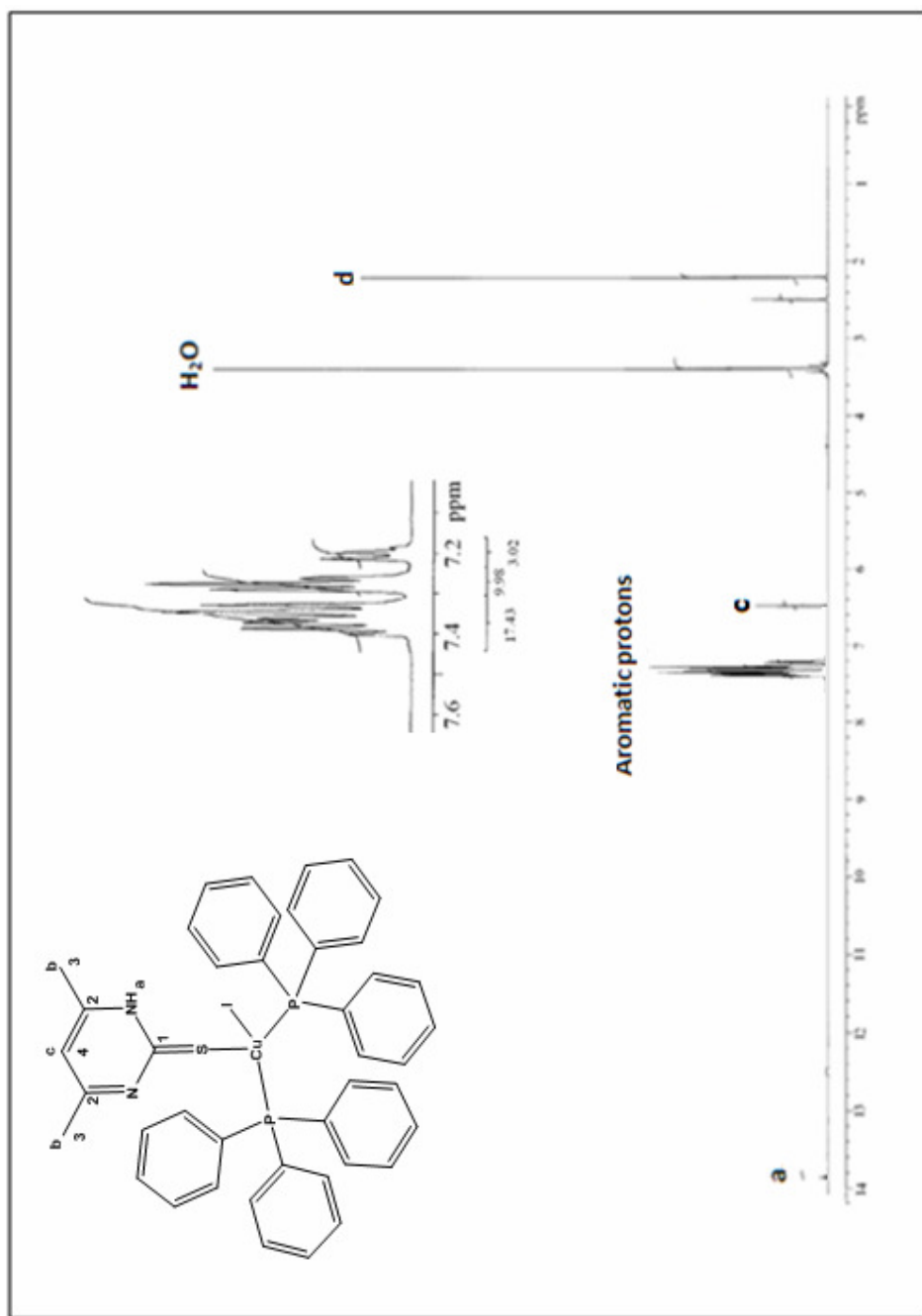


Figure 52 ^1H NMR spectrum of $[\text{CuI}(\text{PPh}_3)_2(\text{dmpytmH})]$ (4).

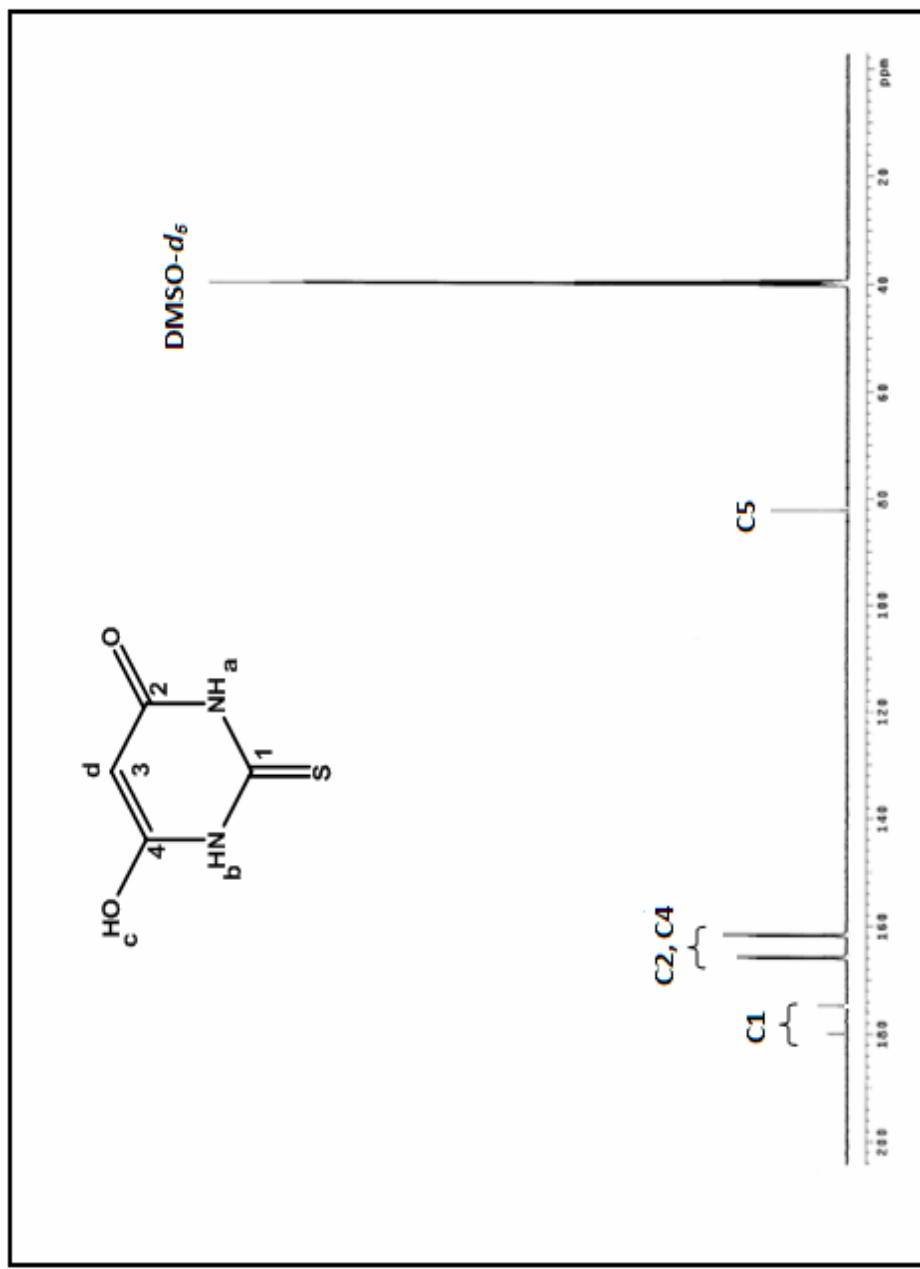


Figure S3 ^{13}C NMR spectrum of TRA

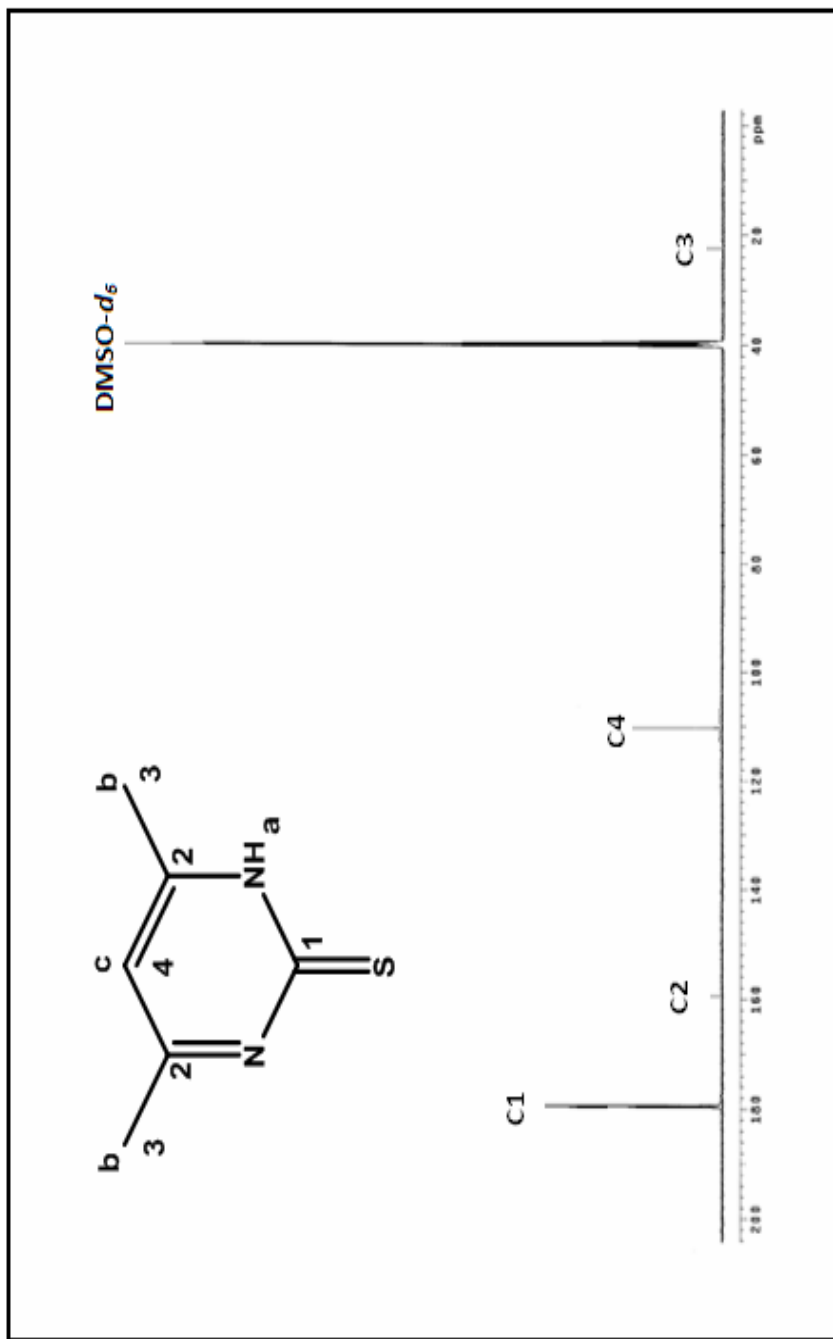


Figure 54 ^{13}C NMR spectrum of dmpymth.

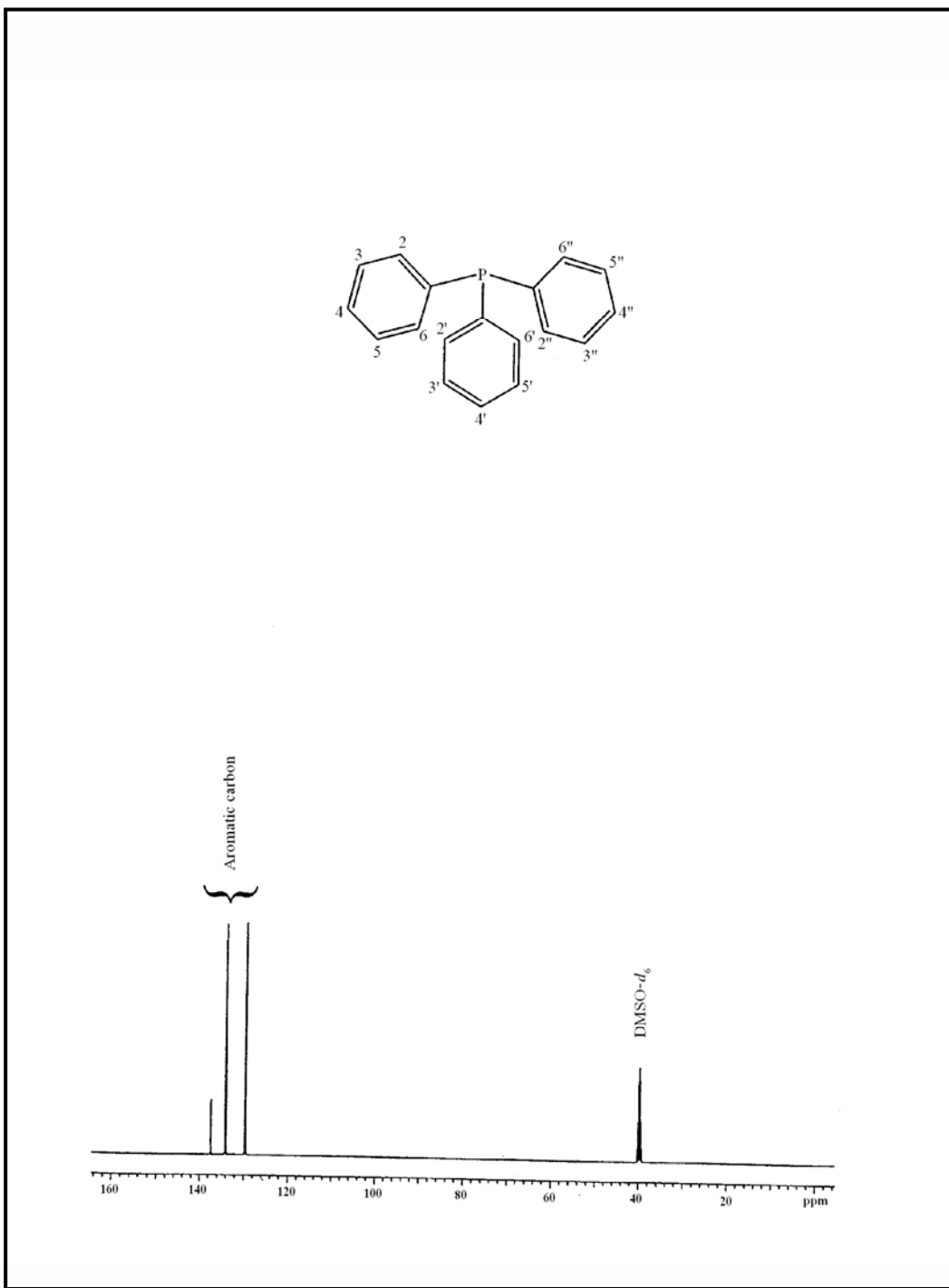


Figure 55 ^{13}C NMR spectrum of triphenylphosphine (PPh_3).

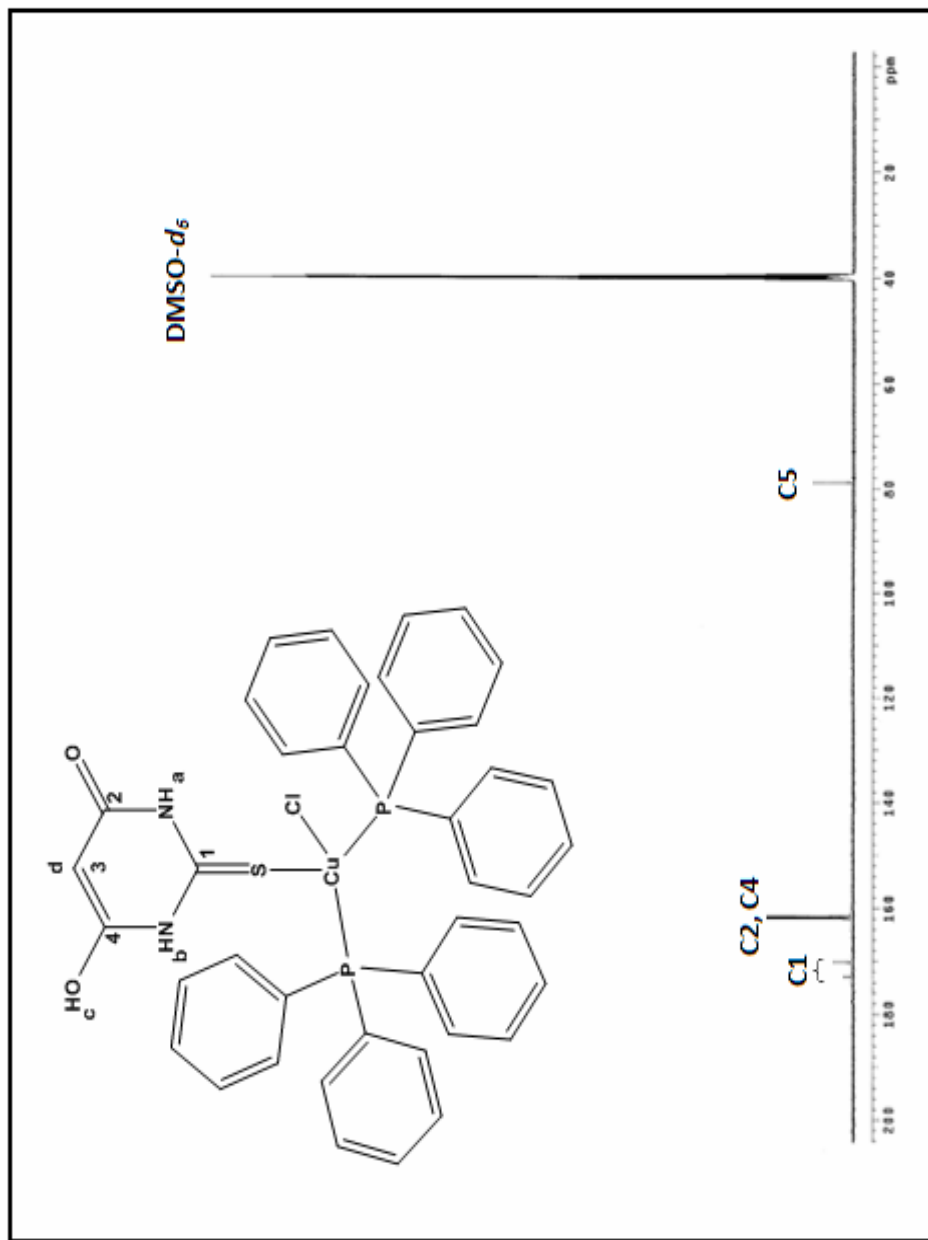


Figure 56 ^{13}C NMR spectrum of $[\text{CuCl}(\text{PPh}_3)_2(\text{TBA})]\cdot\text{H}_2\text{O}$ (1).

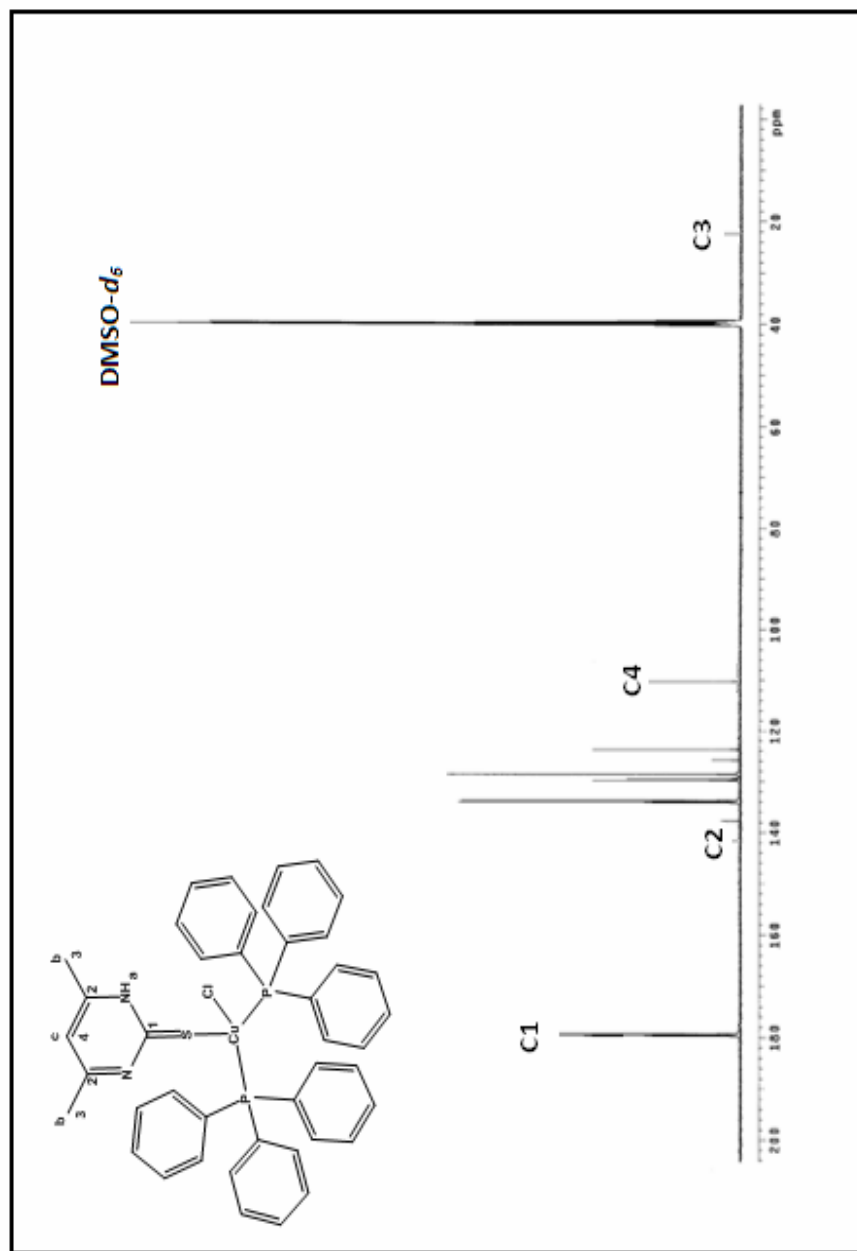


Figure 57 ^{13}C NMR spectrum of $[\text{CuCl}(\text{PPh}_3)_2(\text{dmpymlH})]$ (3).

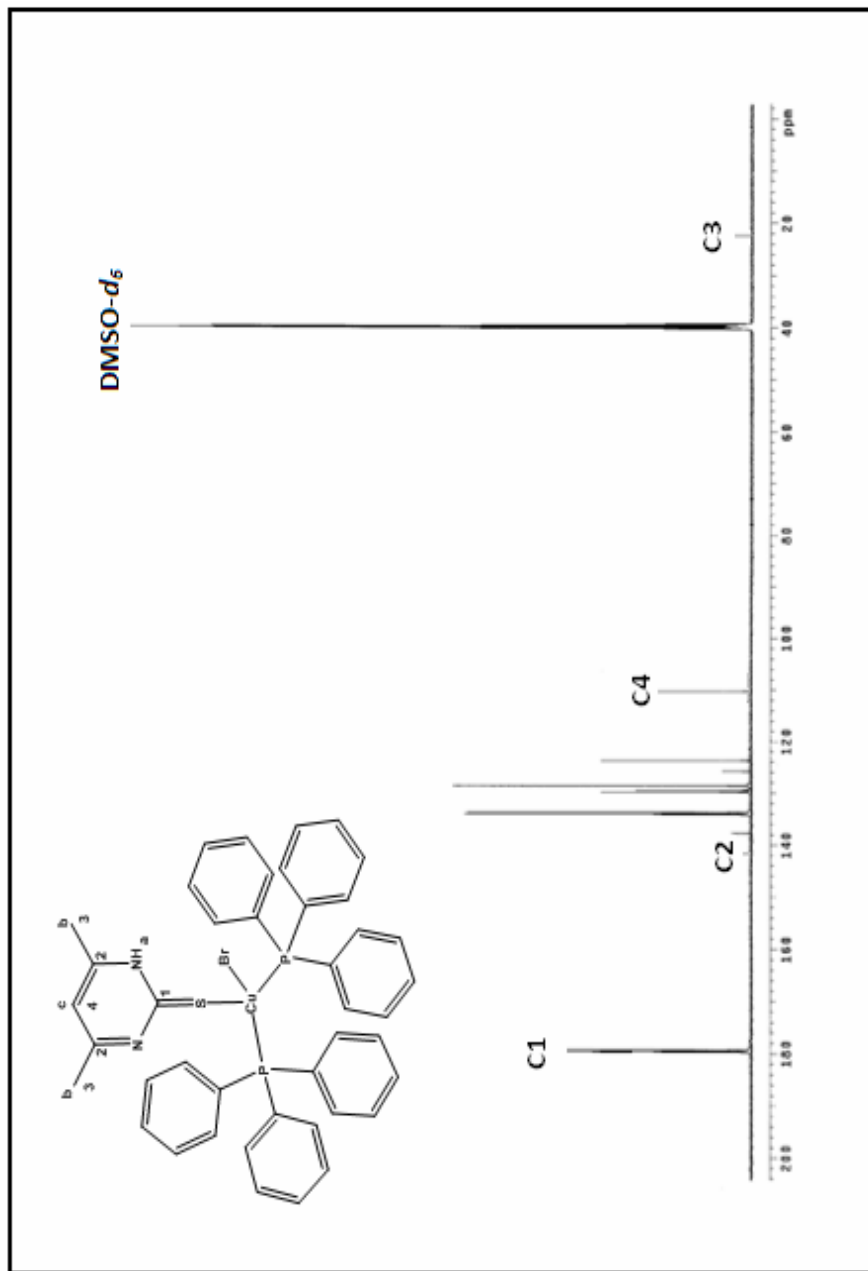


Figure 58 ^{13}C NMR spectrum of $[\text{CuBr}(\text{PPh}_3)_2(\text{dmppytH})]$ (4).

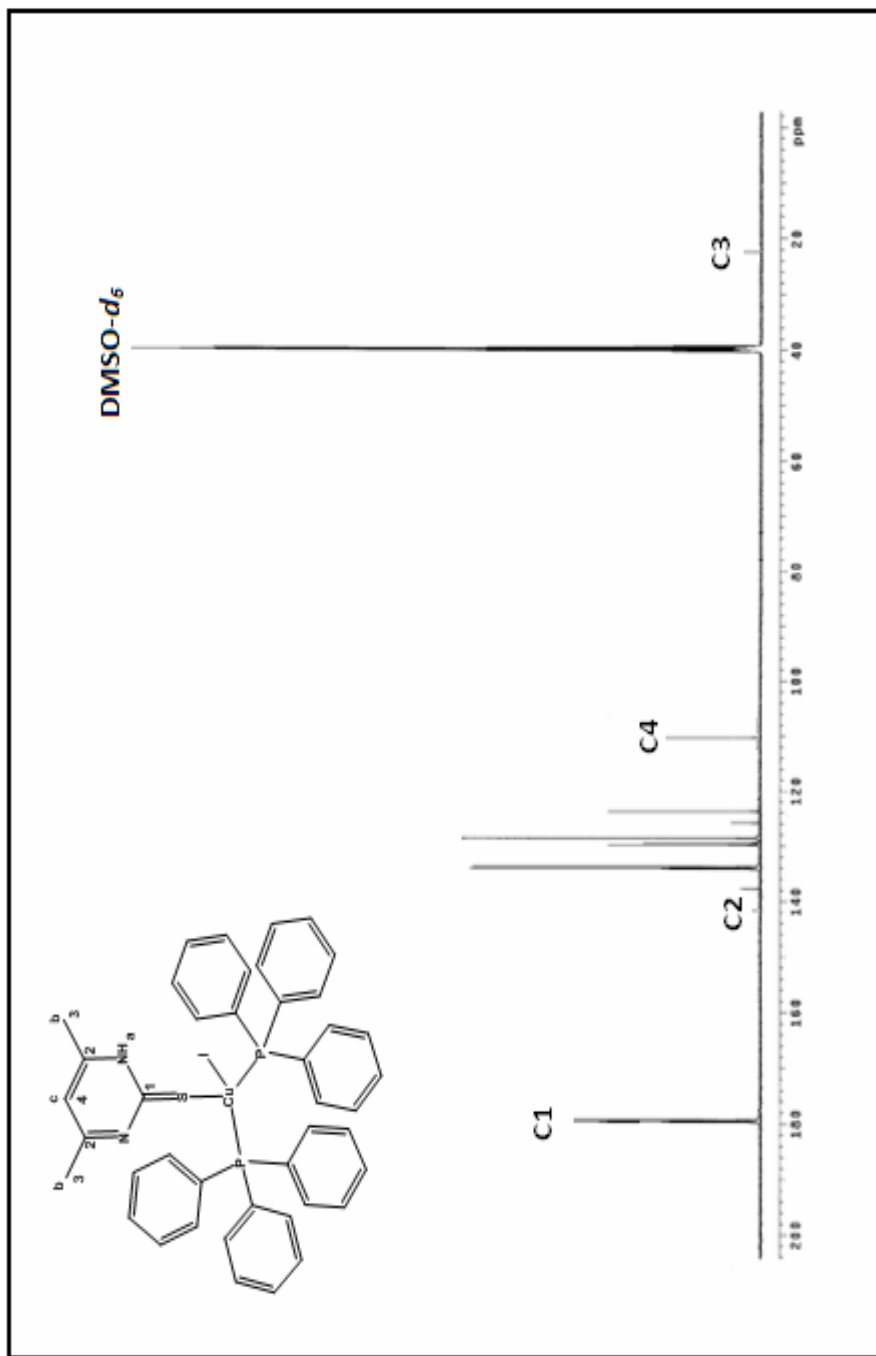


Figure 59 ^{13}C NMR spectrum of $[\text{CuI}(\text{PPh}_3)_2(\text{dmypytmH})]$ (5).

3.6 Single crystal X-ray diffractometry

3.6.1 Crystal Structures

These results from crystal structure determination using SHELXTL (Sheldrick, 2000) and WinGX (Farrugia, 1999) System of complexes 1-5 are shown in Tables 4-15 and Figures 60-63.

Table 4 The crystallographic data for $[\text{CuCl}(\text{PPh}_3)_2(\text{TBA})]\cdot\text{H}_2\text{O}$ (1) and $[\text{CuI}(\text{PPh}_3)_2(\text{CH}_3\text{CN})]$ (2).

	$\text{C}_{42}\text{H}_{37}\text{ClCuN}_2\text{P}_2\text{S}$	$\text{C}_{42}\text{H}_{37}\text{BrCuN}_2\text{P}_2\text{S}$	$\text{C}_{42}\text{H}_{37}\text{CuIN}_2\text{P}_2\text{S}$
Empirical formula	$\text{C}_{42}\text{H}_{37}\text{ClCuN}_2\text{P}_2\text{S}$	$\text{C}_{42}\text{H}_{37}\text{BrCuN}_2\text{P}_2\text{S}$	$\text{C}_{42}\text{H}_{37}\text{CuIN}_2\text{P}_2\text{S}$
Formula weight	762.73	807.19	854.18
Temperature	293(2) K	293(2) K	293(2) K
Wavelength	0.71073 Å	0.71073 Å	0.71073 Å
Crystal system	monoclinic	monoclinic	triclinic
Space group	$P2_1/c$	$P2_1/c$	$P1$
Unit cell dimensions			
a (Å)	9.8469(3)	9.8259(6)	11.5605(7)
b (Å)	17.8683(5)	17.8673(11)	13.0076(8)
c (Å)	22.0555(6)	22.2361(13)	13.6456(8)
α (°)	90	90	92.2430(10)
β (°)	100.9120(10)	100.7390(10)	99.2470(10)
γ (°)	90	90	106.0920(10)
Volume	3810.44(19)	3835.4(4)	1938.3(2)
Z	4	4	2
Final R indices [$I > 2\sigma(I)$]	$R1 = 0.0344$ $wR2 = 0.0881$	$R1 = 0.0444$ $wR2 = 0.0948$	$R1 = 0.0217$ $wR2 = 0.0570$
R indices (all data)	$R1 = 0.0407$ $wR2 = 0.0924$	$R1 = 0.0407$ $wR2 = 0.0924$	$R1 = 0.0235$ $wR2 = 0.0584$

Table 5 The crystallographic data for [CuX(PPh₃)₂(dmpymtH)] (X = Cl, Br, I)

Empirical formula	C ₄₀ H ₃₆ ClCuN ₂ O ₃ P ₂ S	C ₃₆ H ₃₃ CuINP ₂
Formula weight	785.70	732.01
Temperature	293(2) K	293(2) K
Wavelength	0.71073 Å	0.71073 Å
Crystal system	monoclinic	monoclinic
Space group	P2 ₁ /c	P2 ₁ /c
Unit cell dimensions		
a (Å)	9.8090(3)	9.2547(3)
b (Å)	9.8643(3)	19.3814(6)
c (Å)	39.9890(13)	19.4249(6)
α (°)	90	90
β (°)	96.5860(10)	93.0430(10)
γ (°)	90	90
Volume	3843.8(2)	3479.31(19)
Z	4	4
Final <i>R</i> indices [<i>I</i> >2σ(<i>I</i>)]	<i>R</i> 1 = 0.0330 w <i>R</i> 2 = 0.0944	<i>R</i> 1 = 0.0272 w <i>R</i> 2 = 0.0649
<i>R</i> indices (all data)	<i>R</i> 1 = 0.0378 w <i>R</i> 2 = 0.0944	<i>R</i> 1 = 0.0317 w <i>R</i> 2 = 0.0649

Table 6 Non-hydrogen interatomic distances of $[\text{CuCl}(\text{PPh}_3)_2(\text{TBA})]\cdot\text{H}_2\text{O}$ (1).

Atom	Distance (Å)	Atom	Distance (Å)
Cu(1)-Cl(1)	2.3986(8)	Cu(1)-P(1)	2.2943(8)
Cu(1)-P(2)	2.2757(8)	Cu(1)-S(1)	2.3620(8)
C(1)-N(2)	1.338(4)	C(1)-N(1)	1.340(3)
C(1)-S(1)	1.689(3)	C(2)-O(1)	1.254(3)
C(2)-N(1)	1.388(4)	C(2)-C(3)	1.397(4)
C(3)-C(4)	1.355(4)	C(4)-O(2)	1.293(4)
C(4)-N(2)	1.374(4)	C(11A)-C(12A)	1.377(4)
C(11A)-C(16A)	1.385(4)	C(11A)-P(1)	1.831(3)
C(12A)-C(13A)	1.372(5)	C(13A)-C(14A)	1.376(6)
C(14A)-C(15A)	1.348(5)	C(15A)-C(16A)	1.381(4)
C(21A)-C(26A)	1.383(5)	C(21A)-C(22A)	1.388(5)
C(21A)-P(1)	1.829(3)	C(22A)-C(23A)	1.388(5)
C(23A)-C(24A)	1.361(6)	C(24A)-C(25)	1.378(6)
C(31A)-C(32A)	1.370(5)	C(31A)-C(36A)	1.377(5)
C(31A)-P(1)	1.829(3)	C(32A)-C(33A)	1.383(5)
C(33A)-C(34A)	1.360(6)	C(34A)-C(35A)	1.346(6)
C(35A)-C(36A)	1.379(5)	C(11B)-C(16B)	1.379(4)
C(11B)-C(12B)	1.379(5)	C(11B)-P(2)	1.830(3)
C(12B)-C(13B)	1.386(5)	C(13B)-C(14B)	1.368(6)
C(14B)-C(15B)	1.365(6)	C(15B)-C(16B)	1.383(5)
C(21B)-C(22B)	1.379(5)	C(21B)-C(26B)	1.376(4)
C(21B)-P(2)	1.823(3)	C(22B)-C(23B)	1.366(5)
C(23B)-C(24B)	1.369(6)	C(24B)-C(25B)	1.370(6)
C(25B)-C(26B)	1.387(5)	C(31B)-C(32B)	1.371(5)
C(31B)-C(36B)	1.376(4)	C(31B)-P(2)	1.824(3)
C(32B)-C(33B)	1.375(5)	C(33B)-C(34B)	1.355(6)
C(34B)-C(35B)	1.366(6)	C(35B)-C(36B)	1.385(5)
N(2)-C(1)-N(1)	115.5(2)	N(2)-C(1)-S(1)	123.2(2)

Table 7 Non-hydrogen interatomic distances of $[\text{CuCl}(\text{PPh}_3)_2(\text{CH}_3\text{CN})]$ (2).

Atom	Distance (Å)	Atom	Distance (Å)
Cu(1)-N(1)	2.065(3)	Cu(1)-P(1)	2.2784(8)
Cu(1)-P(2)	2.2790(8)	Cu(1)-I(1)	2.6644(4)
C(1)-C(6)	1.384(4)	C(1)-C(2)	1.385(4)
C(1)-P(1)	1.833(3)	C(2)-C(3)	1.384(5)
C(3)-C(4)	1.364(5)	C(4)-C(5)	1.364(5)
C(5)-C(6)	1.375(5)	C(7)-C(8)	1.373(5)
C(7)-C(12)	1.385(5)	C(7)-P(1)	1.828(3)
C(8)-C(9)	1.386(5)	C(9)-C(10)	1.357(7)
C(10)-C(11)	1.362(7)	C(11)-C(12)	1.391(5)
C(13)-C(18)	1.378(4)	C(13)-C(14)	1.386(4)
C(13)-P(1)	1.821(3)	C(14)-C(15)	1.376(5)
C(15)-C(16)	1.366(6)	C(16)-C(17)	1.365(6)
C(17)-C(18)	1.383(5)	C(19)-C(24)	1.371(4)
C(19)-C(20)	1.374(4)	C(19)-P(2)	1.818(3)
C(20)-C(21)	1.377(5)	C(21)-C(22)	1.368(5)
C(22)-C(23)	1.352(5)	C(23)-C(24)	1.377(5)
C(25)-C(30)	1.379(4)	C(25)-C(26)	1.387(4)
C(25)-P(2)	1.833(3)	C(26)-C(27)	1.380(5)
C(27)-C(28)	1.364(5)	C(28)-C(29)	1.367(5)
C(29)-C(30)	1.380(5)	C(31)-C(32)	1.370(5)
C(31)-C(36)	1.390(5)	C(31)-C(36)	1.390(5)
C(31)-P(2)	1.825(3)	C(32)-C(33)	1.400(5)
C(33)-C(34)	1.348(6)	C(34)-C(35)	1.357(6)
C(35)-C(36)	1.376(5)	C(1A)-N(1)	1.107(4)
C(1A)-C(2A)	1.457(6)		

Table 8 Non-hydrogen interatomic distances of $[\text{CuCl}(\text{PPh}_3)_2(\text{dmpymtH})]$ (3).

Atom	Distance (Å)	Atom	Distance (Å)
Cu(1)-Cl(1)	2.4120(8)	Cu(1)-P(1)	2.2966(8)
Cu(1)-P(2)	2.2698(8)	Cu(1)-(S1)	2.4120(8)
C(1)-N(1)	1.339(4)	C(1)-N(2)	1.364(4)
C(1)-S(1)	1.707(3)	C(2)-N(1)	1.333(4)
C(2)-C(3)	1.393(4)	C(2)-C(5)	1.497(5)
C(3)-C(4)	1.356(4)	C(4)-N(2)	1.360(4)
C(4)-C(6)	1.489(4)	C(11)-C(12)	1.373(5)
C(11)-C(16)	1.384(5)	C(11)-P(2)	1.829(3)
C(12)-C(13)	1.395(6)	C(13)-C(14)	1.357(7)
C(14)-C(15)	1.350(7)	C(15)-C(16)	1.390(5)
C(21)-C(26)	1.383(4)	C(21)-C(22)	1.384(4)
C(21)-P(2)	1.829(3)	C(22)-C(23)	1.381(5)
C(23)-C(24)	1.366(6)	C(24)-C(25)	1.363(5)
C(25)-C(26)	1.385(5)	C(31)-C(32)	1.380(4)
C(31)-C(36)	1.386(4)	C(31)-P(2)	1.828(3)
C(32)-C(33)	1.389(5)	C(33)-C(34)	1.352(5)
C(34)-C(35)	1.354(6)	C(35)-C(36)	1.382(5)
C(41)-C(42)	1.378(4)	C(41)-C(46)	1.385(4)
C(41)-P(1)	1.835(3)	C(42)-C(43)	1.380(4)
C(43)-C(44)	1.357(5)	C(44)-C(45)	1.368(5)
C(45)-C(46)	1.371(5)	C(51)-C(52)	1.377(4)
C(51)-C(56)	1.380(4)	C(51)-P(1)	1.826(3)
C(52)-C(53)	1.376(5)	C(53)-C(54)	1.355(5)
C(54)-C(55)	1.365(5)	C(55)-C(56)	1.384(5)
C(61)-C(66)	1.365(4)	C(61)-C(62)	1.376(4)
C(61)-P(1)	1.823(3)	C(62)-C(63)	1.379(5)
C(63)-C(64)	1.355(6)	C(64)-C(65)	1.343(6)
C(65)-C(66)	1.384(6)		

Table 9 Non-hydrogen interatomic distances of $[\text{CuBr}(\text{PPh}_3)_2(\text{dmpymtH})]$ (4).

Atom	Distance (Å)	Atom	Distance (Å)
Cu(1)-Br(1)	2.5527(8)	Cu(1)-P(1)	2.2720(13)
Cu(1)-P(2)	2.2942(13)	Cu(1)-S(1)	2.3690(1)
C(1)-C(6)	1.367(7)	C(1)-C(2)	1.376(7)
C(1)-P(1)	1.832(5)	C(2)-C(3)	1.384(8)
C(3)-C(4)	1.352(9)	C(4)-C(5)	1.343(9)
C(5)-C(6)	1.388(8)	C(7)-C(12)	1.378(7)
C(7)-C(8)	1.388(7)	C(7)-P(1)	1.827(5)
C(8)-C(9)	1.395(8)	C(9)-C(10)	1.362(10)
C(10)-C(11)	1.345(10)	C(11)-C(12)	1.414(9)
C(13)-C(14)	1.380(7)	C(13)-C(18)	1.393(7)
C(13)-P(1)	1.826(5)	C(14)-C(15)	1.396(7)
C(15)-C(16)	1.359(8)	C(16)-C(17)	1.366(9)
C(17)-C(18)	1.373(8)	C(19)-C(24)	1.376(6)
C(19)-C(20)	1.387(6)	C(19)-P(2)	1.829(5)
C(20)-C(21)	1.378(7)	C(21)-C(22)	1.358(8)
C(22)-C(23)	1.365(7)	C(23)-C(24)	1.372(7)
C(25)-C(26)	1.367(7)	C(25)-C(30)	1.371(7)
C(25)-P(2)	1.823(5)	C(26)-C(27)	1.375(8)
C(27)-C(28)	1.357(9)	C(28)-C(29)	1.333(9)
C(29)-C(30)	1.385(7)	C(31)-C(32)	1.366(7)
C(31)-C(36)	1.372(7)	C(31)-P(2)	1.827(5)
C(32)-C(33)	1.389(7)	C(33)-C(34)	1.367(8)
C(34)-C(35)	1.362(8)	C(35)-C(36)	1.367(7)
C(1A)-N(2)	1.346(6)	C(1A)-N(1)	1.365(5)
C(1A)-S(5)	1.711(5)	C(2A)-C(3A)	1.345(7)
C(2A)-N(1)	1.358(6)	C(2A)-C(5A)	1.488(7)
C(3A)-C(4A)	1.402(7)	C(4A)-N(2)	1.318(6)
C(4A)-C(6A)	1.507(7)		

Table 10 Non-hydrogen interatomic distances of $[\text{CuI}(\text{PPh}_3)_2(\text{dmpymtH})]$ (5).

Atom	Distance (Å)	Atom	Distance (Å)
Cu(1)-I(1)	2.6800(3)	Cu(1)-P(1)	2.2894(7)
Cu(1)-P(2)	2.3039(7)	Cu(1)-S(1)	2.3407(7)
C(28)-C(29)	1.370(5)	C(28)-C(27)	1.371(5)
N(1)-C(2A)	1.361(3)	N(1)-C(1A)	1.362(3)
N(2)-C(4A)	1.336(4)	N(2)-C(1A)	1.348(3)
P(1)-C(13)	1.826(3)	P(1)-C(7)	1.830(2)
P(1)-C(1)	1.831(2)	P(2)-C(31)	1.827(2)
P(2)-C(19)	1.833(2)	P(2)-C(25)	1.834(2)
S(1)-C(1A)	1.689(3)	C(25)-C(26)	1.382(4)
C(25)-C(30)	1.387(4)	C(36)-C(35)	1.374(4)
C(36)-C(31)	1.384(4)	C(31)-C(32)	1.378(4)
C(7)-C(8)	1.378(4)	C(7)-C(12)	1.385(4)
C(13)-C(18)	1.377(4)	C(13)-C(14)	1.399(4)
C(20)-C(21)	1.377(4)	C(20)-C(19)	1.389(3)
C(19)-C(24)	1.383(3)	C(15)-C(16)	1.376(5)
C(15)-C(14)	1.378(4)	C(1)-C(6)	1.386(4)
C(1)-C(2)	1.388(4)	C(24)-C(23)	1.383(4)
C(12)-C(11)	1.380(4)	C(23)-C(22)	1.367(4)
C(30)-C(29)	1.375(4)	C(4A)-C(3A)	1.376(4)
C(4A)-C(6A)	1.489(4)	C(3A)-C(2A)	1.346(4)
C(21)-C(22)	1.374(4)	C(26)-C(27)	1.383(4)
C(6)-C(5)	1.384(4)	C(11)-C(10)	1.373(5)
C(8)-C(9)	1.378(4)	C(18)-C(17)	1.390(4)
C(32)-C(33)	1.394(4)	C(10)-C(9)	1.359(5)
C(35)-C(34)	1.360(5)	C(2)-C(3)	1.384(4)
C(2A)-C(5A)	1.490(4)	C(17)-C(16)	1.351(5)
C(33)-C(34)	1.371(5)	C(5)-C(4)	1.374(5)
C(3)-C(4)	1.360(5)		

Table 11 Non-hydrogen interbond angles of $[\text{CuCl}(\text{PPh}_3)(\text{TBA}) \cdot \text{H}_2\text{O}]$ (1) .

Atom	Angle ($^{\circ}$)
P(2)-Cu(1)-P(1)	124.70(3)
P(2)-Cu(1)-S(1)	108.11(3)
P(1)-Cu(1)-S(1)	109.71(3)
P(2)-Cu(1)-Cl(1)	99.30(3)
P(1)-Cu(1)-Cl(1)	107.45(3)
S(1)-Cu(1)-Cl	105.66(3)
O(1)-C(2)-N(1)	116.4(2)
O(1)-C(2)-C(3)	126.9(3)
N(1)-C(2)-C(3)	116.6(3)
C(4)-C(3)-C(2)	119.4(3)
O(2)-C(4)-C(3)	128.5(3)
O(2)-C(4)-N(2)	112.1(3)
C(3)-C(4)-N(2)	119.4(3)
C(12A)-C(11A)-C(16A)	117.7(3)
C(12A)-C(11A)-P(1)	118.5(2)
C(16A)-C(11A)-P(1)	123.8(2)
C(13A)-C(12A)-C(11A)	121.0(3)
C(14A)-C(13A)-C(12A)	120.1(4)
C(15A)-C(14A)-C(13A)	120.2(4)
C(14A)-C(15A)-C(16A)	119.9(3)
C(15A)-C(16A)-C(11A)	121.2(3)
C(26A)-C(21A)-C(22A)	119.0(3)
C(26A)-C(21A)-P(1)	117.5(2)
C(22A)-C(21A)-P(1)	123.5(3)
C(21A)-C(22A)-C(23A)	119.8(4)
C(24A)-C(23A)-C(22A)	120.6(4)
C(23A)-C(24A)-C(25A)	120.2(4)

Table 11 (Continued).

Atom	Angle (°)
C(21A)-C(26A)-C(25A)	120.6(4)
C(32A)-C(31A)-C(36A)	118.2(3)
C(32A)-C(31A)-P(1)	118.2(2)
C(36A)-C(31A)-P(1)	123.6(3)
C(31A)-C(32A)-C(33A)	120.9(3)
C(34A)-C(33A)-C(32A)	120.2(4)
C(35A)-C(34A)-C(33A)	119.2(4)
C(34A)-C(35A)-C(36A)	121.6(4)
C(31A)-C(36A)-C(35A)	119.9(4)
C(16B)-C(11B)-C(12B)	118.5(3)
C(16B)-C(11B)-P(2)	123.4(3)
C(12B)-C(11B)-P(2)	118.1(2)
C(11B)-C(12B)-C(13B)	120.8(4)
C(14B)-C(13B)-C(12B)	119.4(4)
C(15B)-C(14B)-C(13B)	120.9(4)
C(14B)-C(15B)-C(16B)	119.4(4)
C(11B)-C(16B)-C(15B)	121.0(4)
C(22B)-C(21B)-C(26B)	118.3(3)
C(22B)-C(21B)-P(2)	116.8(2)
C(26B)-C(21B)-P(2)	124.9(2)
C(23B)-C(22B)-C(21B)	121.5(4)
C(24B)-C(23B)-C(22B)	119.7(4)
C(25B)-C(24B)-C(23B)	120.3(4)
C(24B)-C(25B)-C(26B)	119.6(4)
C(21B)-C(26B)-C(25B)	120.6(3)
C(32B)-C(31B)-C(36B)	118.1(3)
C(32B)-C(31B)-P(2)	118.0(2)

Table 11 (Continued).

Atom	Angle (°)
C(36B)-C(31B)-P(2)	123.8(2)
C(31B)-C(32B)-C(33B)	121.2(4)
C(34B)-C(33B)-C(32B)	120.2(4)
C(33B)-C(34B)-C(35B)	119.9(4)
C(34B)-C(35B)-C(36B)	119.9(4)
C(31B)-C(36B)-C(35B)	120.6(3)
C(1)-N(1)-C(2)	125.1(2)
C(1)-N(2)-C(4)	124.0(2)
C(31A)-P(1)-C(21A)	104.49(14)
C(31A)-P(1)-C(11A)	102.92(14)
C(21A)-P(1)-C(11A)	101.81(14)
C(31A)-P(1)-Cu(1)	113.72(10)
C(21A)-P(1)-Cu(1)	115.36(10)
C(11A)-P(1)-Cu(1)	116.82(10)
C(21B)-P(2)-C(31B)	104.30(13)
C(21B)-P(2)-C(11B)	102.82(14)
C(31B)-P(2)-C(11B)	102.88(13)
C(21B)-P(2)-Cu(1)	117.33(10)
C(31B)-P(2)-Cu(1)	110.82(9)
C(11B)-P(2)-Cu(1)	117.00(10)
C(1)-S(1)-Cu(1)	109.27(10)

Table 12 Non-hydrogen inerbond angles of [Cu_i(PPh₃)₂(CH₃CN)] (2).

Atom	Angle (°)
N(1)-Cu(1)-P(1)	112.49(8)
N(1)-Cu(1)-P(2)	105.21(8)
P(1)-Cu(1)-P(2)	123.55(3)
N(1)-Cu(1)-I(1)	101.05(9)
P(1)-Cu(1)-I(1)	106.95(2)
P(2)-Cu(1)-I(1)	105.13(2)
C(6)-C(1)-C(2)	117.5(3)
C(6)-C(1)-P(1)	118.9(2)
C(2)-C(1)-P(1)	123.4(2)
C(3)-C(2)-C(1)	120.7(3)
C(4)-C(3)-C(2)	120.5(3)
C(3)-C(4)-C(5)	119.5(3)
C(4)-C(5)-C(6)	120.4(3)
C(5)-C(6)-C(1)	121.3(3)
C(8)-C(7)-C(12)	118.3(3)
C(8)-C(7)-P(1)	123.0(3)
C(12)-C(7)-P(1)	118.3(3)
C(7)-C(8)-C(9)	121.2(4)
C(10)-C(9)-C(8)	120.0(5)
C(9)-C(10)-C(11)	120.0(4)
C(10)-C(11)-C(12)	120.6(4)
C(7)-C(12)-C(11)	119.9(4)
C(18)-C(13)-C(14)	118.4(3)
C(18)-C(13)-P(1)	117.8(2)
C(14)-C(13)-P(1)	123.4(3)
C(15)-C(14)-C(13)	120.1(4)
C(16)-C(15)-C(14)	120.9(4)
C(17)-C(16)-C(15)	119.7(4)

Table 12 (Continued).

Atom	Angle (°)
C(16)-C(17)-C(18)	120.0(4)
C(13)-C(18)-C(17)	120.9(3)
C(24)-C(19)-C(20)	117.9(3)
C(24)-C(19)-P(2)	124.8(2)
C(20)-C(19)-P(2)	117.3(2)
C(19)-C(20)-C(21)	120.7(3)
C(22)-C(21)-C(20)	120.4(4)
C(23)-C(22)-C(21)	119.4(3)
C(22)-C(23)-C(24)	120.4(3)
C(19)-C(24)-C(23)	121.2(3)
C(30)-C(25)-C(26)	118.1(3)
C(30)-C(25)-P(2)	123.3(2)
C(26)-C(25)-P(2)	118.6(2)
C(27)-C(26)-C(25)	120.6(3)
C(28)-C(27)-C(26)	120.5(4)
C(27)-C(28)-C(29)	119.8(3)
C(28)-C(29)-C(30)	120.2(3)
C(25)-C(30)-C(29)	120.9(3)
C(32)-C(31)-C(36)	118.0(3)
C(32)-C(31)-P(2)	124.4(3)
C(36)-C(31)-P(2)	117.5(3)
C(31)-C(32)-C(33)	119.8(4)
C(34)-C(33)-C(32)	121.0(4)
C(33)-C(34)-C(35)	119.8(4)
C(34)-C(35)-C(36)	120.1(4)
C(35)-C(36)-C(31)	121.2(4)
N(1)-C(1A)-C(2A)	179.2(6)

Table 12 (Continued).

Atom	Angle (°)
C(1A)-N(1)-Cu(1)	165.9(3)
C(13)-P(1)-C(7)	104.78(15)
C(13)-P(1)-C(1)	101.72(13)
C(7)-P(1)-C(1)	104.72(14)
C(13)-P(1)-Cu(1)	114.74(10)
C(7)-P(1)-Cu(1)	111.30(10)
C(1)-P(1)-Cu(1)	118.17(9)
C(19)-P(2)-C(31)	103.91(14)
C(19)-P(2)-C(25)	104.49(13)
C(31)-P(2)-C(25)	101.88(14)
C(19)-P(2)-Cu(1)	112.49(10)
C(31)-P(2)-Cu(1)	115.59(10)
C(25)-P(2)-Cu(1)	116.92(10)

Table 13 Non-hydrogen inerbond angles of $[\text{CuCl}(\text{PPh}_3)_2(\text{dmpymtH})]$ (3).

Atom	Angle (°)
P(2)-Cu(1)-P(1)	125.00(3)
P(2)-Cu(1)-S(1)	112.46(3)
P(1)-Cu(1)-S(1)	99.56(3)
P(2)-Cu(1)-Cl(1)	105.81(3)
P(1)-Cu(1)-Cl(1)	104.02(3)
S(1)-Cu(1)-Cl(1)	109.13(3)
P(2)-Cu(1)-P(1)	125.00(3)
P(2)-Cu(1)-S(1)	112.46(3)

Table 13 (Continued).

Atom	Angle (°)
P(1)-Cu(1)-S(1)	99.56(3)
P(2)-Cu(1)-Cl(1)	105.81(3)
P(1)-Cu(1)-Cl(1)	104.02(3)
S(1)-Cu(1)-Cl(1)	109.13(3)
N(1)-C(1)-N(2)	120.5(3)
N(1)-C(1)-S(1)	119.9(2)
N(2)-C(1)-S(1)	119.6(2)
N(1)-C(2)-C(3)	122.6(3)
N(1)-C(2)-C(5)	116.3(3)
C(3)-C(2)-C(5)	121.1(3)
C(4)-C(3)-C(2)	118.7(3)
C(3)-C(4)-N(2)	117.9(3)
C(3)-C(4)-C(6)	124.5(3)
N(2)-C(4)-C(6)	117.5(3)
C(12)-C(11)-C(16)	118.2(3)
C(12)-C(11)-P(2)	124.2(3)
C(16)-C(11)-P(2)	117.7(2)
C(11)-C(12)-C(13)	120.4(4)
C(14)-C(13)-C(12)	120.2(4)
C(15)-C(14)-C(13)	120.6(4)
C(14)-C(15)-C(16)	119.8(4)
C(11)-C(16)-C(15)	120.9(4)
C(26)-C(21)-C(22)	118.2(3)
C(26)-C(21)-P(2)	124.1(2)
C(22)-C(21)-P(2)	117.7(2)
C(23)-C(22)-C(21)	120.5(4)
C(24)-C(23)-C(22)	120.7(4)
C(25)-C(24)-C(23)	119.4(3)

Table 13 (Continued).

Atom	Angle (°)
C(24)-C(25)-C(26)	120.6(4)
C(21)-C(26)-C(25)	120.5(3)
C(32)-C(31)-C(36)	117.6(3)
C(32)-C(31)-P(2)	119.0(2)
C(36)-C(31)-P(2)	123.3(2)
C(31)-C(32)-C(33)	120.4(3)
C(34)-C(33)-C(32)	120.9(4)
C(33)-C(34)-C(35)	119.7(3)
C(34)-C(35)-C(36)	120.5(4)
C(35)-C(36)-C(31)	120.9(4)
C(42)-C(41)-C(46)	117.7(3)
C(42)-C(41)-P(1)	123.8(2)
C(46)-C(41)-P(1)	118.4(2)
C(41)-C(42)-C(43)	120.5(3)
C(44)-C(43)-C(42)	121.1(3)
C(43)-C(44)-C(45)	119.0(3)
C(44)-C(45)-C(46)	120.6(3)
C(45)-C(46)-C(41)	121.1(3)
C(52)-C(51)-C(56)	118.7(3)
C(52)-C(51)-P(1)	117.2(2)
C(56)-C(51)-P(1)	124.1(2)
C(53)-C(52)-C(51)	120.7(3)
C(54)-C(53)-C(52)	120.5(3)
C(53)-C(54)-C(55)	119.7(3)
C(54)-C(55)-C(56)	120.6(3)
C(51)-C(56)-C(55)	119.9(3)
C(66)-C(61)-C(62)	117.7(3)

Table 13 (Continued).

Atom	Angle (°)
C(61)-C(62)-C(63)	121.4(3)
C(64)-C(63)-C(62)	119.5(4)
C(65)-C(64)-C(63)	120.1(4)
C(64)-C(65)-C(66)	120.7(4)
C(61)-C(66)-C(65)	120.5(4)
C(2)-N(1)-C(1)	118.3(3)
C(4)-N(2)-C(1)	122.0(3)
C(61)-P(1)-C(51)	103.56(13)
C(61)-P(1)-C(41)	104.10(13)
C(51)-P(1)-C(41)	103.39(13)
C(61)-P(1)-Cu(1)	110.19(9)
C(51)-P(1)-Cu(1)	118.16(10)
C(41)-P(1)-Cu(1)	115.88(9)
C(31)-P(2)-C(11)	104.29(14)
C(31)-P(2)-C(21)	101.53(13)
C(11)-P(2)-C(21)	101.72(13)
C(31)-P(2)-Cu(1)	115.73(10)
C(11)-P(2)-Cu(1)	113.14(9)
C(21)-P(2)-Cu(1)	118.44(10)
C(1)-S(1)-Cu(1)	109.81(10)

Table 14 Non-hydrogen inerbond angles of [CuBr(PPh₃)₂(dmpyntH)] (4).

Atom	Angle (°)
P(1)-Cu(1)-P(2)	125.16(5)

Table 14 (Continued).

Atom	Angle (°)
P(1)-Cu(1)-S(1)	112.54(5)
P(2)-Cu(1)-S(1)	99.21(5)
P(1)-Cu(1)-Br(1)	104.80(4)
P(2)-Cu(1)-Br(1)	104.28(4)
S(1)-Cu(1)-Br(1)	110.26(4)
C(6)-C(1)-C(2)	116.9(5)
C(6)-C(1)-P(1)	123.5(4)
C(2)-C(1)-P(1)	119.6(4)
C(1)-C(2)-C(3)	121.4(6)
C(4)-C(3)-C(2)	120.3(6)
C(5)-C(4)-C(3)	119.4(6)
C(4)-C(5)-C(6)	120.7(6)
C(1)-C(6)-C(5)	121.3(6)
C(12)-C(7)-C(8)	119.1(5)
C(12)-C(7)-P(1)	123.8(5)
C(8)-C(7)-P(1)	117.0(4)
C(7)-C(8)-C(9)	120.4(6)
C(10)-C(9)-C(8)	119.7(7)
C(11)-C(10)-C(9)	121.0(7)
C(10)-C(11)-C(12)	120.4(7)
C(7)-C(12)-C(11)	119.3(6)
C(14)-C(13)-C(18)	118.4(5)
C(14)-C(13)-P(1)	124.3(4)
C(18)-C(13)-P(1)	117.1(4)
C(13)-C(14)-C(15)	119.8(5)
C(16)-C(15)-C(14)	121.0(6)
C(15)-C(16)-C(17)	119.4(6)

Table 14 (Continued).

Atom	Angle (°)
C(16)-C(17)-C(18)	120.8(6)
C(24)-C(19)-P(2)	124.5(4)
C(20)-C(19)-P(2)	118.3(4)
C(21)-C(20)-C(19)	121.0(5)
C(22)-C(21)-C(20)	121.1(5)
C(21)-C(22)-C(23)	118.1(5)
C(22)-C(23)-C(24)	121.8(5)
C(23)-C(24)-C(19)	120.8(5)
C(26)-C(25)-C(30)	117.9(5)
C(26)-C(25)-P(2)	123.4(4)
C(30)-C(25)-P(2)	118.5(4)
C(25)-C(26)-C(27)	120.4(6)
C(28)-C(27)-C(26)	121.1(7)
C(29)-C(28)-C(27)	119.3(6)
C(28)-C(29)-C(30)	120.7(6)
C(25)-C(30)-C(29)	120.7(6)
C(32)-C(31)-C(36)	118.4(5)
C(32)-C(31)-P(2)	124.3(4)
C(36)-C(31)-P(2)	117.3(4)
C(31)-C(32)-C(33)	120.7(5)
C(34)-C(33)-C(32)	120.0(6)
C(35)-C(34)-C(33)	119.3(6)
C(34)-C(35)-C(36)	120.6(6)
C(35)-C(36)-C(31)	121.1(5)
N(2)-C(1A)-N(1)	120.5(4)
N(2)-C(1A)-S(1)	120.1(4)
N(1)-C(1A)-S(1)	119.3(4)

Table 14 (Continued).

Atom	Angle (°)
C(3A)-C(2A)-N(1)	118.3(5)
C(3A)-C(2A)-C(5A)	124.6(5)
N(1)-C(2A)-C(5A)	117.0(5)
C(2A)-C(3A)-C(4A)	118.6(5)
N(2)-C(4A)-C(3A)	122.7(5)
N(2)-C(4A)-C(6A)	116.9(5)
C(3A)-C(4A)-C(6A)	120.4(5)
C(2A)-N(1)-C(1A)	121.6(4)
C(4A)-N(2)-C(1A)	118.2(4)
C(13)-P(1)-C(7)	101.2(2)
C(13)-P(1)-C(1)	101.3(2)
C(7)-P(1)-C(1)	104.3(2)
C(13)-P(1)-Cu(1)	118.33(16)
C(7)-P(1)-Cu(1)	113.06(16)
C(1)-P(1)-Cu(1)	116.49(16)
C(25)-P(2)-C(31)	103.5(2)
C(25)-P(2)-C(19)	104.1(2)
C(31)-P(2)-C(19)	103.1(2)
C(25)-P(2)-Cu(1)	111.02(15)
C(31)-P(2)-Cu(1)	117.97(16)
C(19)-P(2)-Cu(1)	115.59(15)
C(1A)-S(1)-Cu(1)	110.34(17)

Table 15 Non-hydrogen inerbond angles of $[\text{CuBr}(\text{PPh}_3)_2(\text{dmpymtH})]$ (5).

Atom	Angle ($^{\circ}$)
P(1)-Cu(1)-P(2)	114.86(2)
P(1)-Cu(1)-S(1)	107.15(3)
P(2)-Cu(1)-S(1)	108.78(3)
P(1)-Cu(1)-I(1)	107.865(19)
P(2)-Cu(1)-I(1)	104.911(19)
S(1)-Cu(1)-I(1)	113.45(2)
C(29)-C(28)-C(27)	119.6(3)
C(2A)-N(1)-C(1A)	122.6(2)
C(4A)-N(2)-C(1A)	118.5(2)
C(13)-P(1)-C(7)	102.89(11)
C(13)-P(1)-C(1)	103.01(11)
C(7)-P(1)-C(1)	104.13(11)
C(13)-P(1)-Cu(1)	117.34(8)
C(7)-P(1)-Cu(1)	110.24(8)
C(1)-P(1)-Cu(1)	117.50(8)
C(31)-P(2)-C(19)	104.13(11)
C(31)-P(2)-C(25)	102.53(12)
C(19)-P(2)-C(25)	102.73(11)
C(31)-P(2)-Cu(1)	112.71(8)
C(19)-P(2)-Cu(1)	118.85(8)
C(25)-P(2)-Cu(1)	114.05(8)
C(1A)-S(5)-Cu(1)	113.55(9)
C(26)-C(25)-C(30)	118.6(3)
C(26)-C(25)-P(2)	117.5(2)
C(30)-C(25)-P(2)	123.8(2)
C(35)-C(36)-C(31)	121.5(3)
C(32)-C(31)-C(36)	118.2(2)

Table 15 (Continued).

Atom	Angle (°)
C(32)-C(31)-P(2)	124.2(2)
C(36)-C(31)-P(2)	117.6(2)
C(8)-C(7)-C(12)	118.5(2)
C(8)-C(7)-P(1)	123.14(19)
C(12)-C(7)-P(1)	118.09(19)
C(18)-C(13)-C(14)	118.3(3)
C(18)-C(13)-P(1)	118.8(2)
C(14)-C(13)-P(1)	122.9(2)
C(21)-C(20)-C(19)	120.6(2)
C(24)-C(19)-C(20)	118.6(2)
C(24)-C(19)-P(2)	119.03(18)
C(20)-C(19)-P(2)	122.40(19)
N(2)-C(1A)-N(1)	119.4(2)
N(2)-C(1A)-S(1)	120.94(19)
N(1)-C(1A)-S(1)	119.69(19)
C(16)-C(15)-C(14)	120.2(3)
C(6)-C(1)-C(2)	118.4(2)
C(6)-C(1)-P(1)	123.1(2)
C(2)-C(1)-P(1)	118.6(2)
C(19)-C(24)-C(23)	120.3(2)
C(11)-C(12)-C(7)	120.8(3)
C(22)-C(23)-C(24)	120.5(3)
C(29)-C(30)-C(25)	120.6(3)
N(2)-C(4A)-C(3A)	122.4(2)
N(2)-C(4A)-C(6A)	116.0(3)
C(3A)-C(4A)-C(6A)	121.6(3)
C(2A)-C(3A)-C(4A)	119.6(3)

Table 15 (Continued).

Atom	Angle (°)
C(22)-C(21)-C(20)	120.2(3)
C(25)-C(26)-C(27)	120.3(3)
C(5)-C(6)-C(1)	120.3(3)
C(15)-C(14)-C(13)	120.2(3)
C(10)-C(11)-C(12)	119.8(3)
C(9)-C(8)-C(7)	120.1(3)
C(13)-C(18)-C(17)	120.7(3)
C(31)-C(32)-C(33)	120.2(3)
C(23)-C(22)-C(21)	119.8(3)
C(9)-C(10)-C(11)	119.7(3)
C(34)-C(35)-C(36)	119.8(3)
C(3)-C(2)-C(1)	120.8(3)
C(3A)-C(2A)-N(1)	117.6(3)
C(3A)-C(2A)-C(5A)	125.6(3)
N(1)-C(2A)-C(5A)	116.8(3)
C(16)-C(17)-C(18)	120.3(3)
C(17)-C(16)-C(15)	120.2(3)
C(34)-C(33)-C(32)	120.0(3)
C(35)-C(34)-C(33)	120.3(3)
C(4)-C(5)-C(6)	120.2(3)
C(4)-C(3)-C(2)	120.0(3)
C(3)-C(4)-C(5)	120.2(3)
C(28)-C(29)-C(30)	120.5(3)
C(10)-C(9)-C(8)	121.1(3)
C(28)-C(27)-C(26)	120.4(3)

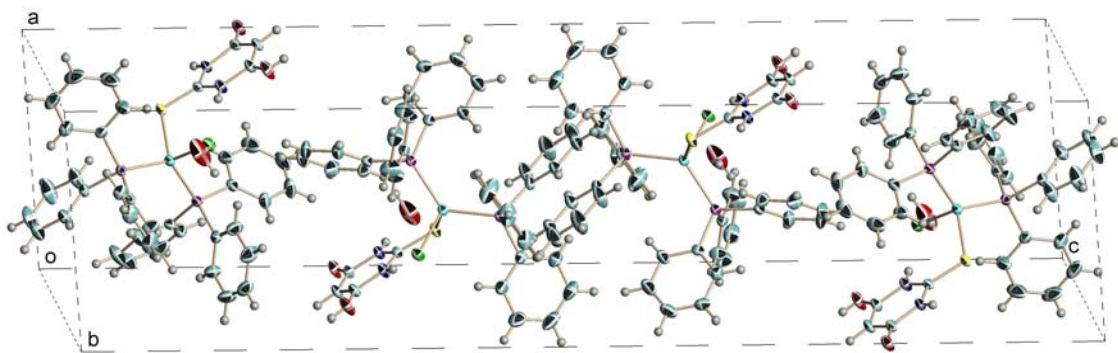


Figure 60 Unit cell contents of $[\text{CuCl}(\text{PPh}_3)_2(\text{TBA})] \cdot 2\text{H}_2\text{O}$ (1).

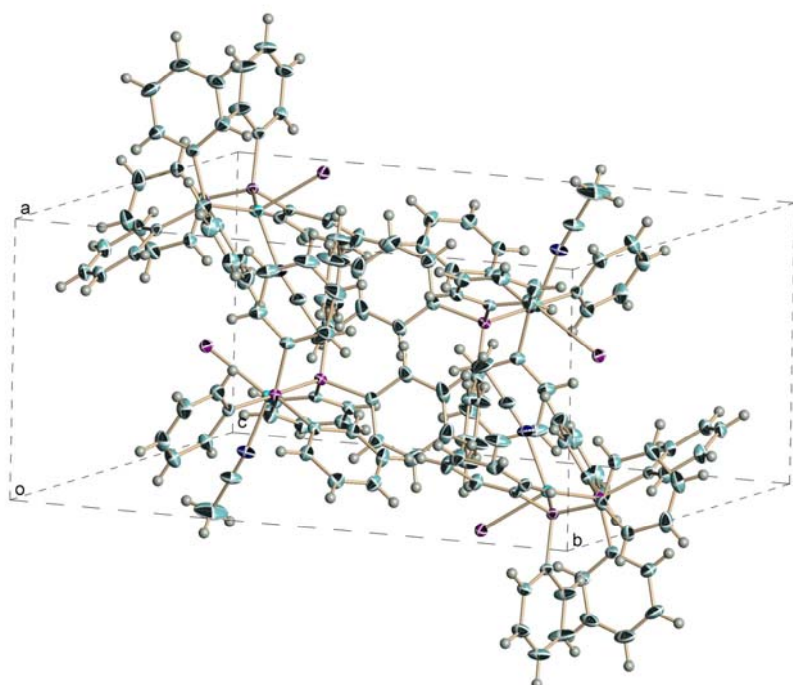


Figure 61 Unit cell contents of $[\text{CuI}(\text{PPh}_3)_2(\text{CH}_3\text{CN})]$ (2).

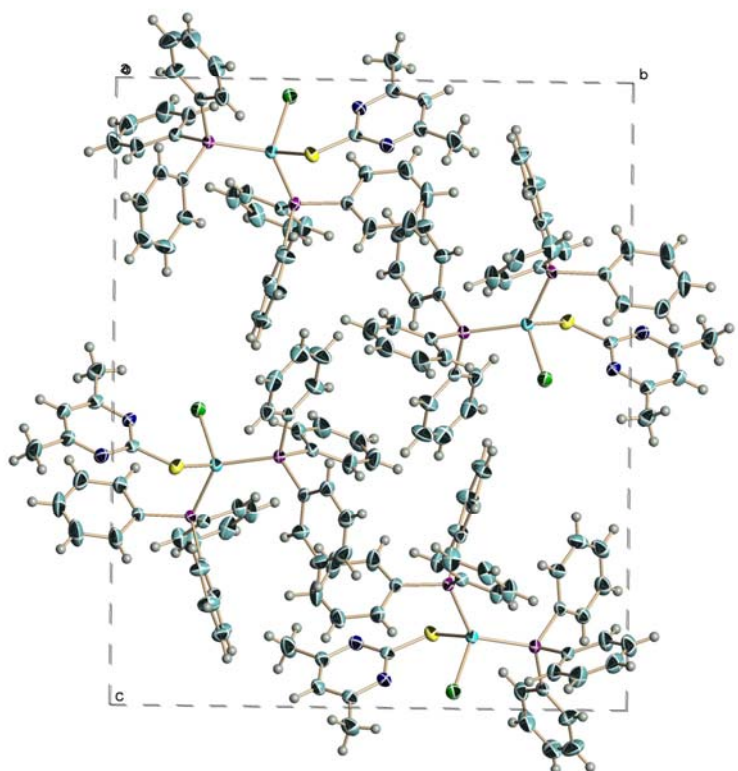


Figure 62 Unit cell contents of $[\text{CuCl}(\text{PPh}_3)_2(\text{dmpymtH})]$ (3) and $[\text{CuBr}(\text{PPh}_3)_2(\text{dmpymtH})]$ (4).

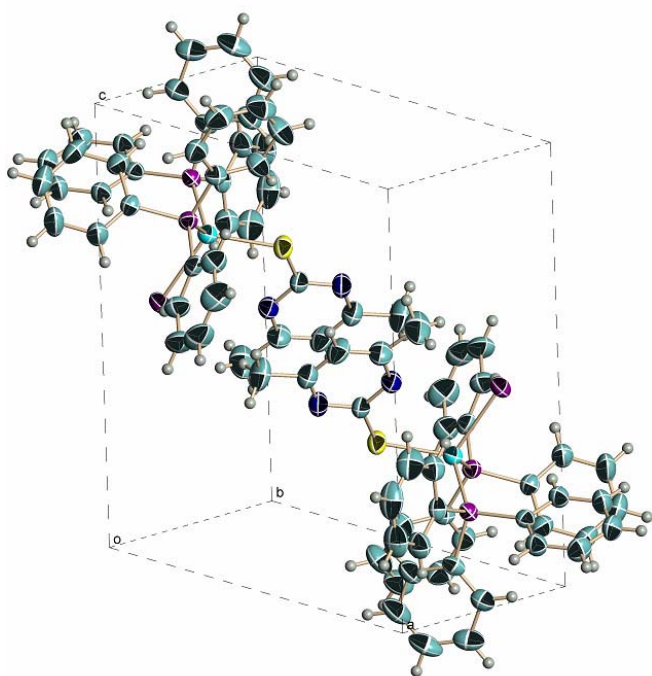


Figure 63 Unit cell contents of $[\text{CuI}(\text{PPh}_3)_2(\text{dmpymtH})]$ (5)

CHAPTER 4

Discussion

4.1 Preparation of complexes

Reaction by refluxing of copper(I) halide with triphenylphosphine in the molar ratio of 1:2 in acetonitrile formed a product of stoichiometry $[\text{Cu}(\text{PPh}_3)_2\text{X}]$ ($\text{X} = \text{Cl}, \text{Br}, \text{I}$) which after addition of one equivalent of heterocyclic thiones, 2-thiobarbituric acid (TBA) or 4,6-dimethylpyrimine-2(1*H*)-thione (dmpytmH) yielded a monomeric tetrahedral complex $[\text{CuCl}(\text{PPh}_3)_2(\text{TBA})]\cdot\text{H}_2\text{O}$ (1), $[\text{CuCl}(\text{PPh}_3)_2(\text{dmpytmH})]$ (3), $[\text{CuBr}(\text{PPh}_3)_2(\text{dmpytmH})]$ (4) or $[\text{CuI}(\text{PPh}_3)_2(\text{dmpytmH})]$ (5). This procedure, frequently used for the preparation copper(I) halide complexes containing both heterocyclic thione and triphenylphosphine ligands, which gave a good yield (70-75%) for this practical synthesis. However, another procedure by ultrasonic irradiation of the reaction of copper(I) iodide with 2-thiobarbituric acid with the presence of triphenylphosphine in acetonitrile did not form a similar complex, it rather formed an unknown $[\text{CuI}(\text{PPh}_3)_2(\text{CH}_3\text{CN})]$ (2) complex in the absence of 2-thiobarbituric acid in low yield (10%). The coordination of counterion is strongly dependent on the reactant mole ratios, the nature of solvent, the reaction time employed as well as the reaction temperature.

The colors of synthesized complexes were different: complex (1) was pink, complex (2) was colorless, complex (3), (4) and (5) were yellow. These complexes are stable in air and moisture without decomposition. Complexes (1) and (2) are generally soluble in common organic solvents such as acetone, methanol, ethanol and dimethylsulfoxide but fairly soluble in chloroform, while complexes (3), (4) and (5) are soluble in acetone, chloroform and are sparingly soluble in dimethylsulfoxide.

4.2 Elemental analysis

The results in determining the contents of carbon, hydrogen, nitrogen sulfur and oxygen in complexes by CHNS-O Elemental Analyzer are reported. The experimental (%) values are given in Table 3 in which they are in close agreement with the corresponding theoretical values and the experimental data are slightly different from the theoretical data because of the impurity, the moisture and how sensitive of samples to the air.

4.3 X-ray Fluorescence spectrometry

X-ray fluorescence (XRF) analysis is a convenient method for identifying elements in a material. From XRF spectra of $[\text{CuCl}(\text{PPh}_3)_2(\text{TBA})]\cdot\text{H}_2\text{O}$ (1), $[\text{CuCl}(\text{PPh}_3)_2(\text{dmpytmH})]$ (3), $[\text{CuBr}(\text{PPh}_3)_2(\text{dmpytmH})]$ (4) and $[\text{CuI}(\text{PPh}_3)_2(\text{dmpytmH})]$ (5) complexes which the $\text{K}\alpha$ spectrum of Cu, Cl, Br and I appears at 8.04, 2.62, 11.92 and 28.65 keV, respectively, represented for copper(I) salts. In addition, S is represented for TBA and dmpytmH, in which the $\text{K}\alpha$ spectrum appears at 2.32 keV and P is represented for PPh_3 , in which the $\text{K}\alpha$ spectrum appears at 2.01 keV. The XRF spectra of all complexes are shown in Figures 29-38.

4.4 Infrared spectroscopy

The main IR data of 2-thiobarbituric acid (TBA), agree with the previous literature (Refat *et al.*, 2003) and its complex ($[\text{CuCl}(\text{PPh}_3)_2(\text{TBA})]\cdot\text{H}_2\text{O}$) (1) are summarized in table 16. The main IR data of 2-thiobarbituric acid in the solid state do not contain $\nu(\text{SH})$ band in the region 2500 cm^{-1} (Sight *et al.*, 2008). This indicates that the ligand does not contain free SH group in the solid state. A comparison of the IR spectra of the TBA ligand and the copper(I) complex as follow:

1. The spectra of the complex exhibit a sharp band at 3613 cm^{-1} , which attributed to symmetric $\nu_s(\text{OH})$ stretching frequency of the hydroxyl group. This indicates an unbounded hydroxyl group, which consistent with the result from X-ray

structure analysis. Furthermore the strong band appears at 3382 is assigned to $\nu_s(\text{OH})$ of associated water molecule.

2. The carbonyl absorption band, $\nu(\text{C=O})$ of the ligand at 1722 cm^{-1} becomes weak appearance at 1732 cm^{-1} , and 1712 cm^{-1} in the spectrum of the complex due to the hydrogen bonding in the complex. Moreover, the $\nu(\text{N-H})$ band shifts towards the lower frequency region by 14 cm^{-1} at 1584 cm^{-1} correspond to the strongly hydrogen bonded NH groups as have been observed for heterocyclic thione complexes (Singh *et al.*, 2008)

3. The sharp bands at 1273 and 1243 cm^{-1} of the ligand are assigned to $\nu(\text{C-N}) + \nu(\text{C=S})$ and $\nu(\text{C=N}) + \nu(\text{C-S})$, respectively which are disappeared in the complex, indicating the involvement of C=S group in coordination. This is also supported by the upward shifts of 14 cm^{-1} at 1584 cm^{-1} for $\sigma(\text{N-H}) + \nu(\text{C=C})$; $\nu(\text{C=O}) + \nu(\text{C=N})$ band and a downward shifts of 26 cm^{-1} at 1325 cm^{-1} for $\nu(\text{C=N}) + \nu(\text{C=S})$ band. All of these bands are typical of the thione structure. Thus, the infrared spectra provide experimental evidence that TBA ligand coordinated to copper atom in the thione forms, in agreement with earlier reports in the literature (Balas *et al.*, 2008).

The bands of a 4,6-dimethylpyrimine-2(1H)-thione (dmpytmH), which agree with the previous literature (Martos-Calvente *et al.*, 2003), and its complexes ($[\text{CuCl}(\text{PPh}_3)_2(\text{dmpytmH})]$ (3), $[\text{CuBr}(\text{PPh}_3)_2(\text{dmpytmH})]$ (4) and $[\text{CuI}(\text{PPh}_3)_2(\text{dmpytmH})]$ (5) are shown in Table 17. The infrared spectra of the ligand provide experimental evidence that thione is dominant species in the solid state, in agreement with earlier report in the literature (Martos-Calvente *et al.*, 2003). A comparison of the IR spectra of the ligand and the copper(I) complexes as follow:

1. A broad band at 3450 cm^{-1} of the ligand is attributed to $\nu(\text{N-H})$ interacting with residual water in the IR wafer, which shifts slightly towards the lower frequency at 3445 cm^{-1} of the three copper(I) complexes. It indicates that in these complexes the NH group is not involved in coordination.

2. A sharp band at 1432 cm^{-1} of the ligand is assigned to $\nu(\text{C=N}) + \delta(\text{CH}) + \delta(\text{NH})$ vibrations, which shifts slightly towards the higher frequency region at 1434 cm^{-1} of the three copper(I) complexes. In addition, the sharp bands at 1230 and 1188 cm^{-1} of the ligand are attributed to $\nu(\text{C=S})$ in NHC=S group, which shift towards the

lower frequency region at 1226 and 1186 cm⁻¹ of the complexes. All these observations clearly indicate the involvement of the C=S group in coordination, in agreement with earlier report in the literature (Singh *et al.*, 2008).

Bonding through the sulfur atom of complexes 1 and 3-5 is favored because copper(I), is a soft acid, should prefer to interact with a soft base such as sulfur donor atom ligand. Furthermore, the characteristic $\nu(P-C_{ph})$ bands at 1092 cm⁻¹ in (1) and 1093 cm⁻¹ in (3)-(5) increase in frequency and intensity compare with PPh₃ ligand. This indicates P-metal coordination which confirms the presence of triphenylphosphine in the coordinated form in the complexes, in a close resemblance with triphenylphosphine complexes analog (Lobana *et al.*, 2006).

Table 16 IR frequencies (cm⁻¹) of TBA and complex [CuCl(PPh₃)₂(TBA)]·H₂O (1).

vibration	Band, cm ⁻¹	
	TBA	Complex (1)
$\nu(O-H)$	3567	3613
$\nu(N-H)$	3109	3047
$\nu(C=O)$	1722, 1690	1732, 1712
$\delta(N-H) + \nu(C=C);$	1570	1584
$\nu(C=O) + \nu(C=N)$		
$\delta(N-H)$	1400	1432
$\nu(C=N) + \nu(C=S)$	1351	1325
$\delta(O-H)$	1305	1267
$\nu(C-N) + \nu(C=S)$	1273	
$\nu(C=N) + \nu(C-S)$	1243	
$\nu(C-O), \nu(CS) + \nu(CN)$	1166	1162
$\delta(C-H)$	934, 801	930, 800
$\nu(P-C_{ph})$		1092

Table 17 IR frequencies (cm^{-1}) of dmpymtH and complexes

[CuCl(PPh₃)₂(dmpymtH)] (3), [CuBr(PPh₃)₂(dmpymtH)] (4) and
 [CuI(PPh₃)₂(dmpymtH)] (5).

vibration	Band, cm^{-1}			
	dmpymtH	complex (3)	complex (4)	complex (5)
$\nu(\text{N-H})$	3450 w	3445w	3445w	3445w
$\nu(\text{C-H})\text{asym}$	3185m, 3140m	3180w, 3134w	3180w, 3134w	3180w, 3134w
$\nu(\text{N-H})\text{sym}$	3030-2920s	3050-2918	3049-2918	3050-2918
$\nu(\text{C=C}) + \nu(\text{C=N})$	1624vs, 1565vs	1617s, 1562s	1615s, 1561s	1614s, 1562s
$\nu(\text{C=N}) + \delta(\text{CH}) + \delta(\text{NH})$	1432s	1434s	1434s	1433s
$\nu(\text{C=S})$ in NHC=S	1230vs, 1188s	1225, 1186	1226, 1186	1226, 1186
CH ₃ rocking	1032m, 952m	1027m, 950m	1027m, 950m	1027m, 950m
Ring streaching, $\beta(\text{N-H})$	980s	978w	979w	979w
$\gamma(\text{N-H})$	850s	848s	849s	849s
$\nu(\text{C=S}), \beta(\text{C=S})$	461s	462s	462s	462s
$\nu(\text{P-C}_{\text{ph}})$		1093vs	1093vs	1093vs

4.2 ^1H NMR and ^{13}C NMR Spectroscopy

The prevailance of the thione tautomer in the complexes is further confirmed by the ^1H NMR spectra of the compounds. The ^1H NMR spectra of TBA, dmpymtH ligands and their complexes are shown in Table 18. To facilitate band identification, the atoms are clearly labeled in Figure 64.

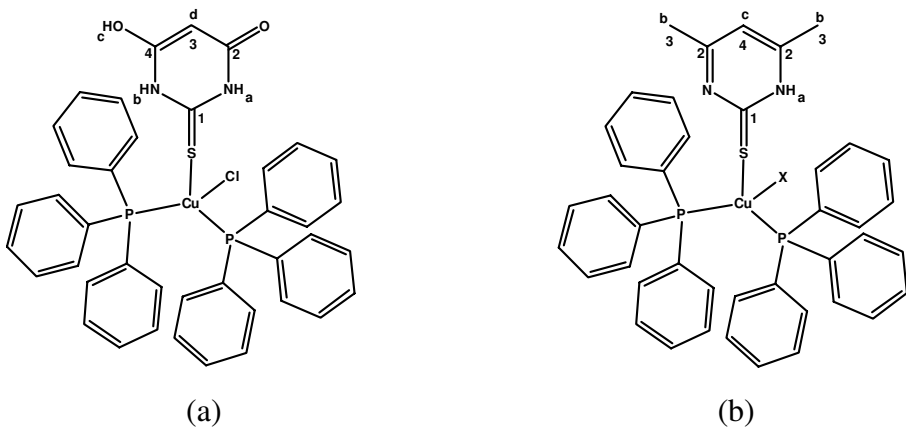


Figure 64 Atom nomenclature employed for NMR assignments, (a) complex (1),
 (b) complexes (3)-(5).

As already reported (Garcia *et al.*, 1996) the ^1H and ^{13}C NMR spectra of TBA suggest that in $\text{DMSO}-d_6$ solution the distribution of charge in this molecule is mainly determined by the two keto-enol tautomeric forms (Figure 64). These keto-enol forms can undergo both $-\text{OH}$ and $-\text{NH}$ deprotonation, and both O- and N-coordination.

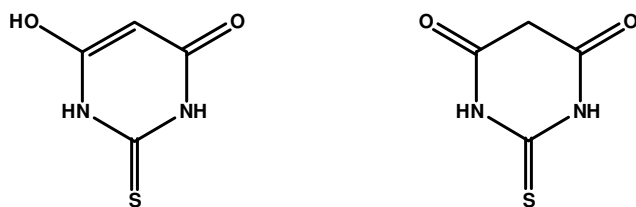


Figure 65 Two keto-enol tautomeric forms of 2-thiobarbituric acid.

The ^1H NMR spectra of TBA in $\text{DMSO}-d_6$ show two peaks, the first at δ 4.92 ppm which is assigned to C3 proton of the pyrimidine ring and the second is at δ 12.23 ppm with integration corresponds to two NH and one OH protons as a result of enol-ketone tautomerisms takes place (Refat *et al.*, 2008). The spectra of complex (1) in $\text{DMSO}-d_6$ like the spectra of TBA but the peaks have been shifted at δ 4.95 and δ 12.59 ppm for C3 proton and NH, respectively, confirming the formation of the complex.

The ^1H NMR spectra of the complexes (3)-(5) in DMSO- d_6 reveal the presence of NH protons in the range of 13.95-13.76 ppm which are downfield compared to the free ligand, indicating that the ligand coordinates to the copper ion as a neutral ligand, probably through the sulfur atom only (Singh *et al.*, 2008). Free dmpyntH ligand also shows resonance signals at δ 2.20 and δ 6.52 ppm due to methyl group and C4 proton, which shifted to δ 2.32 and δ 6.33, respectively.

The ^{13}C NMR spectra of the complexes display signals associated with TBA, dmpyntH and PPh₃ ligands. The position and integrated intensities of various resonances supported well with the presence of TBA or dmpyntH and formulation of the complexes. The thione carbon in the complex (1) resonates at 173.10 and 170.62 ppm due to keto-enol tautomeric forms (Me'ndez *et al.*, 2006), while complexes (3)-(5) resonates at 178.33-179.26 ppm, which upfield compared to the free ligand, suggesting involvement of the thione sulfur in bonding (Singh *et al.*, 2008).

Table 18 Experimental ^1H NMR spectra of the compounds in DMSO- d_6 solvent.

compounds	Atom [*]	signal	Chemical shift
			δ , ppm
Ligand TBA	H _a , H _b (2H)	s	12.23
	H _d (1H)	s	4.92
[CuCl(PPh ₃) ₂ (TBA)]·H ₂ O (1)	H _a , H _b (2H)	s	12.59
	H _d (1H)	s	4.95
	C ₆ H ₅ group (30H)	m	7.26-7.38
Ligand dmpyntH	H _a (1H)	s	13.45
	H _b (6H)	s	2.20
	H _c (1H)	s	6.52
[CuCl(PPh ₃) ₂ (dmpyntH)] (2)	H _a (1H)	s	13.95
	H _b (6H)	s	2.32
	H _c (1H)	s	6.33
	C ₆ H ₅ group (30H)	m	7.26-7.42

compounds	Atom [*]	signal	Chemical shift
			δ , ppm
$[\text{CuBr}(\text{PPh}_3)_2(\text{dmpytmH})]$ (3)	H _a (1H)	s	13.87
	H _b (6H)	s	2.32
	H _c (1H)	s	6.33
	C ₆ H ₅ group (30H)	m	7.26-7.44
$[\text{CuI}(\text{PPh}_3)_2(\text{dmpytmH})]$ (4)	H _a (1H)	s	13.76
	H _b (6H)	s	2.32
	H _c (1H)	s	6.33
	C ₆ H ₅ group (30H)	m	7.26-7.43

^x Proton nomenclature are indicated in the respective compounds in Figure 64.

Table 19 Experimental ¹³C NMR spectra of the compounds in DMSO-d₆ solvent.

compounds	Atom [*]	Chemical shift
		δ , ppm
Ligand TBA	C(1)	181.81, 175.92
	C(2), C(4)	166.85, 162.91
	C(5)	82.84
$[\text{CuCl}(\text{PPh}_3)_2(\text{TBA})]\cdot\text{H}_2\text{O}$ (1)	C(1)	173.10, 170.62
	C(2), C(4)	160.83
	C(5)	78.82
	C ₆ H ₅ group	128.96-133.93
Ligand dmpytmH	C(1)	181.77
	C(2)	159.37
	C(3)	22.01
	C(4)	110.62

compounds	Atom [*]	Chemical shift
		δ , ppm
$[\text{CuCl}(\text{PPh}_3)_2(\text{dmpymtH})]$ (3)	C(1)	179.23
	C(2)	140.21
	C(3)	22.54
	C(4)	110.82
	C_6H_5 group	128.17-134.29
$[\text{CuBr}(\text{PPh}_3)_2(\text{dmpymtH})]$ (4)	C(1)	178.76
	C(2)	140.11
	C(3)	22.50
	C(4)	110.66
	C_6H_5 group	128.15-134.30
$[\text{CuI}(\text{PPh}_3)_2(\text{dmpymtH})]$ (5)	C(1)	178.62
	C(2)	140.08
	C(3)	22.48
	C(4)	110.59
	C_6H_5 group	128.16-134.29

* Carbon numbers are indicated in the respective compounds in Figure 63..

4.6 X-ray structure determination

4.6.1 The structure of $[\text{CuCl}(\text{PPh}_3)_2(\text{TBA})]\cdot\text{H}_2\text{O}$ (1)

Complex (1) crystallizes in the monoclinic unit cell space group $P2_1/c$. The structure of this mixed-ligand complex displays the distorted tetrahedral coordination of the copper(I) center, which is surrounded by the sulfur donor of the 2-thiobarbituric acid ligand, two phosphorous atoms of triphenylphosphine groups one chlorine atom, as well as one lattice water molecule (Figure 66). The arrangement is considerably distorted since the phosphorous angle at metal site, P-Cu-P with a value of $124.70(3)^\circ$, is much larger than the tetrahedral value 109.4° . This higher angle is counterbalanced by the bond angles of Cl-Cu-P(1), Cl-Cu-P(2), S-Cu-P(1) and S-Cu-

P(2) whose values are $107.45(3)^\circ$, $99.30(3)^\circ$, $109.71(3)^\circ$ and $108.11(3)^\circ$, respectively. The tetrahedral distortion is due to steric imposition of the bulky of phosphine ligands and was observed previously in a series of analogous complexes. For instance, the P-Cu-P angles of $122.36(5)^\circ$ in $[\text{Cu}(\text{PPh}_3)_2(\text{bztzdtHCl})\cdot\text{CH}_3\text{COCH}_3]$; where bztzdtH is benz-1,3-thiazolidine-2-thione (Voutsas and Kokkou, 1995) and $[\text{Cu}(\text{PPh}_3)_2(\text{tzdtHCl})]$; where tzdtH is 1,3-thiazolidine-2-thione (Aslanidis, *et al.*, 1998). The two Cu-P(1) and Cu-P(2) bond distances of $2.2943(8)$ Å and $2.2757(8)$ Å are in accordance with that found in the above corresponding complexes.

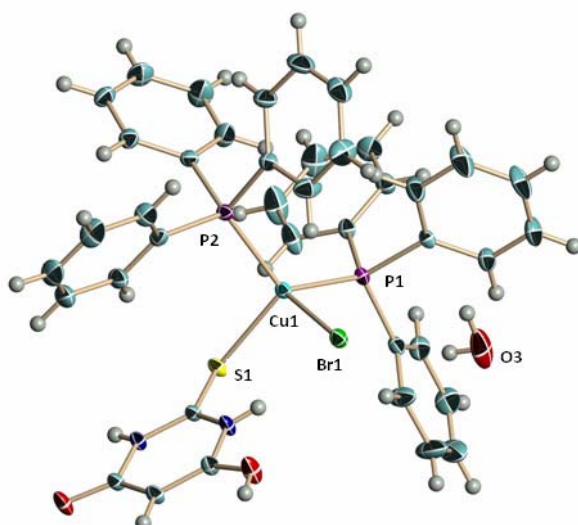


Figure 66 The structure of $[\text{CuCl}(\text{PPh}_3)_2(\text{TBA})]\cdot\text{H}_2\text{O}$ (1). Ellipsoids are drawn at the 30% probability level.

Regarding the geometrical characteristic of heterocyclic ring in the thione unit, coordination to copper(I) causes the Cu-S bond distance of $2.3620(8)$ Å, which is large with the value observed in tetrahedrally coordinated copper(I) halide complexes with thione-S donors such as $[\text{CuBr}(\text{dppe})(\text{py}_2\text{SH})_2]$ with Cu-S bond distance of $2.3456(13)$ Å (Cox *et al.*, 2000). The short non-bonding distance in the molecule $\text{H}(\text{N}(2))\cdots\text{Cl}$ and $\text{O}3(\text{H}_2\text{O})\cdots\text{Cl}$ can be accepted as an intramolecular hydrogen bond with the geometry $\text{N}(2)\cdots\text{Cl} = 3.082(3)$ Å, $\text{H}(\text{N}(2))\cdots\text{Cl} = 2.32(3)$ Å, $\text{N}(2)\cdots\text{H}(\text{N}(2))\cdots\text{Cl} = 169(3)^\circ$ and $\text{O}(3)(\text{H}_2\text{O})\cdots\text{Cl} = 3.140(3)$ Å, $\text{H}(2)(\text{O}(3))\cdots\text{Cl} = 2.43(2)$ Å, $\text{O}3\cdots\text{H}2(\text{H}_2\text{O})\cdots\text{Cl} = 150(3)^\circ$ (Figure 67). Moreover the water molecule of this complex interlinks the neutral $[\text{CuCl}(\text{PPh}_3)_2(\text{TBA})]$ units through hydrogen bonds to

form a one-dimensional (1D) chain (Figure 68). In addition, the hydrogen bonding interactions between TBA ligands of neighbor chains through O-H \cdots O hydrogen bonds combined two chains to form a 1D supramolecular double-chains to stabilize the structure.

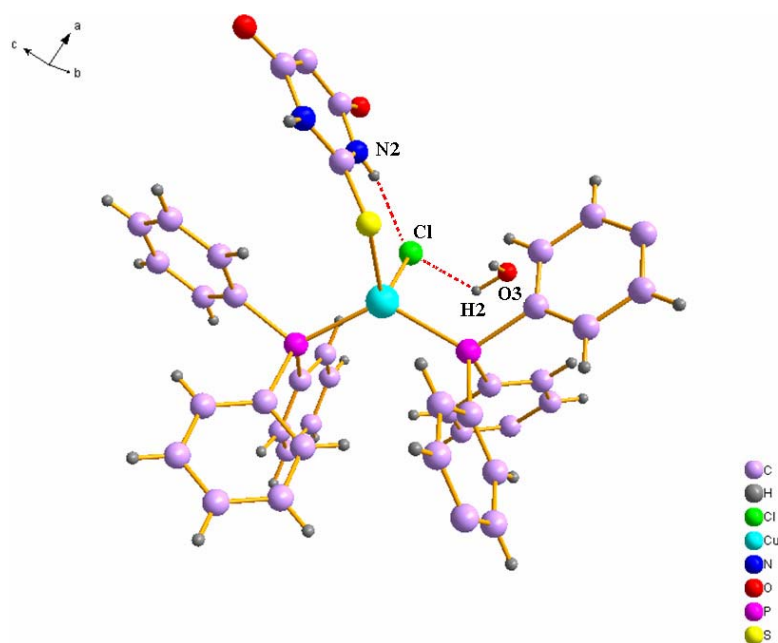


Figure 67 The intra-interaction hydrogen bonding in complex (1).

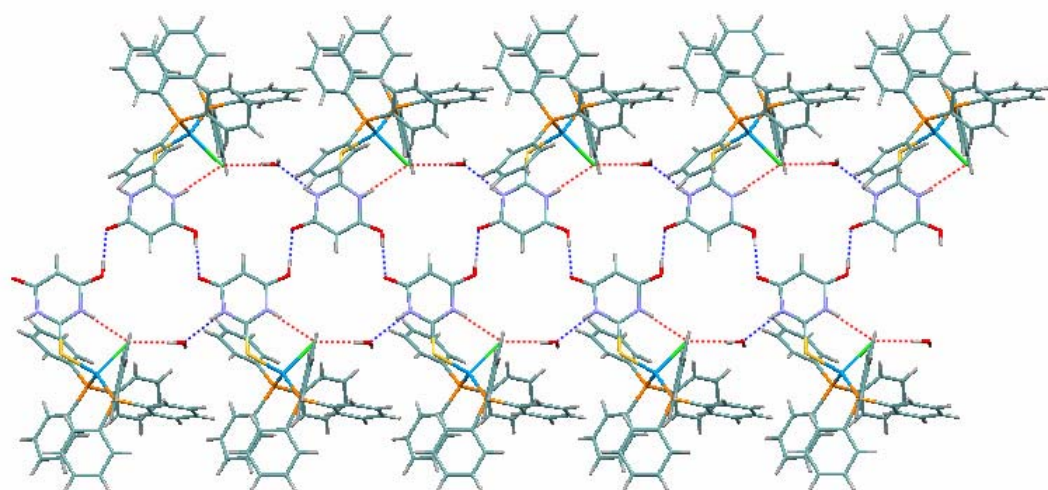


Figure 68 1D supramolecular double-chains of complex (1).

4.6.2 The structures of $[\text{CuI}(\text{PPh}_3)_2(\text{CH}_3\text{CN})]$ (2)

The structure of complex (2) reveals the copper(I) ion residing in a distorted tetrahedral geometry with two triphenylphosphine groups bound through phosphorous atoms, with one iodine atom and with coordination completed by an acetonitrile molecule through nitrogen atom. This complex is mononuclear and crystallizes in the monoclinic space group $P2_1/c$ with four formula units in the unit cell (Figure 69).

Focusing on the geometry of the solvent ligand, the Cu-N bond distance of 2.065(3) Å is slightly longer as compared to the other four-coordinate copper(I)-acetonitrile complexes, 1.939(5) Å for $[\text{Cu}_2([\text{18}]\text{aneS}_6)(\text{NCMe})_2] \cdot (\text{ClO}_4)_2$ (Blake, *et al.*, 1990) and 1.923(4) Å for $[\text{LCu}(\text{CH}_3\text{CN})] \cdot (\text{PF}_6)$ (Conry *et al.*, 1999). The acetonitrile ligand is almost linear with the N-C-C angle of 179.2(6)°, as is typical for copper(I)-acetonitrile complexes, 179.1(4)° for $[\text{LCu}(\text{CH}_3\text{CN})] \cdot (\text{PF}_6)$ (Conry *et al.*, 1999) and 179.0(1)° for $[\text{Cu}_2(\text{L})_2\text{CH}_3\text{CN}] [\text{Cu}(\text{L})\text{CH}_3\text{CN}] \cdot (\text{BF}_4)_3$ (Gennari *et al.*, 2007). The copper-nitrile angle is bent with the Cu-N-C angle of 165.9°, fall within the usual range for transition metal complexes (Endres, 1987).

The distortion is best displayed by the P-Cu-P angles of 123.55(3)° including the two bulkiest ligands , expected to be the largest one within the tetrahedron. The Cu-P(1) and Cu-P(2) bond distances (2.2784(4) Å and 2.2790(8) Å) fall well within the range seen for known tetrahedral mixed ligand copper(I) complexes with triphenylphosphine ligand. In the case of this complex, there is no indication of any specific interaction in the structure.

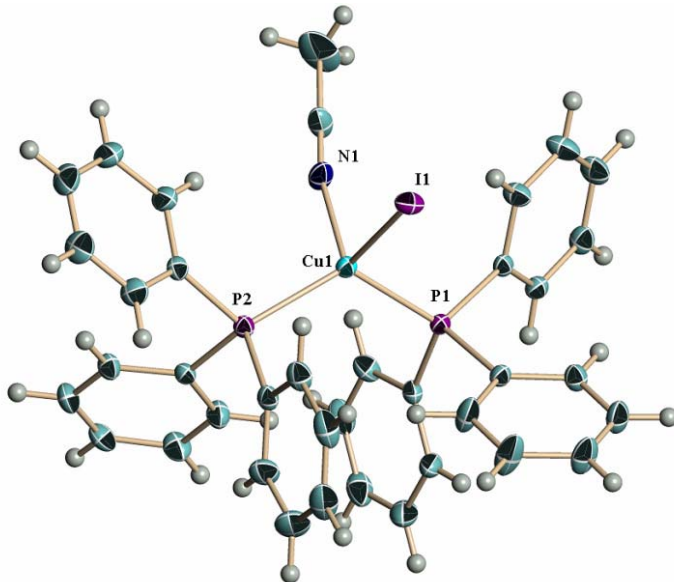


Figure 69 The structure of $[\text{CuI}(\text{PPh}_3)_2(\text{CH}_3\text{CN})]$ (2). Ellipsoids are drawn at the 30% probability level.

4.6.3 The structures of $[\text{CuCl}(\text{PPh}_3)(\text{dmpymtH})]$ (3) and $[\text{CuBr}(\text{PPh}_3)(\text{dmpymtH})]$ (4)

The X-ray structural analyses evidence that the crystal of complex (3) is isomorphous and isostructural with the complex (4) and crystallizes in the monoclinic system with the same space group of $P2_1/c$. Bond distances and bond angles of both complexes are given in Tables 8, 9, 13 and 14 in the chapter result. The both complexes are monomeric and the copper(I) metal ion is four-coordinated forming a distorted tetrahedral geometry. 4,6-Dimethylpyrimidine-2(1*H*)-thione (dmpymtH) ligand acts as monodentate ligand coordinating through the sulfur atom (Figure 70). The other positions of the tetrahedral are occupied by one halogen atom and two triphenylphosphine ligands. The bond angles around copper are approximately in the range of 99-125° in both complexes. Geometrical distortion from ideal angles (109.47°) can be explained by the need to accommodate the bulky triphenylphosphine groups. The nearly equivalent Cu-P bond lengths, average 2.283 Å for both complexes, are as expected for complexes containing two triphenylphosphine ligands. The Cu-S bond lengths are 2.3637(8) Å for complex (3), 2.3691(13) Å for complex (4), as usually found for tetrahedrally coordinated copper(I) and sulfur atom donors.

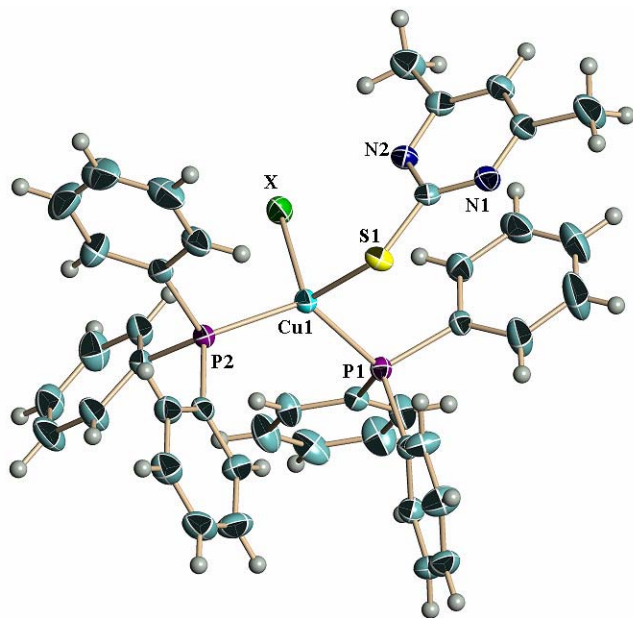


Figure 70 The structure of $[\text{CuX}(\text{PPh}_3)_2(\text{dmpymtH})]$ ($\text{X} = \text{Cl}, \text{Br}$ and I). Ellipsoids are drawn the 30% probability level.

Intramolecular hydrogen bonds are observed between the atoms N(2) and Cl(1) for complex (3), N(2) and Br(1) for complex (4) with $\text{N}(2)\cdots\text{Cl}(1)$ distance of 3.10 Å, $\text{N}(2)\text{-H}(2)\cdots\text{Cl}(1)$ angle of 172.66° and $\text{N}(2)\cdots\text{Br}(1)$ distance of 3.24 Å, $\text{N}(2)\text{-H}(2)\cdots\text{Br}(1)$ angle of 176.22° (Figure 71). Because of the parallel arrangement of the 4,6-dimethylpyrimidine-2(1H)-thione rings of neighbouring units, there exists a $\pi\text{-}\pi$ stacking interaction of 3.370 and 3.410 Å in complexes (3) and (4) respectively as shown in Figure 70. Both hydrogen bonding and $\pi\text{-}\pi$ interactions has been reported for similar systems, for example, in crystal structures of $[\text{Cu}(\text{N}_3)(\text{dmpymtH})(\text{PPh}_3)_2]$ and $[\text{Cu}(\text{NCS})(\text{dmpymtH})(\text{PPh}_3)_2]$ (Lemos, et al., 2001).

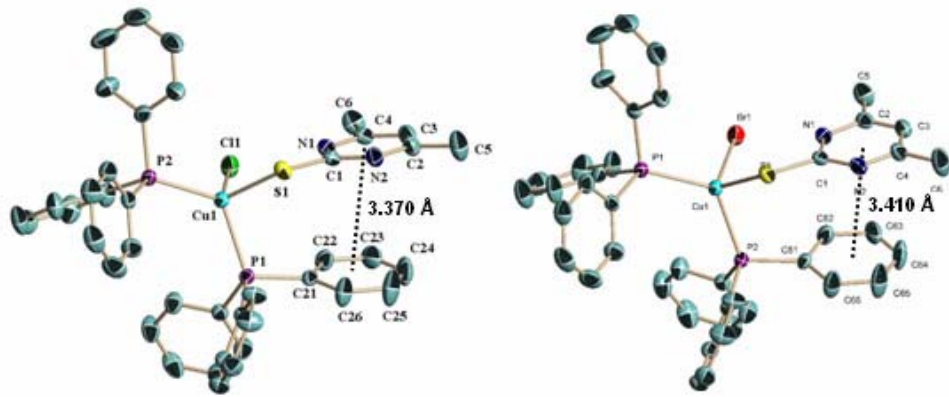


Figure 71 The parallel arrangement of structure of $[\text{CuX}(\text{PPh}_3)_2(\text{dmpymtH})]$ ($\text{X} = \text{Cl}, \text{Br}$).

4.6.4 The structures of $[\text{CuI}(\text{PPh}_3)(\text{dmpymtH})]$ (5)

The structure of complex (5) is similar to the complexes (3) and (4). The space group of complex (5) is identified as triclinic system with space group of $P\bar{1}$. The molecular structure and the packing in unit cell is depicted in Figures 70 and 63, respectively. Selected bond lengths and angles around the Cu(I) atom are presented in table 11 and 16, respectively. Focusing on the comparison of bond distances and bond angles around the metal atom, the Cu-S bond length for complex (5), $2.3407(7)\text{\AA}$, is shorter than complexes (3) and (4), but it is in good agreement with values reported for other copper(I) complexes with heterocyclic thione ligands such as $2.345(3)\text{\AA}$ for $[\text{Cu}(\text{PPh}_3)_2(\text{pymtH})\text{Br}]$ (Aslanidis, 1994) and $2.344(3)\text{\AA}$ for $[\text{CuI}(\text{1ks-imzsH})(\text{PPh}_3)_2]$ (Lobana, 2008). The Cu-P(1) and Cu-P(2) bond distances, $2.2894(7)$ and $2.3039(7)\text{\AA}$, are slightly longer than complexes (3) and (4). The bond distance of Cu-I, $2.6800(3)$, is comparable to those found in $2.6858(10)\text{\AA}$ for $\{[\text{Cu}_2(\text{L1})(\text{PPh}_3)_2\text{I}_2]\cdot 2\text{CH}_2\text{Cl}_2\}_n$ (Zhou, 2006) and $2.6859(4)\text{\AA}$ for $[\text{CuI}(\text{xanthpos})(\text{imdtH}_2)]$ (Cox, 2006). The bond angle P(1)-Cu-P(2) of complexes (5), $114.86(2)^\circ$, is smaller than those found in complexes (3) and (4) cause less distortion than both complexes. In this complex, intramolecular hydrogen bond is also observed between the atoms N(2) and I(1) with N(2) \cdots I(1) distance of $3.485(2)$ \AA and N(2)-H(2) \cdots I(1) angle of $177(3)^\circ$.

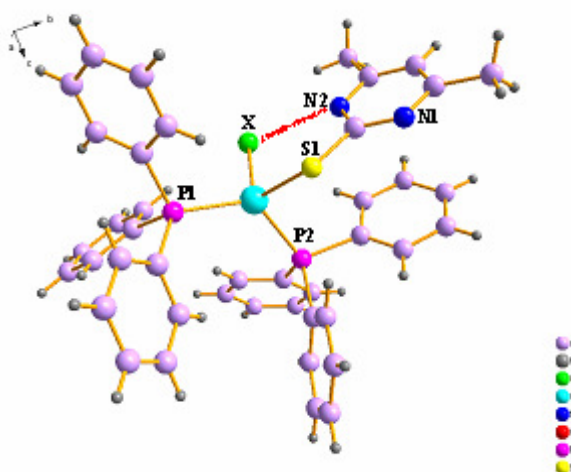


Figure 72 The intra-interaction hydrogen bonding in $[\text{CuX}(\text{PPh}_3)(\text{dmpytmH})]$ ($\text{X}=\text{Cl}, \text{Br}, \text{I}$) complexes.

A literature search of published data on 4,6-dimethylpyrimidine-2(1*H*)-thione ligand, this ligand usually coordinated to Cu(I) atom through the sulfur atom in thione form. In addition, It was found that the intra- and intermolecular hydrogen bonds occurred, which involved the NH group of ligand such as the intramolecular hydrogen bonds $\text{N}(2)\text{-H}\cdots\text{N}(3)$ of $[\text{Cu}(\text{N}_3)(\text{dmpytmH})(\text{PPh}_3)_2]$ and $[\text{Cu}(\text{NCS})(\text{dmpytmH})(\text{PPh}_3)_2]$ (Lemos, et al., 2001), $\text{N}(1)\text{-H}\cdots\text{Br}$ intramolecular interaction of $[\text{CuBr}(\text{binap})(\text{dmpytmH})]\cdot\text{CH}_2\text{Cl}_2$ (Aslanidis, et al., 2008), and two $\text{N}\text{-H}\cdots\text{Cl}$ intermolecular interactions, $\text{N}(11)\text{-H}(11)\cdots\text{Cl}$ and $\text{N}(21)\text{-H}(21)\cdots\text{Cl}$ of $[\text{Cu}(\text{Cl})(\text{dmpytmH})_2]_2$ (Falomer, et al., 2006).

As in complex (3), also in complexes (4) and (5) the shortest C-N and C-C distances in the coordinated 4,6-dimethylpyrimidine-2(1*H*)-thione are C(2)-N(1) and C(3)-C(4), so that they can best be represented by the structure in Figure 73. This is accordance with the coordination of 4,6-dimethylpyrimidine-2(1*H*)-thione in a previous publication (Lemos, et al., 2001).

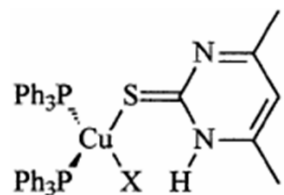


Figure 73 The resonance structure of complexes (3), (4) and (5) ($\text{X}; \text{Cl}, \text{Br}, \text{I}$).

CHAPTER 5

Conclusion

In this study, five new monomeric copper(I) complexes with interesting structural molecules; $[\text{CuCl}(\text{PPh}_3)_2(\text{TBA})]\cdot\text{H}_2\text{O}$ (1), $[\text{CuI}(\text{PPh}_3)_2(\text{CH}_3\text{CN})]$ (2), $[\text{Cu}(\text{PPh}_3)_2(\text{dmpytmH})\text{X}]$; X = Cl, Br, I ((3)-(5), respectively) have been successfully synthesized from the rigid ligands, triphenylphosphine (PPh_3), 4,6-dimethylpyrimidine-2(1*H*)-thione (dmpytmH) and 2-thiobarbituric (TBA) acid with copper(I) halides. We have found that PPh_3 readily forms a copper/triphenylphosphine intermediate, that proves to be a good precursor for the preparation of other derivatives which are the complexes in this study. These complexes have been studied crystallographically. X-ray single crystal determination reveals that each structure is characterized by a distorted tetrahedral arrangement of ligands around the central copper atom with dmpytmH or TBA acting as a neutral S donor ligand in a terminal S-bonding mode. Structures of all complexes have also been characterized by spectroscopic studies.

The structure $[\text{CuCl}(\text{PPh}_3)_2(\text{TBA})]\cdot\text{H}_2\text{O}$ (1) clearly shows a preference for the soft sulphur donor forming pseudo-tetrahedral monomeric with thione ligand acts as terminal coordination mode. $[\text{CuCl}(\text{PPh}_3)_2(\text{TBA})]\cdot\text{H}_2\text{O}$ (1) complex crystallizes in the monoclinic space group $P2_1/c$. and $Z = 4$. This complex has a 1D chain along the c direction by intermolecular hydrogen bonds.

The structure of $[\text{CuI}(\text{PPh}_3)_2(\text{CH}_3\text{CN})]$ (2) is monomeric distorted tetrahedral coordinated by two phosphorus atoms of two triphenylphosphine molecules, one nitrogen atom of acetonitrile molecule and one iodide atom. $[\text{CuI}(\text{PPh}_3)_2(\text{CH}_3\text{CN})]$ complex crystallizes in the monoclinic space group $P2_1/c$ and $Z = 4$.

The structures of $[\text{CuCl}(\text{PPh}_3)(\text{dmpytmH})]$ (3) and $[\text{CuBr}(\text{PPh}_3)(\text{dmpytmH})]$ (4) are monomeric distorted tetrahedral. Both complexes, which are isomorphous and isostructural, crystallize in the monoclinic space group $P2_1/c$ with $Z = 4$. The intramolecular interactions were observed in these complexes.

The structure of $[\text{CuI}(\text{PPh}_3)(\text{dmpymtH})]$ (5) is monomeric distorted tetrahedral. The copper(I) ion in the complex is coordinated by two phosphorus atoms of two triphenylphosphine molecules, one sulfur atom of dmpymtH molecule and one iodide atom. The complex crystallizes in the triclinic space group $P\bar{1}$ and $Z = 2$. The intramolecular interaction of this complex has been observed.

Furthermore, results from X-ray fluorescence spectrometry, elemental analysis, infrared spectroscopy and ^1H , ^{13}C NMR spectroscopy support the structures which give rise from the single-crystal X-ray diffraction technique.

The heterocyclic thiones and triphenylphosphine have attracted considerable attention as ligands in Cu(I) complexes, because of their applications in catalytic functions. In the course of our investigations, much efforts have been empathized to understanding the factors which influence the stoichiometric and structure of these complexes.

Bibliography

- Akrivos, P.D. 2001. Recent studies in the coordination chemistry of heterocyclic thiones and thionates. *Coordination Chemistry Reviews*. 213, 181–210.
- Aslanidis, P., Hadjikakou, S.K., Karagiannidis, P. and Cox, P.J. 1998. Synthesis and characterization of copper(1) complexes with triphenylphosphine and heterocyclic thione ligands: the crystal structure of (thiazolidine-2-thione) (bis-triphenylphosphine) copper(1) chloride. *Inorganica Chimica Acta*. 271, 243-247.
- Aslanidis, P., Cox, P.J. and Tsaliki, P. 2008. Copper(I) halide complexes with 2,20-bis(diphenylphosphano)-1,10-binaphthyl(rac-binap) and heterocyclic thiones. Racemic compounds in chiral and achiral crystal space groups. *Polyhedron*. 27, 3029–3035
- Balas, V.I., Hadjikakou, S.K., Hadjiliadis, N., Kourkoumelis, N., Light, M.E., Hursthouse, M., Metsios, A.K., and Karkabounas, S. 2008. Crystal structure and antitumor activity of the novel zwitterionic complex of tri-*n*-Butyltin(IV) with 2-thiobarbituric acid. *Bioinorganic Chemistry and Applications*. 2008, Article ID 654137, 1-5.
- Barron, P.F., Dyason, J.C., Healy, P.C., Engelhardt, L.M., Pakawatchai, C., Patrick, V.A. and White, A.H. 1987. Lewis-base Adducts of Group 11 Metal(I) Compounds. Part 28. Solid-state Phosphorus-31 Cross-polarization Magic-angle Spinning Nuclear Magnetic Resonance and Structural Studies on the Mononuclear 3:1 Adducts of Triphenylphosphine with Copper(I) Halides. *Journal of the Chemical Society Dalton Transactions*. 1099-1106.

- Bowmaker, G.A., Dyason, J.C., Healy, P.C., Engelhardt, L.M., Pakawatchai, C. and White, A.H. 1987. Lewis-Base Adducts of Group 11 Metal(I) Compounds. Part 27. Solid-state Phosphorus-31 Cross-polarization Magic-angle Spinning Nuclear Magnetic Resonance, Far-infrared, and Structural Studies on the Mononuclear 2:1 Adducts of Triphenylphosphine with Copper(I) and Gold(I) Halides. *Journal of the Chemical Society Dalton Transactions*. 1089-1097.
- Bowmaker, G.A. 1994. Vibrational Spectra and Crystal Structures of Tris- and Tetrakis-(ethylenethiourea)copper(I) Systems. *Australian Journal of Chemistry*. 47, 15-24.
- Bruker. 1998. SMART. Bruker AXS Inc., Madison, Wisconsin, USA.
- Bruker. 2003. SAINT and SADABS. Bruker AXS Inc., Madison, Wisconsin, USA.
- Coles, M.P. and Hitchcock, P.B. 2001. Synthesis and X-ray crystal structure of polymeric and dimeric copper(I) cyanide complexes incorporating a bicyclic guanidine ligand. *Polyhedron*. 20, 3027–3032.
- Cox, P.J., Aslanidis, P. and Karagiannidis, P. 2000. Binuclear copper(I) complexes containing bis(diphenylphosphino)ethane bridges: the crystal structure of bis[{m-bis(diphenylphosphino)ethane } (pyridine-2-thione)copper(I) bromide]. *Polyhedron*. 19, 1615–1620.
- Dehghanpour, S., Bouslimani, N., Welter, R. and Mojahed, F. 2007. Synthesis, spectral characterization, properties and structures of copper(I) complexes containing novel bidentate iminopyridine ligands. *Polyhedron*. 26, 154–162.

- Dyason, J.C., Engelhardt, L.M., Pakawatchai, P., Healy, P.C. and White, A.H. 1985. Lewis-Base Adducts of Group 1B Metal(I) Compounds. XXI+ The Crystal and Molecular Structures of the Unsolvated Forms of Dibromotris(triphenylphosphine)dicopper(I) and ‘step’ Tetrabromotetrakis(triphenylphosphine)tetracopper(I). *Australian Journal of Chemistry*. 38, 1243-1250.
- Falcomer, V.A.S., Lemos, S.S., Batista, A.A., Ellena, J. and Castellano, E.E. 2006. Mono- and dinuclear copper(I) complexes with methyl-substituted pyrimidinethiones. *Inorganica Chimica Acta*. 359, 1064–1070.
- Farrugia, L.J. 1999. WinGX suit for small-molecule single-crystal crystallography. *Journal of Applied Crystallography*. 32, 837-838.
- Hall, S.R., du Boulay, D.J. and Olthof-Hazekamp, R. 1997 Eds. Xtal 3.6 System. University of wastem Astrarea.
- Koshevaya, A.Y. and Starodub, V.A. 2006. Cu(I) Chloride Complexes with 4,5-(2-pyridylethylene)dithio-1,3-dithiol-2-thione and triphenylphosphine. *Koordinatsionnaya Khimiya*. 32, 149–157.
- Kubicki, M., Hadjikakou, S.K. and Xanthopoulou, M.N. 2001. Synthesis, characterisation and study of mercury(II) bromide complexes with triphenylphosphine and heterocyclic thiones. The crystal structures of [bis(triphenylphosphine) dibromo mercury(II)] and [dibromo (pyrimidine-2-thionato) (triphenylphosphine) mercury(II)]. Extended intra-molecular linkages via N-H···Br and C-H···Br interactions. *Polyhedron*. 20, 2179–2185.
- Lang, J. and Tatsumi, K. 1996. Synthesis and crystal structure of a binuclear copper(I) bromide complex of benz-1,3-thiazolidine-2-thione and triphenylphosphine, [Cu(btzdtH)(PPh₃) Br]₂. *Polyhedron*. 15, 2127-2130.

- Lemos S.S., Camargo, M.A., Cardoso Z.Z., Deflon V.M., Försterling, F.H. and Hagenbach, A. 2001. Copper(I) pseudohalide complexes with 4,6-dimethylpyrimidine-2(1H)-thione and triphenylphosphane as ligands. The X-ray crystal structures of $[\text{Cu}(\text{N}_3)(\text{dmpytmH})(\text{PPh}_3)_2]$ and $[\text{Cu}(\text{NCS})(\text{dmpytmH})(\text{PPh}_3)_2]$. *Polyhedron*. 20, 849–854.
- Li, D., Li, R.-Z., Ni, Z., Qi, Z.-Y., Feng, X.-L. and Cai, J.-W. 2003. Synthesis and crystal structure of photoluminescent copper(I)-phosphine complexes with oxygen and nitrogen donor ligands. *Inorganic Chemistry Communications*. 6, 469–473.
- Lobana, T.S., Sultana, R. and Hundal, G. 2008. Heterocyclic thioamides of copper(I): Synthesis and crystal structures of copper complexes with 1,3-imidazoline-2-thiones in the presence of triphenyl phosphine. *Polyhedron*. 27, 1008–1016.
- Macrae, C.E., Edgington, P.R., McCabe, P., Pidcock, E., Shields, G.P., Taylor, R., Towler, M. and van de Streek, J. 2006. Mercury: a visualization and analysis of crystal structures. *Journal of Applied Crystallography*. 39, 453-457.
- Maeyer, J.T., Johnson, T.J., Smith, A.K., Borne, B.D., Pike, R.D., Pennington, W.T., Krawiec, M. and Rheingold, A.L. 2003. Pyrimidine, pyridazine, quinazoline, phthalazine, and triazine coordination polymers of copper(I) halides. *Polyhedron*. 22, 419-431.
- Mamais, M., Cox, P.J. and Aslanidis, P. 2008. Three- and four-coordinate copper(I) halide complexes of 2-(diphenylphosphano)benzaldehyde: Dimerization induced by thione-S ligation. *Polyhedron*. 27, 175–180.
- Martos-Calvente, R., de la Pena O’Shea, V.A., Campos-Martin, J.M. and Fierro, J.L.G. 2003. The usefulness of density functional theory to describe the tautomeric equilibrium of 4,6-dimethyl-2-mercaptopurine in Solution. *Journal of Physical Chemistry A*. 107, 7490-7495.

- Méndez, E., Cerdá, M.F., Gancheff, J.S., Torres, J., Kremer, C., Castiglioni, J., Kieninger, M. and Ventura, O.N. 2007. Tautomeric forms of 2-thiobarbituric acid as studied in the solid, in polar solutions, and on gold nanoparticles. *Journal of Physical Chemistry C*. 111, 3369-3383.
- Battistuzzi, R. and Peyronel, G. 1978. Copper(I) complexes of neutral, deprotonated and protonated 4,6-dimethylpyrimidine-2 (H)-thione. *Transition Metal Chemistry*. 3, 345-351.
- Ramando, F., Pieretti, A., Gontrani, L. and Bencivenni, L. 2001. Hydrogen bonding in barbituric and 2-thiobarbituric acids: a theoretical and FT-IR study. *Chemical Physics*. 271, 293-308.
- Refat, M.S., El-Korashy^b, S.A. and Ahmeda, A.S. 2008. A convenient method for the preparation of barbituric and thiobarbituric acid transition metal complexes. *Spectrochimica Acta Part A*. 71, 1084–1094.
- Rao, C.N.R. and Venkataraghavan, R. 1962. The C=S stretching frequency and the “-N-C=S bands” in the infrared. *Spectrochimica Acta*. 18, 541-547.
- Reznikov, A.N. and Skvortsov, N.K. 2008. Synthesis of 5-[3-(diphenylphosphinoyl)propyl]-2-thiobarbituric acid. *Russian Journal of General Chemistry*. 78, 320-322.
- Sheldrick, G.M. 2000. SHLLXTL NT Version 6.12, Bruker Analytical X-ray System, Inc: Madison, WI, USA.
- Sheldrick, G.M. 2008. A short history of SHELX. *Acta Crystallographica. A64*, 112-122.
- Singh, N.K., Singh, M., Tripathi, P., Srivastava, A.K. and Butcher, R.J. 2008. Synthesis of a new *N,N'*-ethane-1,2-bis(4-methoxyphenyl)carbothioamide ligand and its Cu(I) and Ag(I) complexes. *Polyhedron*. 27, 375–382.

- Garcia Tasende, M.S., Suárez Gimeno, M.I., Sánchez, A., Casas, J.S. and Sordo, J. 1990. Monoorganomercury and diorganothallium derivatives of 2-thiobarbituric acid. *Journal of Organometallic Chemistry.* 390, 293-300.
- Voutsas, P.P., Kokkou, S.C., Cheer, C.J., Aslanidis, P. and Karagiannidis. 1995. Copper(I) Halide coordination compounds with benz-1,3-thiazolidine-2-thione and triarylphosphines: The crystal and molecular structure of $[\text{Cu}(\text{PPh}_3)_2(\text{bztzdtHCl})\text{CH}_3\text{COCH}_3]$. *Polyhedron.* 14, 2287-2292.
- Zaki, Z.M. and Mohamed, G.G. 2000. Spectral and thermal studies of thiobarbituric acid complexes. *Spectrochimica Acta.* 56, 1245–1250.
- Zhou, X.-H., Wu, T. and Li, D. 2006. Structural variations and spectroscopic properties of copper(I) complexes with bis(schiff base) ligands. *Inorganica Chimica Acta.* 359, 1442–1448.
- Zheng, H.-G., Zeng, D.-X., Xin, X.-Q. and Wong, W.-T. 1997. Solid state syntheses and crystal structures of $[\text{Cu}(\text{HOOC}_6\text{H}_4\text{CHNNHCSNH}_2)(\text{PPh}_3)_2\text{X}]$ ($\text{X} = \text{I}, \text{Br}$) *Polyhedron.* 16, 3499-3503.

APPENDIX

Appendix A

Calculation of unit cell volume

Table 20 The equation of calculation of unit cell volume depend on crystal system :

Crystal system	Equation
Cubic	$V \square a^3$
Tetragonal	$V \square a^2 c$
Orthorhombic	$V \square abc$
Hexagonal	$V \square (3a^2 c)/2 \square 0.886 a^2 c$
Monoclinic	$V \square abc \sin\beta$
Triclinic	$V \square abc(1 - \cos^2 \alpha - \cos^2 \beta - \cos^2 \gamma \square 2 \cos \alpha \cdot \cos \beta \cdot \cos \gamma)^{1/2}$

Calculation of number of molecules per unit cell (Z)

$$Z \square \frac{D \times V \times N}{Fw}$$

D = Density of crystal (g/cm^3)

V = Volume of unit cell (cm^3)

N = Avogadro number ($6.02 \times 10^{23} \text{ mol}^{-1}$)

Fw = Formula weight

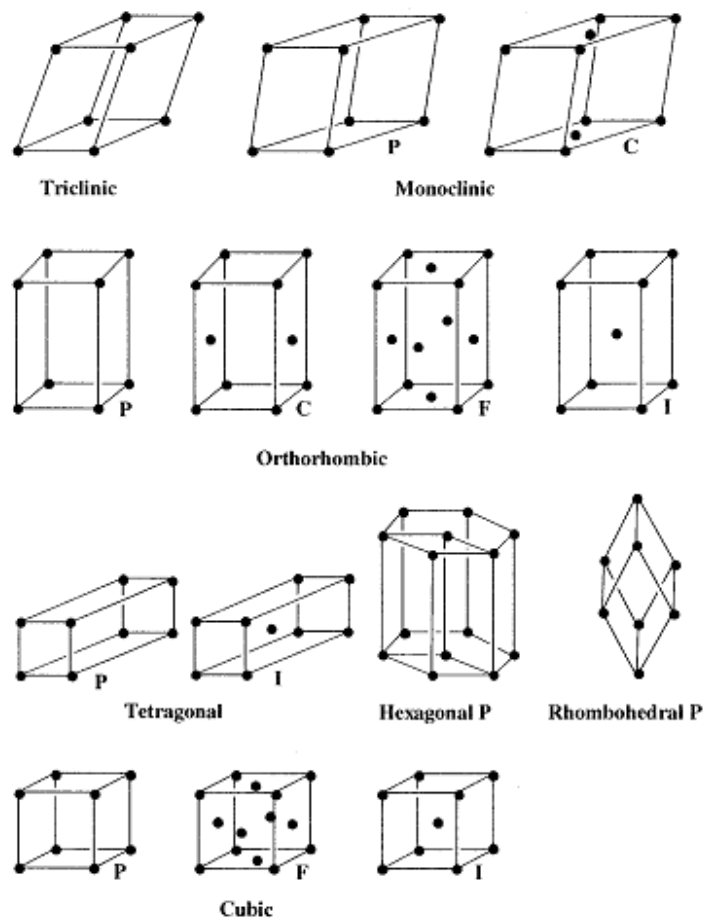


Figure 62 The Bravais lattices.

Appendix B

The crystallographic data

Table 21 Atomic coordinates ($\times 10^4$) and equivalent isotropic displacement parameters ($\text{\AA}^2 \times 10^3$) for $[\text{CuCl}(\text{PPh}_3)_2(\text{TBA})] \cdot \text{H}_2\text{O}$. U(eq) is defined as one third of the trace of the orthogonalized U^{ij} tensor.

Atom	x	y	z	U(eq)
C(1)	7643(3)	242(3)	1675(1)	32(1)
C(2)	8903(3)	-1094(3)	2114(1)	37(1)
C(3)	9313(3)	95(3)	2287(1)	41(1)
C(4)	8852(3)	1306(3)	2160(1)	41(1)
C(11A)	2018(3)	636(3)	1290(1)	39(1)
C(12A)	1618(4)	966(4)	959(1)	64(1)
C(13A)	618(5)	238(5)	769(1)	89(1)
C(14A)	5(4)	-846(4)	908(1)	75(1)
C(15A)	378(3)	-1192(4)	1232(1)	56(1)
C(16A)	1380(3)	-458(3)	1424(1)	48(1)
C(21A)	3655(3)	725(3)	1923(1)	43(1)
C(22A)	3114(4)	1075(4)	2217(1)	59(1)
C(23A)	3345(5)	248(5)	2499(1)	79(1)
C(24A)	4089(5)	-913(5)	2489(1)	81(1)
C(25A)	4645(4)	-1268(4)	2200(1)	75(1)
C(26A)	4432(3)	-445(4)	1918(1)	58(1)
C(31A)	2351(3)	3164(3)	1641(1)	41(1)
C(32A)	3063(4)	4245(4)	1789(1)	69(1)
C(33A)	2387(5)	5405(4)	1873(1)	83(1)
C(34A)	1000(5)	5499(4)	1803(1)	72(1)
C(35A)	295(4)	4438(5)	1660(1)	79(1)

Table 21 (Continued).

Atom	x	y	z	U(eq)
C(36A)	946(4)	3268(4)	1577(1)	61(1)
C(11B)	6825(3)	3358(3)	584(1)	41(1)
C(12B)	7974(4)	3659(5)	804(1)	75(1)
C(13B)	9230(4)	3885(6)	686(1)	104(2)
C(14B)	9334(5)	3770(5)	349(1)	98(2)
C(15B)	8216(5)	3449(5)	127(1)	80(1)
C(16B)	6960(4)	3253(4)	246(1)	59(1)
C(21B)	4088(3)	2402(3)	411(1)	40(1)
C(22B)	4124(5)	1007(4)	390(1)	77(1)
C(23B)	3340(6)	320(4)	141(1)	107(2)
C(24B)	2468(5)	1021(5)	-89(1)	96(2)
C(25B)	2399(4)	2407(5)	-74(1)	73(1)
C(26B)	3217(3)	3097(3)	177(1)	51(1)
C(31B)	4575(3)	4930(3)	765(1)	36(1)
C(32B)	3446(4)	5190(4)	928(1)	71(1)
C(33B)	2971(6)	6490(5)	959(1)	101(2)
C(34B)	3634(6)	7549(4)	834(1)	86(2)
C(35B)	4761(5)	7321(4)	671(1)	71(1)
C(36B)	5228(4)	6010(3)	634(1)	52(1)
Cl(1)	6471(1)	3930(1)	1606(1)	43(1)
Cu(1)	5232(1)	2210(1)	1274(1)	33(1)
N(1)	8073(2)	-945(2)	1812(1)	35(1)
N(2)	8022(3)	1342(3)	1858(1)	42(1)
O(1)	9203(2)	-2286(2)	2205(1)	55(1)
O(2)	9090(3)	2504(2)	2284(1)	67(1)
O(3)	7170(5)	6910(3)	1409(1)	121(2)
P(1)	3325(1)	1682(1)	1530(1)	35(1)
P(2)	5184(1)	3185(1)	757(1)	32(1)

Table 21 (Continued).

Atom	x	y	z	U(eq)
S(1)	6716(1)	319(1)	1292(1)	38(1)

Table 22 Anisotropic displacement parameters ($\text{\AA}^2 \times 10^3$) for $[\text{CuCl}(\text{PPh}_3)_2(\text{TBA})] \cdot \text{H}_2\text{O}$.

The anisotropic displacement factor exponent takes the form:

$$-2\pi^2 [h^2 a^*{}^2 U^{11} + \dots + 2 h k a^* b^* U^{12}]$$

Atom	U ¹¹	U ²²	U ³³	U ²³	U ¹³	U ¹²
C(1)	33(2)	32(2)	31(2)	0(1)	-1(1)	3(1)
C(2)	39(2)	37(2)	35(2)	2(1)	-3(1)	6(1)
C(3)	46(2)	39(2)	33(2)	0(1)	-16(1)	4(2)
C(4)	48(2)	36(2)	36(2)	-3(1)	-12(1)	-2(2)
C(11A)	33(2)	43(2)	41(2)	1(1)	2(1)	0(1)
C(12A)	67(2)	72(3)	48(2)	15(2)	-16(2)	-20(2)
C(13A)	90(3)	105(4)	62(3)	19(2)	-31(2)	-30(3)
C(14A)	63(3)	82(3)	73(3)	-10(2)	-18(2)	-20(2)
C(15A)	46(2)	53(2)	69(3)	-6(2)	9(2)	-11(2)
C(16A)	48(2)	52(2)	46(2)	2(2)	7(2)	-2(2)
C(21A)	37(2)	54(2)	38(2)	9(2)	-2(1)	-8(2)
C(22A)	67(2)	70(2)	39(2)	2(2)	4(2)	-4(2)
C(23A)	97(3)	109(4)	32(2)	13(2)	8(2)	-20(3)
C(24A)	84(3)	99(4)	56(3)	38(2)	-11(2)	-10(3)
C(25A)	65(3)	78(3)	81(3)	40(2)	2(2)	7(2)
C(26A)	51(2)	68(2)	55(2)	22(2)	9(2)	8(2)
C(31A)	40(2)	49(2)	35(2)	2(1)	8(1)	3(2)
C(32A)	49(2)	72(3)	87(3)	-31(2)	8(2)	4(2)
C(33A)	84(3)	63(3)	104(3)	-32(2)	24(3)	2(2)

Table 22 (Continued).

Atom	U^{11}	U^{22}	U^{33}	U^{23}	U^{13}	U^{12}
C(34A)	81(3)	67(3)	74(3)	2(2)	28(2)	29(2)
C(35A)	53(2)	87(3)	98(3)	2(3)	12(2)	28(2)
C(36A)	43(2)	64(2)	77(3)	-2(2)	9(2)	9(2)
C(11B)	44(2)	39(2)	41(2)	9(1)	11(2)	11(1)
C(12B)	47(2)	122(4)	55(2)	27(2)	8(2)	3(2)
C(13B)	42(2)	177(6)	92(4)	46(3)	9(2)	0(3)
C(14B)	65(3)	134(4)	105(4)	50(3)	49(3)	23(3)
C(15B)	90(3)	91(3)	68(3)	10(2)	47(3)	13(3)
C(16B)	69(2)	54(2)	56(2)	0(2)	23(2)	4(2)
C(21B)	51(2)	38(2)	30(2)	1(1)	2(1)	-1(2)
C(22B)	129(4)	40(2)	53(2)	-2(2)	-28(2)	1(2)
C(23B)	183(5)	52(3)	74(3)	-13(2)	-36(3)	-20(3)
C(24B)	130(4)	88(4)	60(3)	-10(2)	-30(3)	-40(3)
C(25B)	74(3)	90(3)	50(2)	8(2)	-20(2)	-10(2)
C(26B)	56(2)	51(2)	45(2)	3(2)	-6(2)	1(2)
C(31B)	46(2)	33(2)	27(2)	3(1)	0(1)	6(1)
C(32B)	82(3)	50(2)	88(3)	20(2)	39(2)	23(2)
C(33B)	137(4)	71(3)	108(4)	27(3)	71(3)	60(3)
C(34B)	143(4)	41(2)	77(3)	3(2)	20(3)	39(3)
C(35B)	104(3)	35(2)	74(3)	7(2)	13(2)	3(2)
C(36B)	66(2)	37(2)	54(2)	1(2)	13(2)	2(2)
Cl(1)	47(1)	32(1)	47(1)	-3(1)	-6(1)	-1(1)
Cu(1)	35(1)	35(1)	29(1)	4(1)	-1(1)	2(1)
N(1)	45(2)	27(1)	30(1)	-2(1)	-10(1)	4(1)
N(2)	56(2)	25(1)	40(2)	1(1)	-15(1)	5(1)
O(1)	77(2)	34(1)	47(1)	0(1)	-23(1)	15(1)
O(2)	98(2)	35(1)	57(2)	-7(1)	-40(1)	-4(1)
O(3)	196(4)	40(2)	109(3)	-2(2)	-59(3)	-24(2)

Table 22 (Continued).

Atom	U^{11}	U^{22}	U^{33}	U^{23}	U^{13}	U^{12}
P(1)	32(1)	41(1)	32(1)	4(1)	2(1)	1(1)
P(2)	38(1)	30(1)	28(1)	4(1)	2(1)	4(1)
S(1)	45(1)	37(1)	30(1)	-4(1)	-11(1)	10(1)

Table 23 Atomic coordinates ($\times 10^4$) and equivalent isotropic displacement parameters ($\text{\AA}^2 \times 10^3$) for $[\text{CuI}(\text{PPh}_3)_2(\text{CH}_3\text{CN})]$. $U(\text{eq})$ is defined as one third of the trace of the orthogonalized U^{ij} tensor.

Atom	x	y	z	$U(\text{eq})$
C(1)	3135(3)	4942(2)	1225(1)	40(1)
C(2)	2418(4)	5061(2)	592(2)	52(1)
C(3)	1581(4)	5646(2)	483(2)	63(1)
C(4)	1457(4)	6120(2)	996(2)	63(1)
C(5)	2187(4)	6020(2)	1616(2)	68(1)
C(6)	3003(4)	5435(2)	1734(2)	59(1)
C(7)	6031(3)	4371(2)	1375(2)	47(1)
C(8)	6528(4)	5038(2)	1416(2)	71(1)
C(9)	7997(5)	5182(3)	1462(2)	96(2)
C(10)	8972(5)	4659(3)	1458(2)	96(2)
C(11)	8507(4)	3993(3)	1404(2)	82(1)
C(12)	7036(4)	3842(2)	1366(2)	62(1)
C(13)	3687(3)	3618(2)	679(2)	44(1)
C(14)	4439(4)	3652(2)	82(2)	63(1)
C(15)	3951(5)	3294(2)	-496(2)	80(1)
C(16)	2719(6)	2906(2)	-495(2)	83(1)

Table 23 (Continued).

Atom	x	y	z	U(eq)
C(17)	1968(5)	2867(2)	90(2)	79(1)
C(18)	2463(4)	3213(2)	679(2)	61(1)
C(19)	6105(3)	4147(2)	3765(1)	41(1)
C(20)	7055(4)	4291(2)	3265(2)	82(1)
C(21)	8524(4)	4306(3)	3420(2)	108(2)
C(22)	9062(4)	4171(3)	4076(2)	85(1)
C(23)	8137(4)	4025(2)	4572(2)	69(1)
C(24)	6666(3)	4018(2)	4420(2)	52(1)
C(25)	3322(3)	3755(2)	4244(1)	41(1)
C(26)	3084(4)	3048(2)	4249(2)	58(1)
C(27)	2413(5)	2741(2)	4788(2)	75(1)
C(28)	1955(4)	3131(2)	5320(2)	71(1)
C(29)	2180(4)	3827(2)	5323(2)	59(1)
C(30)	2871(3)	4137(2)	4792(2)	49(1)
C(31)	3642(3)	5037(2)	3561(1)	44(1)
C(32)	4573(4)	5572(2)	3715(2)	64(1)
C(33)	4052(6)	6250(2)	3712(2)	89(1)
C(34)	2642(6)	6388(2)	3562(2)	84(1)
C(35)	1705(5)	5863(2)	3416(2)	76(1)
C(36)	2195(4)	5193(2)	3407(2)	61(1)
C(1A)	691(4)	2923(2)	2605(2)	72(1)
C(2A)	-592(6)	2520(3)	2741(4)	164(3)
Cu(1)	3735(1)	3621(1)	2462(1)	42(1)
I(1)	5308(1)	2469(1)	2509(1)	57(1)
N(1)	1669(3)	3224(2)	2495(1)	61(1)
P(1)	4125(1)	4144(1)	1438(1)	39(1)
P(2)	4188(1)	4135(1)	3507(1)	38(1)

Table 24 Anisotropic displacement parameters ($\text{\AA}^2 \times 10^3$) for $[\text{CuI}(\text{PPh}_3)_2(\text{CH}_3\text{CN})]$.

The anisotropic displacement factor exponent takes the form:

$$-2\pi^2 [h^2 a^*{}^2 U^{11} + \dots + 2 h k a^* b^* U^{12}]$$

Atom	U^{11}	U^{22}	U^{33}	U^{23}	U^{13}	U^{12}
C(1)	42(2)	42(2)	37(2)	5(1)	5(1)	-5(1)
C(2)	63(2)	53(2)	39(2)	3(2)	5(2)	4(2)
C(3)	73(3)	65(2)	50(2)	17(2)	-2(2)	11(2)
C(4)	72(3)	50(2)	66(2)	16(2)	10(2)	12(2)
C(5)	93(3)	49(2)	62(2)	-5(2)	8(2)	14(2)
C(6)	75(2)	56(2)	45(2)	1(2)	-2(2)	7(2)
C(7)	41(2)	61(2)	39(2)	10(2)	4(1)	-4(2)
C(8)	54(2)	75(3)	85(3)	14(2)	6(2)	-15(2)
C(9)	64(3)	108(4)	116(4)	21(3)	3(3)	-40(3)
C(10)	46(3)	160(5)	82(3)	42(3)	4(2)	-23(3)
C(11)	49(3)	130(4)	68(3)	39(3)	13(2)	18(3)
C(12)	50(2)	81(3)	57(2)	16(2)	11(2)	2(2)
C(13)	49(2)	43(2)	40(2)	2(1)	0(1)	6(2)
C(14)	67(2)	72(2)	51(2)	-7(2)	13(2)	-5(2)
C(15)	110(4)	84(3)	48(2)	-18(2)	15(2)	-1(3)
C(16)	123(4)	74(3)	50(2)	-16(2)	-10(2)	-2(3)
C(17)	92(3)	75(3)	70(3)	-9(2)	-7(2)	-27(2)
C(18)	72(3)	60(2)	49(2)	-3(2)	1(2)	-13(2)
C(19)	37(2)	48(2)	38(2)	-1(1)	0(1)	-5(1)
C(20)	49(2)	153(4)	41(2)	7(2)	-2(2)	-27(2)
C(21)	44(2)	223(6)	57(3)	5(3)	6(2)	-39(3)
C(22)	34(2)	152(4)	67(3)	3(3)	-6(2)	-8(2)
C(23)	50(2)	103(3)	53(2)	10(2)	-10(2)	0(2)
C(24)	44(2)	65(2)	48(2)	8(2)	3(2)	3(2)
C(25)	34(2)	49(2)	39(2)	5(2)	-2(1)	-3(1)
C(26)	68(2)	50(2)	58(2)	2(2)	16(2)	-7(2)

Table 24 (Continued).

Atom	U^{11}	U^{22}	U^{33}	U^{23}	U^{13}	U^{12}
C(27)	90(3)	52(2)	84(3)	11(2)	30(2)	-11(2)
C(28)	69(3)	83(3)	62(2)	18(2)	20(2)	-13(2)
C(29)	55(2)	79(3)	44(2)	-2(2)	10(2)	-5(2)
C(30)	49(2)	53(2)	45(2)	-1(2)	0(2)	-9(2)
C(31)	51(2)	48(2)	33(2)	5(1)	-1(1)	0(2)
C(32)	78(3)	50(2)	61(2)	3(2)	-23(2)	-8(2)
C(33)	135(4)	46(2)	82(3)	-2(2)	-33(3)	-11(3)
C(34)	128(4)	58(3)	65(3)	0(2)	-11(3)	27(3)
C(35)	80(3)	81(3)	68(3)	14(2)	11(2)	29(3)
C(36)	62(2)	54(2)	67(2)	11(2)	10(2)	6(2)
C(1A)	40(2)	106(3)	67(2)	33(2)	-2(2)	-11(2)
C(2A)	68(3)	227(8)	197(6)	115(6)	15(4)	-50(4)
Cu(1)	39(1)	46(1)	39(1)	1(1)	0(1)	-6(1)
I(1)	49(1)	43(1)	78(1)	2(1)	5(1)	-2(1)
N(1)	39(2)	89(2)	54(2)	6(2)	-2(1)	-12(2)
P(1)	38(1)	44(1)	37(1)	2(1)	3(1)	-1(1)
P(2)	36(1)	41(1)	37(1)	1(1)	-1(1)	-4(1)

Table 25 Atomic coordinates ($\times 10^4$) and equivalent isotropic displacement parameters ($\text{\AA}^2 \times 10^3$) for $[\text{CuCl}(\text{PPh}_3)_2(\text{dmpymtH})]$. $U(\text{eq})$ is defined as one third of the trace of the orthogonalized U^{ij} tensor.

Atom	x	y	z	$U(\text{eq})$
C(1)	1051(3)	4629(2)	869(1)	42(1)
C(2)	555(3)	5882(2)	756(2)	54(1)

Table 25 (Continued).

Atom	x	y	z	U(eq)
C(3)	1394(3)	5959(2)	317(2)	54(1)
C(4)	2069(3)	5347(2)	161(1)	49(1)
C(5)	-214(5)	6537(2)	946(2)	89(1)
C(6)	2946(4)	5338(2)	-319(2)	70(1)
C(11)	799(3)	1619(2)	326(1)	45(1)
C(12)	900(4)	1115(2)	-132(2)	73(1)
C(13)	-200(6)	1015(3)	-626(2)	100(2)
C(14)	-1387(6)	1410(3)	-653(2)	98(2)
C(15)	-1512(4)	1910(2)	-208(2)	86(1)
C(16)	-414(4)	2024(2)	281(2)	64(1)
C(21)	1449(3)	1296(2)	1608(1)	42(1)
C(22)	2172(4)	1353(2)	2209(2)	60(1)
C(23)	1738(5)	967(2)	2680(2)	79(1)
C(24)	578(5)	531(2)	2564(2)	79(1)
C(25)	-152(4)	475(2)	1975(2)	69(1)
C(26)	272(3)	856(2)	1497(2)	54(1)
C(31)	3547(3)	1146(2)	897(1)	43(1)
C(32)	4573(4)	1407(2)	605(2)	61(1)
C(33)	5679(4)	950(2)	542(2)	80(1)
C(34)	5767(4)	241(2)	760(2)	77(1)
C(35)	4760(5)	-30(2)	1041(2)	86(1)
C(36)	3649(4)	414(2)	1110(2)	72(1)
C(41)	3882(3)	3249(2)	2743(1)	37(1)
C(42)	4858(3)	3010(2)	3238(1)	48(1)
C(43)	4475(4)	2820(2)	3788(2)	59(1)
C(44)	3140(4)	2873(2)	3860(2)	63(1)
C(45)	2162(4)	3113(2)	3374(2)	71(1)
C(46)	2521(3)	3292(2)	2820(2)	58(1)

Table 25 (Continued).

Atom	x	y	z	U(eq)
C(51)	6096(3)	3224(2)	2061(1)	40(1)
C(52)	6402(3)	2535(2)	1843(2)	57(1)
C(53)	7753(4)	2304(2)	1896(2)	73(1)
C(54)	8805(4)	2747(2)	2173(2)	76(1)
C(55)	8524(3)	3434(2)	2390(2)	77(1)
C(56)	7172(3)	3679(2)	2335(2)	60(1)
C(61)	4276(3)	4490(2)	1957(1)	39(1)
C(62)	4785(4)	4840(2)	1491(2)	58(1)
C(63)	4728(4)	5607(2)	1422(2)	75(1)
C(64)	4136(5)	6026(2)	1814(3)	92(1)
C(65)	3613(6)	5695(2)	2266(3)	111(2)
C(66)	3693(4)	4927(2)	2346(2)	78(1)
N(1)	376(3)	5229(1)	1023(1)	50(1)
N(2)	1892(2)	4689(1)	446(1)	44(1)
P(1)	4270(1)	3469(1)	1981(1)	35(1)
P(2)	2154(1)	1779(1)	1005(1)	38(1)
S(1)	821(1)	3778(1)	1185(1)	47(1)
Cl(1)	3749(1)	3353(1)	272(1)	57(1)
Cu(1)	2748(1)	3002(1)	1148(1)	40(1)

Table 26 Anisotropic displacement parameters ($\text{\AA}^2 \times 10^3$) for $[\text{CuCl}(\text{PPh}_3)_2(\text{dmpymtH})]$.

The anisotropic displacement factor exponent takes the form:

$$-2\pi^2 [h^2 a^*{}^2 U^{11} + \dots + 2 h k a^* b^* U^{12}]$$

Atom	U^{11}	U^{22}	U^{33}	U^{23}	U^{13}	U^{12}
C(1)	39(2)	47(2)	37(2)	5(1)	2(1)	2(1)
C(2)	63(2)	46(2)	51(2)	5(2)	12(2)	10(2)
C(3)	62(2)	44(2)	56(2)	10(2)	12(2)	2(2)
C(4)	43(2)	54(2)	47(2)	8(2)	5(1)	0(2)
C(5)	122(4)	57(2)	101(3)	16(2)	53(3)	29(2)
C(6)	71(2)	74(2)	73(2)	18(2)	34(2)	2(2)
C(11)	53(2)	38(2)	43(2)	4(1)	5(1)	-15(2)
C(12)	77(3)	81(3)	59(2)	-21(2)	6(2)	-11(2)
C(13)	118(4)	109(4)	63(3)	-30(3)	-8(3)	-24(3)
C(14)	104(4)	87(3)	81(3)	7(3)	-36(3)	-37(3)
C(15)	70(3)	63(3)	107(4)	22(3)	-30(2)	-15(2)
C(16)	61(2)	47(2)	76(2)	5(2)	-11(2)	-9(2)
C(21)	49(2)	34(2)	44(2)	3(1)	13(1)	7(1)
C(22)	69(2)	65(2)	46(2)	3(2)	9(2)	4(2)
C(23)	99(3)	96(3)	44(2)	14(2)	17(2)	23(3)
C(24)	107(3)	71(3)	73(3)	25(2)	52(3)	25(3)
C(25)	79(3)	58(2)	78(3)	9(2)	39(2)	-3(2)
C(26)	62(2)	49(2)	54(2)	3(2)	20(2)	-2(2)
C(31)	49(2)	38(2)	43(2)	-5(1)	6(1)	-2(1)
C(32)	69(2)	46(2)	73(2)	-3(2)	27(2)	1(2)
C(33)	74(3)	74(3)	103(3)	-13(2)	47(2)	1(2)
C(34)	70(3)	73(3)	89(3)	-15(2)	17(2)	26(2)
C(35)	107(3)	53(2)	106(3)	16(2)	38(3)	32(2)
C(36)	85(3)	46(2)	92(3)	11(2)	38(2)	11(2)
C(41)	37(2)	34(2)	40(2)	-2(1)	3(1)	-4(1)
C(42)	47(2)	48(2)	48(2)	0(2)	7(2)	2(1)

Table 26 (Continued).

Atom	U^{11}	U^{22}	U^{33}	U^{23}	U^{13}	U^{12}
C(43)	68(2)	62(2)	42(2)	8(2)	1(2)	5(2)
C(44)	78(3)	70(2)	42(2)	6(2)	16(2)	-8(2)
C(45)	52(2)	109(3)	56(2)	8(2)	20(2)	-5(2)
C(46)	43(2)	87(3)	43(2)	11(2)	7(2)	-2(2)
C(51)	35(2)	42(2)	43(2)	1(1)	8(1)	0(1)
C(52)	46(2)	47(2)	80(2)	-7(2)	16(2)	0(2)
C(53)	57(2)	54(2)	113(3)	-4(2)	30(2)	14(2)
C(54)	41(2)	70(3)	118(3)	22(2)	23(2)	15(2)
C(55)	34(2)	74(3)	119(3)	-4(2)	3(2)	-4(2)
C(56)	41(2)	52(2)	87(3)	-10(2)	10(2)	-3(2)
C(61)	34(2)	37(2)	44(2)	-3(1)	3(1)	-1(1)
C(62)	70(2)	46(2)	60(2)	0(2)	15(2)	-9(2)
C(63)	85(3)	51(2)	84(3)	14(2)	5(2)	-17(2)
C(64)	98(3)	35(2)	141(4)	2(3)	14(3)	-4(2)
C(65)	145(5)	48(3)	160(5)	-19(3)	78(4)	5(3)
C(66)	102(3)	43(2)	102(3)	-8(2)	52(3)	1(2)
N(1)	59(2)	47(2)	47(2)	4(1)	15(1)	11(1)
N(2)	44(1)	44(2)	43(1)	7(1)	10(1)	-1(1)
P(1)	33(1)	34(1)	38(1)	-3(1)	6(1)	0(1)
P(2)	43(1)	32(1)	38(1)	-1(1)	6(1)	-2(1)
S(1)	44(1)	45(1)	52(1)	11(1)	10(1)	4(1)
Cl(1)	78(1)	47(1)	52(1)	1(1)	28(1)	5(1)
Cu(1)	45(1)	34(1)	40(1)	-1(1)	4(1)	-2(1)

Table 27 Atomic coordinates ($\times 10^4$) and equivalent isotropic displacement parameters ($\text{\AA}^2 \times 10^3$) for $[\text{CuBr}(\text{PPh}_3)_2(\text{dmpymtH})]$. U(eq) is defined as one third of the trace of the orthogonalized U^{ij} tensor.

Atom	x	y	z	U(eq)
Br(1)	1183(1)	3343(1)	4793(1)	57(1)
C(1)	1465(5)	1139(3)	4097(2)	41(1)
C(2)	433(6)	1376(3)	4394(3)	68(2)
C(3)	-670(7)	917(4)	4452(3)	84(2)
C(4)	-749(7)	215(4)	4220(3)	81(2)
C(5)	253(8)	-33(4)	3934(3)	94(2)
C(6)	1354(7)	427(3)	3868(3)	77(2)
C(7)	4213(5)	1618(3)	4666(2)	44(1)
C(8)	5432(6)	2022(3)	4702(3)	60(2)
C(9)	6537(7)	1904(4)	5186(3)	84(2)
C(10)	6399(9)	1407(5)	5635(4)	98(3)
C(11)	5224(9)	1013(5)	5613(3)	103(3)
C(12)	4100(7)	1109(4)	5120(3)	74(2)
C(13)	3572(5)	1316(3)	3398(2)	41(1)
C(14)	4730(5)	863(3)	3504(2)	51(1)
C(15)	5141(7)	490(3)	3016(3)	68(2)
C(16)	4402(8)	553(4)	2437(3)	79(2)
C(17)	3260(7)	1005(4)	2330(3)	77(2)
C(18)	2845(6)	1387(3)	2801(3)	59(2)
C(19)	1146(5)	3282(2)	2296(2)	36(1)
C(20)	2508(5)	3346(3)	2217(2)	57(2)
C(21)	2877(6)	3175(4)	1665(3)	70(2)
C(22)	1921(7)	2932(3)	1182(3)	63(2)
C(23)	580(6)	2866(3)	1259(2)	59(2)
C(24)	188(5)	3040(3)	1803(2)	47(1)

Table 27 (Continued).

Atom	x	y	z	U(eq)
C(25)	733(5)	4515(2)	3077(2)	37(1)
C(26)	1297(7)	4958(3)	2685(3)	79(2)
C(27)	1346(8)	5722(4)	2762(4)	110(3)
C(28)	826(8)	6053(4)	3219(4)	93(2)
C(29)	267(7)	5628(3)	3602(3)	74(2)
C(30)	225(6)	4857(3)	3541(2)	56(2)
C(31)	-1078(5)	3245(3)	2965(2)	40(1)
C(32)	-2148(5)	3691(3)	2695(3)	60(2)
C(33)	-3510(6)	3450(4)	2637(3)	79(2)
C(34)	-3790(6)	2759(4)	2850(3)	78(2)
C(35)	-2721(6)	2314(3)	3116(3)	74(2)
C(36)	-1382(6)	2553(3)	3174(3)	57(2)
C(1A)	3965(5)	4652(3)	4138(2)	38(1)
C(2A)	2993(5)	5377(3)	4848(2)	46(1)
C(3A)	3618(5)	5986(3)	4670(2)	53(1)
C(4A)	4425(6)	5906(3)	4217(2)	54(1)
C(5A)	2145(6)	5372(3)	5337(3)	68(2)
C(6A)	5139(8)	6574(3)	4001(3)	93(2)
Cu(1)	2264(1)	3012(1)	3869(1)	39(1)
N(1)	3157(4)	4713(2)	4572(2)	41(1)
N(2)	4604(4)	5257(2)	3960(2)	49(1)
P(1)	2853(1)	1785(1)	3999(1)	38(1)
P(2)	751(1)	3495(1)	3050(1)	33(1)
S(1)	4200(1)	3791(1)	3836(1)	45(1)

Table 28 Anisotropic displacement parameters ($\text{\AA}^2 \times 10^3$) for $[\text{CuBr}(\text{PPh}_3)_2(\text{dmpymtH})]$.

The anisotropic displacement factor exponent takes the form:

$$-2\pi^2 [h^2 a^*{}^2 U^{11} + \dots + 2 h k a^* b^* U^{12}]$$

Atom	U^{11}	U^{22}	U^{33}	U^{23}	U^{13}	U^{12}
Br(1)	80(1)	46(1)	50(1)	0(1)	30(1)	0(1)
C(1)	48(3)	35(3)	41(3)	2(2)	10(2)	2(2)
C(2)	78(4)	45(3)	93(5)	-1(3)	44(4)	-3(3)
C(3)	80(5)	70(5)	118(6)	11(4)	56(4)	-6(4)
C(4)	77(5)	82(5)	86(5)	19(4)	18(4)	-21(4)
C(5)	112(6)	63(5)	117(6)	-19(4)	48(5)	-35(4)
C(6)	85(5)	45(4)	112(5)	-14(3)	50(4)	-18(3)
C(7)	53(3)	37(3)	40(3)	-6(3)	2(3)	13(3)
C(8)	61(4)	45(3)	65(4)	-4(3)	-10(3)	11(3)
C(9)	71(5)	60(4)	106(6)	-17(4)	-25(4)	16(4)
C(10)	108(7)	85(6)	82(6)	-9(5)	-34(5)	34(5)
C(11)	123(7)	111(7)	66(5)	36(4)	-7(5)	25(6)
C(12)	84(5)	82(5)	53(4)	19(3)	4(4)	12(4)
C(13)	53(3)	34(3)	38(3)	-1(2)	14(3)	-7(3)
C(14)	58(4)	42(3)	53(3)	-1(3)	17(3)	5(3)
C(15)	81(4)	52(4)	83(5)	-6(3)	42(4)	3(3)
C(16)	112(6)	70(5)	68(5)	-27(4)	54(5)	-23(4)
C(17)	99(5)	88(5)	43(4)	-13(3)	15(4)	-11(4)
C(18)	60(4)	65(4)	52(4)	-5(3)	10(3)	2(3)
C(19)	38(3)	31(3)	38(3)	0(2)	6(2)	4(2)
C(20)	44(3)	84(4)	43(3)	-6(3)	6(3)	3(3)
C(21)	50(4)	103(5)	60(4)	-11(4)	20(3)	1(3)
C(22)	77(4)	63(4)	51(4)	-8(3)	19(4)	3(3)
C(23)	76(4)	57(4)	39(3)	-8(3)	-2(3)	-7(3)
C(24)	46(3)	46(3)	46(3)	2(3)	4(3)	-2(3)
C(25)	36(3)	30(3)	44(3)	6(2)	5(2)	5(2)

Table 28 (Continued).

Atom	U^{11}	U^{22}	U^{33}	U^{23}	U^{13}	U^{12}
C(26)	115(5)	46(4)	91(5)	9(3)	54(4)	-1(4)
C(27)	146(7)	44(4)	159(8)	13(5)	79(6)	-12(4)
C(28)	102(6)	29(4)	143(7)	3(4)	14(5)	10(4)
C(29)	93(5)	43(4)	84(5)	-17(3)	5(4)	18(4)
C(30)	75(4)	43(3)	53(4)	1(3)	17(3)	11(3)
C(31)	35(3)	41(3)	45(3)	-1(2)	9(2)	-2(2)
C(32)	38(3)	55(4)	86(4)	12(3)	6(3)	1(3)
C(33)	32(3)	82(5)	119(6)	5(4)	2(3)	5(3)
C(34)	42(4)	75(5)	123(6)	-17(4)	28(4)	-13(4)
C(35)	60(4)	53(4)	117(6)	-5(4)	40(4)	-13(3)
C(36)	46(4)	50(4)	78(4)	2(3)	21(3)	-1(3)
C(1A)	37(3)	41(3)	33(3)	-5(2)	3(2)	1(2)
C(2A)	42(3)	51(3)	44(3)	-6(3)	3(3)	5(3)
C(3A)	64(4)	43(3)	50(3)	-10(3)	5(3)	2(3)
C(4A)	67(4)	44(3)	48(3)	-6(3)	9(3)	-13(3)
C(5A)	71(4)	68(4)	73(4)	-20(3)	32(3)	2(3)
C(6A)	136(6)	57(4)	100(5)	-17(4)	60(5)	-32(4)
Cu(1)	45(1)	32(1)	38(1)	1(1)	5(1)	3(1)
N(1)	41(2)	42(2)	41(2)	-6(2)	11(2)	3(2)
N(2)	60(3)	48(3)	41(2)	-7(2)	14(2)	-12(2)
P(1)	45(1)	31(1)	37(1)	-1(1)	7(1)	3(1)
P(2)	33(1)	32(1)	36(1)	2(1)	7(1)	1(1)
S(5)	43(1)	43(1)	50(1)	-10(1)	7(1)	-3(1)

Table 29 Atomic coordinates ($\times 10^4$) and equivalent isotropic displacement parameters ($\text{\AA}^2 \times 10^3$) for $[\text{CuI}(\text{PPh}_3)_2(\text{dmpymtH})]$. U(eq) is defined as one third of the trace of the orthogonalized U^{ij} tensor.

Atom	x	y	z	U(eq)
C(28)	1737(3)	7345(3)	7626(4)	84(1)
N(1)	3053(2)	4778(2)	5482(2)	51(1)
N(2)	5011(2)	5811(2)	6252(2)	54(1)
I(1)	599(1)	2493(1)	5363(1)	53(1)
Cu(1)	2077(1)	2923(1)	7147(1)	38(1)
P(1)	2331(1)	1335(1)	7668(1)	36(1)
P(2)	1116(1)	3767(1)	8138(1)	37(1)
S(1)	4026(1)	4068(1)	7110(1)	55(1)
C(25)	1368(2)	5201(2)	7976(2)	43(1)
C(36)	2936(3)	4208(2)	9800(2)	60(1)
C(31)	1691(2)	3774(2)	9467(2)	42(1)
C(7)	863(2)	429(2)	7829(2)	40(1)
C(13)	3305(2)	1389(2)	8875(2)	42(1)
C(20)	-1228(2)	3857(2)	8424(2)	49(1)
C(19)	-551(2)	3269(2)	8025(2)	37(1)
C(1A)	4037(2)	4947(2)	6230(2)	45(1)
C(15)	3914(3)	618(3)	10378(2)	70(1)
C(1)	2921(2)	537(2)	6845(2)	42(1)
C(24)	-1161(2)	2273(2)	7523(2)	47(1)
C(12)	371(3)	650(2)	8646(2)	53(1)
C(23)	-2417(3)	1873(2)	7432(2)	59(1)
C(30)	1609(3)	5987(2)	8759(2)	61(1)
C(4A)	4970(2)	6485(2)	5543(2)	53(1)
C(3A)	3968(3)	6332(2)	4797(2)	60(1)
C(21)	-2478(3)	3451(2)	8328(2)	60(1)

Table 29 (Continued).

Atom	x	y	z	U(eq)
C(26)	1310(3)	5507(2)	7015(2)	58(1)
C(6)	3863(3)	100(2)	7178(2)	61(1)
C(14)	3146(3)	531(2)	9476(2)	56(1)
C(11)	-781(3)	54(3)	8762(2)	65(1)
C(8)	174(3)	-398(2)	7131(2)	59(1)
C(18)	4260(3)	2300(2)	9199(2)	56(1)
C(32)	972(3)	3336(2)	10146(2)	53(1)
C(22)	-3072(3)	2460(3)	7829(2)	61(1)
C(10)	-1455(3)	-762(3)	8055(3)	74(1)
C(35)	3453(3)	4211(3)	10780(3)	75(1)
C(2)	2405(3)	364(2)	5840(2)	58(1)
C(2A)	2999(3)	5461(3)	4758(2)	61(1)
C(17)	5033(3)	2370(3)	10107(2)	75(1)
C(16)	4857(3)	1540(3)	10685(2)	75(1)
C(6A)	6069(3)	7429(3)	5612(3)	81(1)
C(33)	1499(3)	3341(3)	11140(2)	71(1)
C(34)	2736(4)	3777(3)	11444(2)	77(1)
C(5A)	1861(3)	5183(4)	3992(3)	104(2)
C(5)	4258(3)	-508(3)	6520(3)	83(1)
C(3)	2792(3)	-261(3)	5192(2)	72(1)
C(4)	3710(4)	-693(3)	5533(3)	81(1)
C(29)	1789(3)	7048(2)	8580(3)	77(1)
C(9)	-979(3)	-982(3)	7251(3)	80(1)
C(27)	1491(3)	6577(3)	6844(3)	78(1)

Table 30 Anisotropic displacement parameters ($\text{\AA}^2 \times 10^3$) for [CuI(PPh₃)₂(dmpymtH)].

The anisotropic displacement factor exponent takes the form:

$$-2\pi^2 [h^2 a^*{}^2 U^{11} + \dots + 2 h k a^* b^* U^{12}]$$

Atom	U ¹¹	U ²²	U ³³	U ²³	U ¹³	U ¹²
C(28)	64(2)	43(2)	142(4)	23(2)	14(2)	12(2)
N(1)	42(1)	61(1)	44(1)	14(1)	2(1)	7(1)
N(2)	41(1)	55(1)	58(2)	7(1)	6(1)	3(1)
I(1)	49(1)	58(1)	39(1)	0(1)	-4(1)	3(1)
Cu(1)	39(1)	38(1)	35(1)	3(1)	6(1)	9(1)
P(1)	38(1)	36(1)	36(1)	2(1)	9(1)	10(1)
P(2)	35(1)	37(1)	36(1)	-1(1)	3(1)	10(1)
S(1)	38(1)	68(1)	49(1)	20(1)	0(1)	1(1)
C(25)	31(1)	40(1)	56(2)	4(1)	5(1)	9(1)
C(36)	50(2)	73(2)	51(2)	-10(1)	-4(1)	20(2)
C(31)	48(2)	42(1)	37(1)	-6(1)	0(1)	20(1)
C(7)	38(1)	37(1)	45(1)	7(1)	10(1)	12(1)
C(13)	42(1)	48(2)	41(1)	4(1)	9(1)	20(1)
C(20)	47(2)	47(2)	53(2)	-3(1)	8(1)	13(1)
C(19)	36(1)	41(1)	34(1)	4(1)	5(1)	11(1)
C(1A)	34(1)	53(2)	45(2)	5(1)	8(1)	6(1)
C(15)	69(2)	95(3)	58(2)	34(2)	14(2)	40(2)
C(1)	43(1)	33(1)	50(2)	2(1)	19(1)	7(1)
C(24)	42(2)	49(2)	48(2)	-4(1)	8(1)	11(1)
C(12)	56(2)	54(2)	50(2)	5(1)	18(1)	13(1)
C(23)	47(2)	56(2)	62(2)	-10(1)	9(1)	-1(1)
C(30)	61(2)	45(2)	71(2)	-4(1)	9(2)	9(1)
C(4A)	48(2)	46(2)	66(2)	7(1)	17(1)	9(1)
C(3A)	58(2)	57(2)	68(2)	27(2)	19(2)	14(2)
C(21)	51(2)	67(2)	68(2)	0(2)	20(2)	24(2)
C(26)	56(2)	58(2)	59(2)	13(1)	1(1)	19(1)

Table 31 (Continued).

Atom	U^{11}	U^{22}	U^{33}	U^{23}	U^{13}	U^{12}
C(6)	61(2)	65(2)	65(2)	2(2)	19(2)	26(2)
C(14)	51(2)	63(2)	57(2)	16(1)	11(1)	19(1)
C(11)	58(2)	77(2)	67(2)	21(2)	33(2)	19(2)
C(8)	50(2)	60(2)	60(2)	-8(1)	14(1)	6(1)
C(18)	56(2)	51(2)	56(2)	2(1)	-3(1)	18(1)
C(32)	60(2)	53(2)	45(2)	2(1)	2(1)	18(1)
C(22)	38(2)	74(2)	68(2)	2(2)	13(1)	9(2)
C(10)	47(2)	71(2)	98(3)	17(2)	24(2)	2(2)
C(35)	63(2)	96(3)	63(2)	-23(2)	-17(2)	37(2)
C(2)	67(2)	61(2)	51(2)	-1(1)	19(2)	23(2)
C(2A)	56(2)	71(2)	52(2)	18(2)	3(1)	14(2)
C(17)	66(2)	73(2)	72(2)	-6(2)	-22(2)	20(2)
C(16)	70(2)	104(3)	54(2)	7(2)	-9(2)	42(2)
C(6A)	63(2)	58(2)	111(3)	19(2)	22(2)	-3(2)
C(33)	98(3)	76(2)	43(2)	11(2)	8(2)	35(2)
C(34)	99(3)	90(2)	45(2)	-9(2)	-18(2)	52(2)
C(5A)	76(2)	126(3)	83(3)	55(2)	-20(2)	-4(2)
C(5)	85(2)	86(2)	100(3)	1(2)	36(2)	49(2)
C(3)	86(2)	73(2)	58(2)	-11(2)	28(2)	20(2)
C(4)	97(3)	72(2)	88(3)	-9(2)	50(2)	30(2)
C(29)	74(2)	40(2)	111(3)	-6(2)	12(2)	10(2)
C(9)	54(2)	72(2)	94(3)	-17(2)	18(2)	-12(2)
C(27)	73(2)	70(2)	91(3)	39(2)	6(2)	24(2)

VITAE

Name Miss Patcharanan Choto

Student ID 5010220207

Educational Attainment

Degree	Name of Institution	Year of Graduation
Bachelor of Science (Chemistry)	Prince of Songkla University	2007

Scholarship Awards during Enrolment

Center of Excellence for Innovation in Chemistry (PERCH-CIC), Commission on Higher Education, Ministry of Education.

List of Publication and Proceedings

Presentations

Poster presentation

1. Patcharanan Choto and Chaveng Pakawatchai: Crystal Structure of Copper(I) Chloride Complex containing Triphenylphosphine and 2-Thiobarbituric Acid, The 34th Congress on Science and Technology of Thailand (STT.34), Bangkok, Thailand, October 31-November 2, 2008.
2. Patcharanan Choto and Chaveng Pakawatchai: Synthesis and Crystal Structure of Copper(I) Complexes with Triphenylphosphine and 2-Thiobarbituric Acid, The International Congress for Innovation in Chemistry (PERCH-CIC Congress VI), Pattaya, Thailand, May 3-6, 2009.
3. Patcharanan Choto and Chaveng Pakawatchai: Synthesis, Crystal Structure, and Spectroscopic Characterization of Copper(I) Complexes. A Novel 1D Supramolecular Double-Chains of $[\text{Cu}(\text{PPh}_3)_2(\text{TBA})\text{Cl}]\cdot\text{H}_2\text{O}$, 60th Anniversary Conference on Coordination Chemistry in Osaka (60CCCO), Japan, September 27-30, 2010.